Cocaine-inducible circuitry reorganization as a basis for addiction-related memory traces

Dissertation

for the award of the degree

Doctor of Philosophy (PhD)

Division of Mathematics and Natural Sciences
of the Georg-August-Universität Göttingen

submitted by

Anna Elżbieta Suska

from Kraków, Poland

Göttingen, 2012

Thesis committee members

Dr. Dr. Oliver Schlüter (reviewer)

Molecular Neurobiology, European Neuroscience Institute, Göttingen

Prof. Dr. André Fischer (reviewer)

Epigenetics and Neurodegenerative Diseases, University Medical Center, Göttingen

Prof. Dr. Tobias Moser

Department of Otolaryngology, University Medical Center, Göttingen

Extended committee members

Prof. Dr. Michael Hörner

Dept. of Cell Biology, Johann-Friedrich-Blumenbach-Institute for Zoology and Anthropology, Göttingen

Camin Dean, PhD

Trans-synaptic Signaling, European Neuroscience Institute, Göttingen

Prof. Dr. Silvio Rizzoli

STED Microscopy of Synaptic Function, European Neuroscience Institute, Göttingen

Date of oral examination: **June 18th, 2012**

I hereby declare that I prepared this PhD thesis on my own and with no other sources and aids than quoted.

Anna Elżbieta Suska

Table of contents

List of figures

Abstract

Drug addiction has been conceptualized as an extreme, pathological form of memory. One potential mechanism underlying addiction-related memories is drug-induced plastic changes at glutamatergic synapses within the brain reward pathway. Presumably the changes in glutamatergic projections from the prefrontal cortex (PFC) and amygdala onto GABAergic neurons in the nucleus accumbens (NAc) transmit differential aspects of addiction-associated information. However the synaptic properties of specific glutamatergic afferents and their contribution to cocaine-induced plasticity changes are largely unknown. Using a combination of optogenetic tools to dissect specific afferents and variance-mean analysis to examine synaptic properties, I demonstrate that repeated exposure to cocaine via either i.p. injections or self-administration increased the release probability of medial PFC-to-NAc synapses but not basolateral amygdala–to-NAc synapses. Those presynaptic adaptations were long-lasting and further strengthened specifically in a contingent cocaine procedure. These data identified a presynaptic mechanism in altering the synaptic drive onto NAc medium spiny neurons, which might chronically shift the balance between amygdala and PFC inputs onto MSNs and contribute to the pathology of the addicted state.

Exposure to cocaine generates nascent excitatory synaptic connections in the NAc that could be the key substrates for the development of addiction. These nascent synapses critically contributed to the formation and persistence of cocaine-induced memories in a conditioned place preference paradigm. Silent synapses were increased in the NAc of PSD-95 KO and the number was further increased after cocaine procedures. In control animals these silent synapses were presumably incorporated in new neuronal connections during and after the CPP training, demonstrated by the recovery of the reduced AMPAR/NMDAR ratio and the accumulation of CP-AMPARs at 21 days of withdrawal. Although PSD-95 KO animals acquired initially a higher CPP score, the CPP extinguished after 21 days. Furthermore the AMPAR/NMDAR ratio remained low and no CP-AMPARs accumulated in the synapses. These findings are consistent with a role of the cocaine-induced silent synapses as plasticity substrates for new drug-related memories, which require PSD-95 and a mechanism through CP-AMPARs for consolidation. Together with the selective presynaptic enhancement of specific projections to the NAc, these data

support the conclusion of drug related shifts in synaptic drive of different NAc projection pathways and drug-related new connections in the mesocorticolimbic pathways.

1. Introduction

The human brain is the most complex, and amazing organ of the body that builds itself by adapting to its environment. It contains 100 billion nerve cells that have the unique ability to communicate with each other through highly specialized contacts - synapses. Each neuron can form on average 10.000 – 100.000 synaptic contacts, which in the whole brain results in 10^{15} synapses. It is more connections than there are stars in our galaxy. This enormous degree of connectivity is what makes the brain so exceptional. The capacity to create or loose connections and strengthen or weaken them in response to the surrounding world is the cellular basis of learning.

1.1. Synaptic transmission

Communication between neurons occurs via functional contacts called synapses. There are two types of synaptic connections: electrical and chemical. Electrical synapses are tight junctions, 2-3nm apart that propagate neuronal signals (action potential, AP) from one neuron to another very rapidly. Due to this rapid electrical transmission, electrical synapses are generally responsible for synchronising the activity of populations of neurons, important for example in the brain stem, where rhythmic activity controls breathing (Rekling et al., 2000). Electrical synapses can conduct the signal in both directions, depending on which of the two connected neurons is firing the action potential at the moment. Because the ionic current flows passively through gap junction channels, modification of the strength of such connection is very limited.

The vast majority of synapses in the brain are chemical. In contrast to electrical synapses, chemical ones have a more complex structure, with a higher capacity for long-lasting modulation of the strength of synaptic transmission (synaptic plasticity) that is essential for more complex behaviours in higher organisms. At the chemical

synapses, the presynaptic and postsynaptic neurons are separated by a gap, the synaptic cleft, which is wider than that in electrical synapses (20-40nm). The conveyance of the action potential through a chemical synapse requires the conversion of the electrical signal into a chemical, carried by the neurotransmitter across the synaptic cleft and back to an electrical one on the postsynaptic site.

The arrival of an action potential into the presynaptic terminal causes voltage-gated calcium channels to open, which then results in a rapid increase in the calcium concentration at the active zone, a specialized compartment for neurotransmitter secretion. The calcium triggers the fusion of synaptic vesicles with the presynaptic membrane and the neurotransmitter is released. The neurotransmitter diffuses through the synaptic cleft and binds to ion channel-linked receptors located in the postsynaptic membrane. This leads to the opening of the channels and the ion flow alters the membrane potential of the receiving neuron. The postsynaptic response caused by the content of a single synaptic vesicle is referred to as a quantal response. These alterations in membrane potential summate in the soma (neuron cell body), and once they overcome the action potential threshold, a new action potential is generated and propagated along the axon to another neuron.

Neurotransmitters can be very diverse: single amino acids like glycine, glutamate, GABA; biogenic amines like dopamine, adrenaline, serotonin or peptides – e.g. endorphins. Functionally they can be categorized into three groups: i) excitatory, those cause the postsynaptic neuron to fire a new action potential (glutamate), inhibitory that reduce the probability of the receiving neuron to fire an AP by hyperpolarizing its membrane potential (GABA, glycine) and iii) modulatory that through secondary messengers alter the neuron's metabolism and membrane permeability (e.g. dopamine, serotonin). The action of a certain neurotransmitter – whether it is excitatory, inhibitory or modulatory depends on the type of receptors with which it interacts. Excitatory neurotransmitters open cation channels and therefore depolarize the cell while inhibitory neurotransmitters, act on Cl^- specific channels. Increase in negatively charged ions inside the cell causes hyperpolarization and the action potential in the postsynaptic neuron will not be generated.

1.2. Glutamatergic excitatory synapse

Excitatory synapses are formed primarily on dendritic protrusions called spines. The spine head contains a protein rich structure called the postsynaptic density (PSD, visible as an electron rich region in electron microscopy) that is composed of neurotransmitter receptors as well as their scaffolds, transsynaptic cell adhesion molecules, cytoskeletal elements and downstream signaling components.

1.2.1. Glutamate receptors

Glutamate is the major excitatory neurotransmitter in the brain. It acts on two types of receptors: ionotropic receptors that comprise of a cation channel and metabotropic receptors that belong to a family of G-protein coupled receptors and influence intracellular signaling pathways through secondary messengers. There are three major subtypes of glutamate ionotropic receptors: AMPA receptors (AMPARs), NMDA receptors (NMDARs) and kainate receptors, named after their agonists: α-amino-3-hydroxy-5-methylisoxasole-4-propionic acid, N-methyl-D-aspartate and kainate respectively. They all are nonselective cation channels that are permeable to sodium and potassium. Furthermore, depending on the subunit composition these channels can also pass calcium ions (Seeburg et al., 1998). AMPARs and kainate receptors are activated directly by glutamate and have a relatively low conductance (<20pS) (Howe et al., 1991). They generate the early component of the evoked postsynaptic potential (EPSP). NMDARs on the other hand have a higher conductance (50pS) but have slower kinetics and therefore play a role in the late component of EPSPs (Lieberman and Mody, 1999). They require two more elements (apart from glutamate) for their activation. They need glycine as a co-agonist and membrane depolarization that removes the magnesium block. At the resting membrane potential (-65mV) extracellular magnesium blocks the ion pore of the channel and only upon depolarization Mg^{2+} ions are pushed out of the channel, allowing Na^{+} and Ca^{2+} ions to pass through (Schoepfer et al., 1994). Calcium is second messenger in synaptic plasticity, activating specific enzymes, including kinases, which contribute to long-lasting modifications in the synapse (Berridge, 1998).

All AMPA, NMDA and kainate receptors are tetramers and modifications of their subunit composition define their properties.

NMDA receptors in the forebrain are typically composed of an obligatory NR1 subunit, containing the glycine binding site and one or more NR2 subunits. The most abundant NR2 subunits are NR2A and B, while NR2C and D are expressed in cerebellum and superior colliculus respectively (Goebel and Poosch, 1999). Early in development diheteromeric receptors made of NR1 and NR2B are the most abundant. These receptors have higher calcium permeability and are characterized by large, long-lasting excitatory postsynaptic currents (EPSCs). During maturation, the NR1/NR2B containing receptors are substituted by NR1/NR2A (and perhaps triheteromeric NR1/NR2B/NR2A), which results in the acceleration of NMDA receptors kinetics (Gray et al., 2011; Liu et al., 2004).

AMPA receptors are tetramers made up of GluR1-GluR4 subunits, mainly diheteromers of two GluR1 and GluR2 or GluR3 and GluR2 (Mansour et al., 2001). GluR4 subunits resemble the structure of GluR1 and are expressed early in development – e.g. their expression levels in hippocampus become very low by postnatal day 10 (reviewed by (Malinow and Malenka, 2002). Receptors containing GluR1 and GluR3 subunits are permeable to calcium while through a posttranslational modification (substitution of glutamine to arginine in the channel pore), GluR2 subunit is calcium impermeable (Seeburg et al., 1998). Insertion of GluR2 subunits therefore modifies the receptor properties.

1.2.2. Scaffolding proteins

Glutamate receptors, clustered at the postsynaptic membrane are a part of the postsynaptic density. This protein rich structure is responsible for mediating basal synaptic transmission as well as modifying the strength of the synapse during induction and maintenance of synaptic plasticity. At the excitatory synapses, major scaffolding proteins, involved in AMPAR trafficking are the DLG-MAGUKs (disc-large membrane-associated guanylate kinases). This family of proteins contains 4 members: PSD-95 (postsynaptic density protein 95 kD MW), PSD-93, SAP-97 (synapse associated protein 97) and SAP102. They all show a very similar domain structure, having three N-terminal PDZ domains (named after three proteins in which they were first discovered: PSD-95/Discs large/zona-occludens-1), SH3 domain (Src

homology 3 domain) and GK domain (catalytically inactive guanylate kinase domain). This family of proteins regulates the surface expression of glutamate receptors in the synapse. Overexpression of PSD-95 enhances AMPA receptor-mediated synaptic transmission due to increase in function of AMPARs in the synapse (El-Husseini et al., 2000; Schluter et al., 2006) and has no effect on NMDAR-mediated synaptic transmission. These results were unexpected because the PDZ domain of PSD-95 was first shown to directly interact with the NR2 subunits of NMDA receptors (Kornau et al., 1995; Roche et al., 2001), but not with AMPA receptors. Consistent with the overexpression studies, knockdown of PSD-95 or PSD-93 with RNAi (RNA interference) revealed a 50% decrease in AMPAR EPSCs amplitude with no change in NMDAR-mediated transmission (Elias et al., 2006; Schluter et al., 2006). These results show that PSD-95 and PSD-93 are important in trafficking and retention of AMPA receptors at the synapse.

Knockout studies demonstrated that different members of the DLG-MAGUK family can compensate for one another. SAP102, PSD-93 and PSD-95 single knockouts showed normal basal synaptic transmission (Cuthbert et al., 2007; McGee et al., 2001; Migaud et al., 1998). In PSD-95 and PSD-93 double knockout studies however, a 55% reduction of AMPAR EPSCs was observed. Simultaneous knock down of SAP102 with shRNA (short hairpin RNA) reduced this remaining AMPAR EPSCs for further 50%. It seems that SAP102, which has predominant role in AMPAR trafficking in the immature synapses, compensates for the loss of other DLG-MAGUKs in matured contacts (Elias et al., 2006).

1.2.3. Cellular substrates of learning and memory

The brain has the unique capacity to change in response to past experiences. This is our basis to learn new skills and acquire new memories. This process, called neural plasticity is mediated by the ability of the brain to form new synaptic connections and to modify the existing ones by changing their strength. The processes underlying changes in synaptic strength are long-term potentiation (LTP), a long-lasting increase in synaptic strength and long-term depression (LTD), a decrease in synaptic strength. LTP and LTD can be further divided into NMDAR-dependent and independent mechanisms. The best-studied cellular correlates of learning are NMDAR-dependent LTP and LTD, well described in excitatory synapses between CA3 (cornu amonis 3)

and CA1 region of the hippocampus – a brain structure responsible for acquisition and retrieval of declarative memory (Bear, 1996). The induction of this form of LTP is a result of the distinctive properties of NMDA receptors – calcium permeability upon glutamate binding paired with sufficient membrane depolarization. Generally, the postsynaptic cell can be depolarized by back-propagating action potentials (Magee and Johnston, 1997) or dendritic spikes (APs generated in the dendrite, (Golding et al., 2002)). NMDA receptors serve as coincidence detectors of presynaptic and postsynaptic activity that is necessary for induction of Hebbian forms of plasticity. High-frequency stimulation leads to the rapid increase of postsynaptic calcium concentration, which triggers a cascade of events involving Calcium-calmodulin protein kinase II (CaMKII) and protein kinase C (PKC). This eventually leads to insertion of new AMPA receptors into the synapse and thereby increases the cells response to glutamate release. On the contrary, low-frequency synaptic stimulation (typically 1Hz) leads to a small increase of intracellular calcium levels and activates calcium-dependent phosphatases that in turn trigger the removal of synaptic AMPA receptors, weakening the synaptic connection (Bear and Malenka, 1994; Shepherd and Huganir, 2007). DLG-MAGUKs that play an important role in AMPA receptors trafficking and stability at the synapse are also crucial in the process of LTP and LTD induction. In PSD-95 KO animals the LTP is increased and LTD is absent (Beique et al., 2006; Migaud et al., 1998; Xu et al., 2008) whereas PSD-93 knockouts showed normal LTD and an increased threshold for LTP (Carlisle et al., 2008).

In developing neuronal networks, an important phenomenon underlying synaptic plasticity is activation of silent (or nascent) synapses. Such synapses contain functional NMDA receptors, but AMPA receptors are either absent or highly labile (Groc et al., 2006; Kullmann, 1994; Xiao et al., 2004). As a result, at resting membrane potential, this synapse is unable to conduct current and it is therefore called “silent”. A developing brain contains a high number of silent synapses. For instance during the first postnatal week, almost all Schaffer collaterals synapses (CA3-CA1) in the hippocampus are silent. It is a form of reserve capacity, ready to be activated by the network’s increased activity (Kerchner and Nicoll, 2008). During development (or learning) such increased activity leads to unsilencing of nascent synapses by recruitment and retention of AMPA receptors, making the synapse fully functional. Similarly to LTP induction, postsynaptic depolarization paired with presynaptic

stimulation strengthens the connection by increasing the number of functional AMPA receptors in the synapse, a mechanism involving the activity of CaMKII (Isaac et al., 1995; Liao et al., 1995; Wu et al., 1996). PSD-95, which is involved in LTP induction, is also important in unsilencing of nascent synapses. Knockout studies showed a 30% decrease in AMPA/NMDA ratio of EPSCs amplitudes and a decrease of mEPSCs frequency (without a change in a probability of glutamate release) suggesting an increase in the number of AMPAR-lacking synapses (Beique et al., 2006). It seems that the absence of PSD-95 makes AMPA receptors more labile – nonfunctional in basal conditions and easily recruited during LTP induction.

1.3. Drug addiction as a model of learning

Drug addiction is a state of compulsive, out-of-control drug use despite its obviously negative consequences to health, quality of life and social relationships of afflicted individuals. Repeated drug administration results in homeostatic changes in the brain like tolerance and dependence. Tolerance is a requirement for increased doses of the substance in order to maintain the desired pleasurable effect. Dependence is a state, in which if the drug use is ceased, distressing symptoms of withdrawal occur. Neither of these two adaptations however is responsible for making addiction a chronic illness. It is a long-term form of associative memory that makes addicts vulnerable to relapse, even years after a person had stopped using drugs. Underlying mechanisms are very similar to natural reward-related learning, but in addiction, drug intake overvalues natural rewards, which makes this form of memory pathological.

1.3.1. Reward-related learning

The brain interprets rewards as positive values of certain objects or actions. Natural rewards like food, mating opportunities, shelter are associated with the survival of the species. Behaviours with rewarding goals tend to be repeated increasingly over time; such phenomenon is called reinforced learning. The motivational state of an organism e.g. hunger can increase the value of a reward (food tastes better when hungry) and stimulate an action to obtain the desired reward (Kelley and Berridge, 2002). Similarly, drug use is both rewarding (pleasurable feeling) and reinforcing (sequences of actions performed to obtain the drug are often

repeated). The fear of withdrawal symptoms or positive associations to drug-related cues initiate drug craving and increase the motivation to engage active usage. Unlike natural learning however, drug-associated rewards, which have detrimental rather than beneficial consequences, tend to be valued more than others and obtaining the drug becomes the main life goal.

Dopamine (DA) plays a central role in both natural and addiction-related learning (Schultz et al., 1997), as it is required for motivated behaviours aimed to obtain the reward. Drugs of abuse and natural rewards increase the dopamine level in the synapses between ventral tegmental area (VTA) of the midbrain and the nucleus accumbens (NAc) shell in ventral striatum (Di Chiara, 1998). Findings of Schultz and co-workers shed much light on our understanding of importance of dopamine in reinforced learning. Studying a model called reward prediction error, they were monitoring the activity of VTA dopamine neurons in monkeys, as they received a reward (apple juice) synchronized with a conditioning stimulus (sound or light). When an animal was trained to obtain a reward, dopamine neurons exhibited a stable tonic activity pattern - the reward is "as expected" – no prediction error. It means that the brain doesn't increase dopamine levels in response to reward because it stores in memory rewards experienced in the past. However, if the reward does not appear after prediction cue, there is a pause of activity (negative prediction error). On the other hand if the reward exceeds expectations, bursts of activity signal a positive prediction error (Schultz et al., 1993). In this model, drugs of abuse such as cocaine, which is a dopamine reuptake inhibitor, have a great advantage over natural rewards because of their ability to immediately increase the dopamine levels in the synapse. Regardless of the expectations, the brain will anyways interpret this signal as "better than predicted" and shape the behaviour in order to maximize the reward – increase the drug use even when its pleasure is long gone.

1.3.2. Key brain circuits involved in reward-related learning and addiction

Both natural rewards and addictive drugs have the ability to increase dopamine levels in the mesolimbic dopamine system, which controls motivated behaviours and reward learning (Hyman et al., 2006). The source of DA in this system is the VTA, which projects to other brain areas: NAc, prefrontal cortex (PFC), hippocampus and

amygdala (Swanson, 1982). In turn, PFC, hippocampus and amygdala send glutamatergic afferents to the NAc. Within these structures, dopamine modulates the strength of excitatory synaptic transmission gating the establishment of reward-related memories. The NAc is a key element in circuits associated with addiction (Di Chiara, 2002). It creates a platform for integrating the motivational state of the organism with cognitive and associative abilities. The NAc output affects (among others) motor regions necessary for execution of motivated behaviours.

The PFC is responsible for representing goals, means to achieve them and their emotional valuation as well as future planning (Miller and Cohen, 2001). Neuroimaging studies revealed that in addicted individuals the activity of PFC is altered, leading to reduced self-control, increased impulsivity, drug craving and relapse (Goldstein and Volkow, 2011).

Formation of memories associated with emotions, for example fear conditioning is a result of synaptic plasticity happening in the amygdala, located in the temporal lobe (Rodrigues et al., 2004). In addiction, afferents to the NAc shell are important in drug-seeking behaviour, choice and decision-making (Mameli and Luscher, 2011).

1.3.3. Synaptic plasticity underlying addiction

Drugs of abuse, such as cocaine, induce long-term neuroadaptations that affect behaviour. Modifications of synaptic strength that begin with LTP and LTD mechanisms are consolidated by altered gene and protein expression that result in rewiring of brain circuitry, making addiction-related memories long-lasting.

Twenty-four hours after a single i.p. injection of cocaine in mice, new AMPA receptors are inserted in VTA dopamine neurons, leading to an increase of AMPA/NMDA EPSCs ratio (Bellone and Luscher, 2006; Ungless et al., 2001). A substantial number of those AMPA receptors lack GluR2 subunits, which leads to their calcium permeability (CP-AMPAR). This phenomenon lasts for around a week and can be reversed by activation of the metabotropic glutamate receptor, mGluR1, causing mGluR-dependent LTD, during which GluR2 subunits are locally, de novo synthesised (Bellone and Luscher, 2006; Mameli et al., 2007). This increased AMPAR-mediated transmission in VTA neurons is responsible for the cocaine-induced decrease in AMPA/NMDA ratio observed in mouse NAc shell medium spiny neurons (Kourrich et al., 2007; Mameli et al., 2009; Thomas et al., 2001). This

decrease in ratio was attributed to a decrease in AMPARs number and/or function as a consequence of an LTD-type of mechanism. Again after a week-long withdrawal this plasticity is reversed, leading to an increase of AMPA/NMDA ratio. In the study of Huang et al. (2009), an interesting observation was made that repeated cocaine exposure leads to generation of silent synapses in rat NAc shell. These silent synapses are created primarily by insertion of new NR2B-containing NMDA receptors to new synaptic contacts (Brown et al., 2011). The generation of silent synapses explains the reduced AMPA/NMDA ratio, previously attributed to LTD-like mechanism. It remains to be shown, whether the silent synapses are all de novo generated or whether indeed LTD-type mechanisms contribute to their silencing. The number of nascent synapses that gradually increases throughout the cocaine treatment goes down during the withdrawal period. A possible unsilencing of nascent synapses by recruitment of new AMPAR could explain the potentiation of AMPAR-mediated transmission during withdrawal. According to Kourrich and colleagues (2007), accumulation of AMPARs does not involve insertion of GluR2-lacking AMPA receptors. Conrad et al. (2008) however reported that in rats self-administrating cocaine for 10 days, there is a gradual increase of CP-AMPA receptors expression during prolonged (45 days) withdrawal. This increase of AMPAR mediated transmission in NAc correlates with incubation of drug craving. Similarly to VTA, accumulation of CP-AMPARs can be reversed in mGluR1-dependent manner, by a mechanism involving protein kinase C (McCutcheon et al., 2011).

PSD-95, a protein strongly involved in natural learning processes through an impact on AMPAR trafficking, plays an important role in cocaine-induced plasticity as well. It was reported that PSD-95 mRNA levels were decreased in the NAc and protein levels decreased in the dorsal striatum after chronic but not acute cocaine i.p. treatment in mice (Yao et al., 2004). Similarly PSD-95 levels decreased during withdrawal from repeated morphine injections in the rat NAc (Zhang et al., 2011). Previously reported increased LTP and high number of silent synapses in the absence of PSD-95 (Beique et al., 2006; Migaud et al., 1998) correlate with a hypothesis of nascent synapses being important elements underlying cocaine-associated plasticity.

The scope of the study

Repeated cocaine experience generates silent synapses (Huang et al., 2009) that I hypothesize to be the substrates for learning and depending on subsequent experiences, they may develop into fully functional connections, contributing to cocaine-associated rewiring. Several observations were made, linking PSD-95 with silent synapses and cocaine-induced adaptations. PSD-95 KO animals have a higher number of silent synapses in the hippocampus (Béïque et al., 2006) and display higher locomotor activity in response to a single cocaine injection, but they do not develop behavioural sensitization after repeated cocaine treatment (Yao et al., 2004). Furthermore, in the striatum and NAc, the levels of PSD-95 are decreasing, after exposure to cocaine and morphine (Yao et al., 2004, Zhang et al. 2011). Consistent with an essential role of silent synapses in locomotor sensitization (Brown et al., 2012) a potentially high number of silent synapses in the NAc of PSD-95 KO mice might be responsible for a stronger response to cocaine. The lack of locomotor sensitization might be caused by an occlusion of the saturating initial response. These features render the PSD-95 KO mice an attractive model system to study the importance of silent synapses in formation of cocaine-induced memories. In this study, I aimed on elucidating the impact of cocaine experience on the formation of silent synapses in the NAc of PSD-95-deficient mice. The incorporation of CP-AMPARs in the synapse might potentially be involved in the conversion of silent synapses to functional ones, during development of addiction-related, long-term memories. Given the role of PSD-95 in AMPARs trafficking, I investigated the fate of silent synapses and the requirement of CP-AMPARs in regard to the establishment of short-and long-term, cocaine-associated memories, by using a conditioned place preference test.

Whereas extensive studies on postsynaptic alterations following cocaine exposure led to a discovery of increasing synaptic strength of NAc afferents during withdrawal, it remains largely elusive, whether presynaptic sites of these glutamatergic synaptic transmissions are also affected. Moreover, the pathway-specific alterations of the NAc afferents may represent the ongoing reorganization of the neuronal network, shaping the drug-related pathological behaviour. So far no changes in presynaptic properties were reported (Kourrich et al., 2007; Thomas et al., 2001), however in these studies the results were sampled over all glutamatergic afferents projecting to the NAc. Each

of those pathways may contribute different properties and possible cocaine evoked changes might be masked. It would therefore be necessary to address the glutamatergic afferents separately in order to elucidate possible cocaine-induced changes of the presynaptic properties in the NAc. As the second aim, I analyzed the afferents to the NAc shell from the PFC and the amygdala specifically and elucidated their presynaptic properties in respect to repeated cocaine exposure and subsequent prolonged withdrawal.

2. Materials and methods

2.1. Molecular biology

2.1.1. Genotyping

The PSD-95 KO mouse line was generated by Yao and colleagues (2004). The genotype was evaluated based on the PCR reaction (Saiki et al., 1985) on DNA samples obtained from tail pieces. At postnatal days between 1 and 3, a 1-2mm tail sample was cut from each animal. The tissue was digested overnight in 200µl of PBND lysis buffer at 55°C with constant shaking. Sample was heated up to 99°C for 10 min in order to inactivate the proteinase K present in the lysis buffer. Two µl of the lysate was used as a template for a PCR reaction:

Sample mix:

2.2µl	10x TNK buffer
2µl	dNTP mix (2,5mM each, Bioline)
0.2µl	GKoptFor2 forward primer (50 µM)
0.2µl	GKoptRev2 reverse primer (50 µM)
2µl	lysate
15.2µl	H_2O
0.2µl	Mango Taq Polymerase (Bioline)

Program:

5’ 94°C	initialization	
45’’ 94°C	denaturation	x35
45’’ 55°C	annealing	
1’ 72°C	elongation	
10’ 72°C	final elongation	

PCR products were analysed on 1% agarose gels in sodium tetraborate buffer supplemented with ethidium bromide. Bands were separated by horizontal electrophoresis at 120V for 45 min and visualized on UV-illuminator with INTAS imaging system. Product from a wild-type allele is of a size of 255bp, while KO allele 355bp.

Primer sequence (5’ – 3’):

GKoptFor2: CAGGTGCTGCTGGAAGAAGG

GKoptRev2: CTACCCTGTGATCCAGAGCTG

Solutions:

PBND buffer: 10mM Tris, 50mM KCl, 2.5mM $MgCl_2 \cdot 6H_2O$, 0.1mg/ml gelatine, 0.45% (v/v) Nonident P40, 0.45% (v/v) Tween 20, supplemented with proteinase K (Roth) to a final concentration of 1,2mg/ml

10x TNK: 100mM TrisHCl (pH 8.5), 15mM $MgCl_2$, 500mM KCl, 50mM NH_4Cl

1% agarose gel: 4g of agarose in 400ml 1x sodium tetraborate buffer, supplemented with 6µl 1% ethidium bromide (Roth).

20x sodium tetraborate buffer: 100mM sodium tetraborate decahydrate (Sigma)

2.1.2. Electro-competent bacteria

The bacterial strain of *Escherichia coli* used in this study was SURE, purchased from Stratagene (CA, USA). In order to render the bacteria able to acquire plasmids through electroporation, the following protocol was used.

A single colony of SURE bacteria was picked from LB-Agar (Roth, Germany) plate, put into 5ml of LB-medium (Roth, Germany) and incubated overnight at 37°C with vigorous shaking (300rpm, INNOVA 4230, Brunswick Scientific shaker). Two ml of overnight culture was used to inoculate 500ml LB-medium and grown at 37°C with vigorous shaking (300rpm) until it reached the density of 0.6 (BioPhotometer, Eppendorf, Germany). Bacterial culture was then quickly placed into ice-cold bath and cooled down. After 30min incubation in ice-cold bath, bacterial suspension was spinned down at 8000rpm (Beckman J2-21 centrifuge, JA-10 rotor) in 500ml centrifuge bottles (Nalgene). Bacterial pellet was washed three times by resuspending in 50ml of sterile ice-cold water, filling up to 500ml with water and centrifugation again at 8000rpm. After washing three times the pellet was resuspended again in 50ml of ice-cold water, but filled up with 450ml of 10% glycerol solution (Roth) and spinned down as previously. Next, bacteria were resuspended in 30ml of 10% glycerol, transferred to 35ml centrifugation tubes (Beckman) and spinned at 8000rpm (JA-20 rotor). Lastly, bacteria were resuspended in 4ml of 10% glycerol solution, aliquoted (50µl) in 1,5ml Eppendorf tubes and quickly frozen in liquid nitrogen.

2.1.3. Large-scale plasmid preparation

AAV vector plasmid containing CAG promoter followed by channelrhodopsin-2 fused with Venus (Figure 1, Addgene plasmid 20071: pACAGW-ChR2-Venus-AAV (Petreanu et al., 2009)) was transformed into SURE bacteria (Stratagene, CA, USA) by electroporation (1800V, time constant between 4 and 6 ms, Eppendorf 2510 electroporator). Cells were streaked out and grown overnight on Agar-LB plate in 37°C incubator. A single colony of transformed bacteria was used to inoculate 50ml of LB medium (Roth) and grown overnight in 37°C, with constant shaking (350rpm, INNOVA 4230, Brunswick Scientific shaker). Cells were then harvested by 30 min centrifugation at 4°C (4000rpm, A-4-44 rotor, Eppendorf Centrifuge 5804R) and lysed by a standard alkaline lysis procedure using Qiagen solutions P1, P2 and P3, according to the Qiagen protocol. DNA was then precipitated in 0.7x volume of isopropanol (AppliChem), spinned down (as above) and resuspended in 600µl of buffer TE. To remove the residual RNA, 150µl of 1M NaCl with 1µl RNase (100mg/ml, Qiagen) was added and the sample was incubated at 55°C for 5 min. To remove the proteins from the sample the phenol/chloroform extraction was performed. The sample was mixed with an equal volume of phenol/chloroform/isoamyl alcohol (25:24:1, AppliChem) and vortexed vigorously. The phases were separated by centrifugation, upper (aqueous) phase was transferred to a new tube and an equal volume of chloroform was added (to remove the residual phenol). After vigorous shaking the aqueous phase was collected and the DNA was precipitated with 0.7x volume of isopropanol. The pellet was resuspended in 100µl of EB buffer.

Solutions:

P1: 50mM Tris-HCl pH8.0, 10mM EDTA, 100µg/mL RNase A

P2: 200mM NaOH, 1%SDS w/v

P3: 3.0 M Potassium acetate pH5.5

EB : 10mM Tris/HCl, pH 8.5, (Qiagen).

2.2. Cell culture

2.2.1. HEK 293T cells

Human embryonic kidney cells (HEK), expressing large T-antigen were used to produce adeno-associated viral (AAV) vectors. Cells were cultured in Dulbecco's Modified Eagle's Medium (Biochrom, Germany) supplemented with 10% fetal bovine serum (Biochrom). Cells were passaged using standard trypsin-mediated cell dissociation (both trypsin and phosphate-buffered saline (PBS) were purchased from Biochrom) and grown in 10cm culture dishes in a 37°C incubator with 5% CO_2.

2.2.2. Hippocampal slice cultures

Hippocampal organotypic slice cultures were prepared from P7-P8 Wistar rats (both genders). Animals were anesthetised with isoflurane (Abott, USA) and decapitated. Brains were removed and hippocampi were dissected out in ice-cold sucrose cutting buffer. Three thin layers of 0.8% agarose gel were placed on the base of a guillotine. The hippocampi were placed on top of the upper most layer of agarose and cut into 300µm thin slices by releasing the guillotine's wire frame. Slices were scooped out of the guillotine base with the upper most layer of agarose and transferred back to the sucrose cutting solution. After separation from one another the slices were transferred to ACSF solution for recovery (room temperature). After 30 min the slices were transferred to Basal Medium Eagle (BME, Biochrom) and plated on membrane discs inserts (Millicell-CM, 0.4µm pore size, Millipore, Germany) inside 35mm Petri dishes, 3 slices per dish. Slices were cultured in 20%HK medium for the first 3 days and transferred to 5% HK medium for the remaining culture time. The medium was exchanged with fresh one every 2 days. Slices were kept in the incubator in 34°C in the atmosphere of 5% CO_2.

Solutions:
20% HK: 49% BME (Biochrom), 25% EBSS, 25mM HEPES (Biochrom), 20% Donor Equine Serum (heat-inactivated for 30min at 55°C, Gibco, Germany), 28mM glucose, 1mM Glutamax (Biochrom), 88µg/ml l-ascorbic acid, 1µg/ml insulin, 0.25% 100X MEM-vitamins, 0.49% 50X MEM-amino acids.

5% HK: 63.3% BME (Biochrom), 25% EBSS, 25mM HEPES (Biochrom), 5% Donor Equine Serum HI (Gibco), 28mM glucose, 2mM Glutamax (Biochrom), 88µg/ml l-ascorbic acid, 1µg/ml insulin, 0.32% 100X MEM-vitamins, 0.63% 50X MEM-amino acids.

EBSS: 1.8mM $CaCl_2 \cdot 2H_2O$, 1mM $NaH_2PO_4 \cdot H2O$, 0.8mM $MgSO_4 \cdot 7H_2O$, 116mM NaCl, 26.2mM $NaHCO_3$, 5.4mM KCl, 5mM D-glucose·H2O.

Sucrose Cutting Buffer: 204mM sucrose, 26mM $NaHCO_3$, 10mM d-glucose, 2.5mM KCl, 1mM $NaH_2PO_4 \cdot H_2O$, 4mM $MgSO_4 \cdot 7H_2O$, 1mM $CaCl_2 \cdot 2H_2O$, 4mM l-ascorbic acid.

ACSF (recovery): 119mM NaCl, 26mM $NaHCO_3$, 20mM D-glucose, 2.5mM KCl, 1mM NaH_2PO_4, 4mM $MgSO_4 \cdot 7H_2O$, 4mM $CaCl_2$, bobbled with carbogene (95% O_2, 5% CO_2).

2.3. AAV preparation

2.3.1. Transfection of HEK 293T cells

Polyethyleneimine (PEI) was used as a transfection reagent in a procedure modified from Kuroda and co-workers (Kuroda et al., 2009). 3,36ml of 15mM linear PEI (Polysciences) was mixed with 24ml of 150mM NaCl solution and incubated for 10 min in room temperature. In a separate tube, 150mM NaCl was mixed with a combination of helper AAV plasmids: 127.5µg pRVI (AAV serotype 1), 127.5µg pH21 (AAV serotype 2), 315µg pFΔ6 and 150µg of vector plasmid (pACAGWChR2V-AAV) and incubated for 10 min in RT. Subsequently, the PEI mixture was added to the DNA mixture, vortexed and incubated for 10 min. Meanwhile HEK 293T cells (70-80% confluent) were harvested from 10x 15cm cell culture dishes, trypsinized and spinned down. The cell pellet was resuspended in 240ml of DMEM medium. The PEI/DNA mixture was added to the cell suspension

and mixed gently. HEK cells were plated on 15x 15cm cell culture dishes with 19ml of cell suspension per dish and cultured at 37°C in the atmosphere of 5% CO_2 for 48h.

2.3.2. Harvesting and purification of AAV

The medium was removed from the cells substituted by 4ml of PBS/dish and the cells were harvested by scraping off the dish surface. Cells were collected in 50ml Falcon tubes and centrifuged at 1000×g for 10 min. The pellet was resuspended in 9 ml of a buffer containing 20mM Tris, 150mM NaCl, pH 8.0. To lyse the cells and release the virus, 500µl of 10% NaDOC was added (to a final concentration of 0.5%) and mixed, followed by adding 2µl of benzonase nuclease HC (250u/µl, Novagen) and mixing thoroughly. The sample was incubated at 37°C for 30 min, with occasional vigorous shaking. 584mg of NaCl was added to the solution and the sample was incubated at 56°C for another 30 min. At this stage sample can be frozen in liquid nitrogen and stored over night at -80°C. After thawing the AAV-containing sample at 37°C, the remainings of the lysed cells were spinned down by centrifugation at 4000xg for 30 min (in 30ml Corex tubes). The supernatant was carefully transferred into the ultracentrifuge tube (Beckman) onto the discontinuous gradient of iodixanol: (from the bottom) 3ml of 56% layer, 3ml of 40%, 4ml of 25% and 7ml of 15%. The sample was centrifuged for 1,5h at 60000rpm using Beckman 70Ti rotor, during which the AAV particles are collected in the 40% iodixanol layer. To collect this layer, a cannula (20G, 0,9×70mm, Dispomed) attached to the syringe was placed at the interphase between 40% and 56% layer and the 40% phase was gently sucked into the syringe. The solution containing AAV particles was placed in a Falcon tube and diluted with PBS-MK up to 10ml and then concentrated with Amicon 100K concentrator by spinning at 2000g for 5-10 min, at room temperature. After repeating the concentrating step 3 times, the virus solution was filled with PBS-MK up to 500µl volume and sterilized by filtration through 0.22µm Millex-GV syringe-driven filter. The purified virus was stored at 4°C.

Solutions:

10% NaDOC: 10g of deoxycholic acid sodium salt dissolved in 100ml water. Filter sterilized (0.22µm).

10x PBS-MK: 0.2g $MgCl_2 \cdot 6H_2O$ (Merck), 0.19g KCl (Sigma) dissolved in 100ml 10xPBS. Filter sterilized (0.22μm).

Iodixanol solutions:
54%: 97.2ml of 60% iodixanol stock solution (in 1xPBS-MK) and 10.8ml of 1xPBS-MK
40%: 32ml of 54% iodixanol solution and 11.2ml 1xPBS-MK
25%: 20ml of 54% iodixanol solution and 32.1ml 1xPBS-MK
15%: 12ml of 54% iodixanol solution, 21.6 2M NaCl and 9.6ml 1xPBS-MK
(stored in the dark)

2.4. Viral infection

2.4.1. Injections into organotypic hippocampal slices

The organotypic hippocampal slice cultures were infected with AAV 2 days after preparation. 1μl of AAV virus solution was filled into a glass capillary mounted on Nanoject II microinjector (Drummond). The virus was injected into a single spot in the CA3 region (identified visually using binocular) by a single injection of 9.2nl at 46nl/s speed. The slices were transferred into fresh 20%HK medium and cultured at 34°C in the atmosphere of 5% CO_2.

2.4.2. Injections of AAV into PFC of newborn mice

P0-P2 C57BL/6 mouse pups were anesthetised on ice (10min) and immobilized in a styrofoam, home-made holder under the binocular. The thin skin of the newborns allows identifying the injection site visually. Similarly to slice culture injection, a glass capillary was filled with 2μl AAV encoding ChR2-Venus solution. Four injections of the AAV solution (13.4nl each, 23nl/s) were delivered into PFC (approx. AP +1.50, ML ±0.50, DV -1.3) by Nanoject II microinjector (Drummond). The tip of the capillary was placed on the pup's skin directly above the injection site, at a 90° angle and one quick move of the microinjector pierced both the skin and the skull, placing the capillary 1,3mm deep in the brain. After the injection, the capillary was slowly removed from the brain and animals were put on a heating plate (25-30°C)

where they were allowed to recover for a few minutes. Afterwards, they were returned back to their home cage.

2.4.3. Stereotaxic injections of AAV into PFC and amygdala of adult rats

Stereotaxic injections in rats were carried out by Brian R. Lee (Department of VCAPP, Washington State University, Pullman, WA, USA). Briefly, male Sprague-Dawley rats, 4-7 weeks old, were anesthetised by a ketamine, xylazine, and acepromazine mixture (0.1ml/100g) and placed in a stereotactic frame (Stoelting). 1 µl of AAV solution was injected bilaterally using 26G injection needle attached to Hamilton syringe and a Thermo Orion M365 pump, at 0.2µl/min speed (PFC: AP +3.00, ML ±0.75, DV -4.00, amygdala: AP -2.50, ML ±4.80, DV -8.50). After the surgery half of the animals were placed in their home cages to recover while other half underwent a surgery for implantation of a catheter for self-administration.

2.5. Cocaine treatment

2.5.1. Passive injections of cocaine in rats

Male Spraque Dalwey rats (9-16 weeks old) were used for all experiments. At least 3 weeks after stereotactic viral injection, rats received cocaine treatment. For 5 days, once-daily they received an intraperitoneal (i.p.) injection of either cocaine HCl (15mg/kg, Sigma, Germany) or saline – control group (Braun, Germany). They were sacrificed either on the next day (short-term withdrawal) or kept in their home cages for next 45-50 days (long-term withdrawal).

2.5.2. Self-administration of cocaine in rats

A surgery for implantation of a catheter for self-administration (SA) was performed by Brian R. Lee (Department of VCAPP, Washington State University, Pullman, WA, USA). The procedure directly followed the stereotactic viral injection. Briefly, a catheter was inserted into the jugular vein, passed under the skin and connected to a Quick Connect Harness (SAI Infusion). During recovery the catheter

was flushed daily with 0.1 ml of heparin (10 U/ml) and gentamicin antibiotics (5 mg/ml) in sterile saline, which protected against infection and catheter occlusion. After successful SA treatment, rats subjected to long-term withdrawal had the tubing blocked and harnesses removed.

For cocaine treatment, rats were first placed in an operant conditioning chamber (Med Associates) for an overnight session, during which they had time to accommodate to the new environment and learn the cocaine self-administration procedure. The animal activated the cocaine flow by poking an active button. Each poke resulted in 0,75mg/kg of cocaine HCl in 0,1ml of sterile saline, infused within 6s and activation of a conditioned stimulus (green light inside the active nose poke); poking inactive button had no effect, but was monitored as well. Simultaneously, a house light was switched on for 20 seconds during which the active button was deactivated (to prevent overdose). After overnight session, rats were put back to their home cages and after one day, 5 days of 2-hour self-administration sessions were performed. A session was successful when animal received at least 10 doses of cocaine. Again rats were sacrificed on the next day or after 45-50 days of withdrawal (short- and long-term withdrawal respectively).

2.5.3. Conditioned place preference in mice

Conditioned place preference procedure was performed according to Roux et al. (2003), with slight modifications. Male and female PSD95 KO mice (Yao et al. 2004) and their wild-type littermates, 3-6 weeks old, were used for all experiments. Animals were allowed to acclimate to the environmental conditions of the laboratory room for about 5 days, during which they received once-daily intraperitoneal injections of saline to familiarize them with injection procedure. They were housed in a dark/light cycle with illumination from 8am to 8pm, with free access to food and water. The conditioned place preference was measured in the two-compartment cage. Each of the 15cm x 15cm chambers differed in the texture of interior, visual cues (thick, vertical, black and white stripes versus small, black dots on white background) and scent (a piece of tissue with a drop of scented oils – cinnamon or vanilla, hidden in an Eppendorf tube). Compartments were connected by a triangular, neutral, grey-colored area and a pair of guillotine doors separated the conditioning chambers. One day before starting the conditioning, the animals were placed in the neutral area of the

two-compartment cage with a free access to both compartments. During 18min time, the location of the mouse was recorded in order to test for unconditioned preference or aversion towards one of the compartments. If such preference existed: less than 25% or over 75% of time spent in one compartment, the animal was discarded from the study. Animals were randomly assigned to receive cocaine/saline in one of the two compartments and for the next 10 days, they received alternate i.p. injections, once daily – cocaine (20mg/kg in 125µl volume of saline, Sigma, Germany) in one compartment and saline (Braun, Germany) in the second compartment. Control animals received saline injections in alternate compartments. After each injection, the animals were immediately placed in the assigned compartment for 20 min. One day after the conditioning period, a place preference test was performed where animals were again placed in the middle area with free access to both chambers and the time spent in each compartment was recorded during 18 min. The place preference score (PPS) was calculated from the equation below:

$$\mathrm{PPS} = \frac{time\ in\ the\ conditioned\ compertment\ (s) \times total\ time\ (s)}{total\ time\ (s) - time\ in\ the\ neutral\ area\ (s)}$$

Animals were sacrificed for the electrophysiological recordings either immediately after the test (1 day withdrawal) or returned to their home cages for 21-25 days of withdrawal. After that time, the place preference test was repeated and animals sacrificed for electrophysiology.

2.5.4. Tissue preparation

Coronal brain slices, 300µm thick, were prepared using Leica VTS1200 vibratome in ice-cold NMDG cutting solution (for rat preparations) or sucrose cutting buffer (for mouse preparations). Slices containing NAc were collected, transferred to ACSF solution, incubated for 30min at 36ºC and later for 30 min at room temperature. All solutions were constantly bubbled with carbogene (95% O_2, 5% CO_2).

Solutions:

NMDG cutting buffer: 135mM NMDG, 1mM KCl, 1,2mM KH_2PO_4, 1,5mM $MgCl_2 \cdot 6H_2O$, 0,5mM $CaCl_2 \cdot 2\ H_2O$, 20mM choline bicarbonate, 10mM D-glucose (all chemicals purchased from Sigma)

Sucrose cutting buffer: 25mM NaCl (Roth), 1,9mM KCl (Sigma), 1,2mM NaH_2PO_4 (Sigma), 26mM $NaHCO_3$ (Sigma), 10mM $MgSO_4 \cdot 7H_2O$ (Merck), 2,5mM $CaCl_2$ (Roth) 10mM D-glucose (Merck), 168mM sucrose (Roth)

ACSF: 119mM NaCl (Roth), 2,5mM KCl (Sigma), 1mM NaH_2PO_4 (Sigma), 26mM $NaHCO_3$ (Sigma), 1,3mM $MgCl_2$, 2,5mM $CaCl_2$ (Roth) 10mM D-glucose (Merck)

2.6. Electrophysiology

All electrophysiological recordings were conducted using two experimental setups:

Setup 1:

- Olympus BX51WI microscope
- Micromanipulator MP-255 (Sutter Instruments),
- Multiclamp700B amplifier (Molecular Devices),
- ITC-18 data acquisition board (HEKA),
- 473nm DPSS laser (IkeCool)
- pClamp data acquisition software (Molecular Devices).

Setup 2:

- ZEISS AXIO Examiner D1 microscope
- Micromanipulator SM-5 (Luigs & Neumann)
- ELC-03XS amplifier (npi),
- ITC-18 data acquisition board (HEKA),
- ISO-FLEX stimulator (A.M.P.I.)
- 473nm DPSS laser (IkeCool)
- Igor Pro data acquisition software (Wave Metrics)

The recording chamber was perfused with an ACSF solution, heated up to 29-31°C, constantly bobbled with carbogene (95% O_2, 5% CO_2). Recorded cells (medium spiny

neurons in NAc shell or CA1 pyramidal neurons in hippocampus) were identified visually and patched with a glass pipette (Borosilicate (KG-33) glass, King Precision Glass Inc.) of 3-5 MΩ resistance. The patch pipette was filled with internal solutions: (1) for rat NAc acute preparations and (2) for rat hippocampal organotypic cultures and mouse acute NAc slices. Recordings were carried out in whole-cell voltage clamp configuration, filtered at 3 kHz. Series and input resistance were monitored throughout the experiment.

Solutions:
ACSF: 119mM NaCl (Roth), 2.5mM KCl (Sigma), 1mM NaH_2PO_4 (Sigma), 26mM $NaHCO_3$ (Sigma), 1.3mM $MgCl_2$ (Sigma) 2.5mM $CaCl_2$ (Roth), 10mM D-glucose (Merck)

Internal solution (1): 139.6mM CsMeS (Sigma), 117.5 mM $MeSO_3H$ (Fluka), 20mM HEPES (Sigma), 5mM TEA-Cl (Fluka), 0.4mM EGTA (Sigma), 2.5mM MgATP (Sigma), 0.25mM NaGTP (Sigma), 1mM QX-314 bromide (Sigma). pH was adjusted to 7.3 using CsOH; osmolarity ~290mOsm.

Internal solution (2): 50%w/v CsOH (Sigma), 117,5 mM $MeSO_3H$ (Fluka), 10mM HEPES (Roth), 17.75mM CsCl (Sigma), 10mM TEA-Cl (Fluka), 0.25mM EGTA (Roth), 10mM Glucose (Merck), 2mM $MgCl_2 \cdot 6H_2O$ (Sigma), 4mM Na_2ATP (Sigma), 0.3mM NaGTP (Sigma). pH was adjusted to 7.0-7.3 using CsOH and osmolarity to 285-300mOsm with CsCl.

2.6.1. Light stimulation in hippocampal organotypic slice cultures

Light-mediated stimulation of pyramidal neurons in CA1 region of hippocampus was performed by using 473nm DPSS laser (IkeCool, USA) coupled to 200µm optic fibre. Recordings were made at least 8 days after viral injection, to allow sufficient ChR2-Venus expression. Axons from neurons in CA3 region were activated either in the vicinity of recorded cell (in CA1 region), in the Schaffer collaterals or in CA3 region itself. Moving the illumination spot closer to CA3 region made the postsynaptic response bigger, as more of the CA3 axons were recruited. For variance-

mean analysis, a train of 5 light pulses of 20Hz frequency and 1ms duration was stimulating the cell every 10s. 50-100 stable sweeps were recorded. For paired pulse recordings two pulses, 50ms apart, 1ms long were applied every 5s. 50 stable sweeps were recorded. Postsynaptic responses (EPSCs) of CA1 pyramidal neurons were recorded at -60mV. ACSF solution contained additionally 50µM picrotoxin (Ascent, UK), 5µM 4-aminopiridine (Aldrich, Germany), 1µM 2-chloroadenosine (BioLog, Germany), or 0,5mM kynurenic acid (Sigma, Germany) where indicated.

2.6.2. Pathway specific recordings form NAc shell

Pathway specific stimulation of medium spiny neurons in NAc shell was done by the illumination of axons expressing ChR2-Venus in the vicinity of a patched cell. Light pulses were generated by 473nm DPSS laser (IkeCool, USA) coupled to an optic fibre of 62.5µm (setup 1, rat slices) or 200µm diameter (setup 2, mouse slices). For variance mean analysis, a train of 5 light pulses of 20Hz frequency and 0.03-2.5ms duration was used to stimulate the axons every 10s. AMPAR EPSCs were recorded at -70mV (rat slices) and at -60mV (mouse slices) NMDAR EPSCs were recorded from mouse slices at +40mV. ACSF solution contained additionally 50µM picrotoxin, 100µM 4-aminopiridine, 5µM NBQX (Ascent, UK) or 20µM MK-801 maleate (Ascent, UK) where indicated.

2.6.3. Generation of action potentials by optical stimulation

The ability of the ChR2-Venus to generate action potentials was tested on pyramidal neurons in the somatosensory cortex. Once a channelrhodopsin-2-expressing cell was selected and patched in a voltage clamp mode, the configuration was switched to current clamp. Light flashes (1ms duration) were generated by the 473 DPSS laser (IkeCool, USA) and illuminated the cell at the following frequencies: 20Hz, 50Hz, 100Hz, 200Hz. The external ACSF solution contained additionally 50µM picrotoxin, 5µM NBQX and 50µM APV.

2.6.4. Electrical stimulation

Electrical stimulation of NAc slices was performed using a bipolar silver chloride electrode, put inside a borosilicate, 2-barrel glass capillary (World Precision Instruments) filled with the ACSF solution. A single electric stimulus of 0.2ms

duration was applied every 5 seconds. The intensity of the impulse was adjusted to obtain responses of amplitude between 50-300pA. For AMPA/NMDA ratio, 50 stable sweeps were recorded at -60mV and +40mV (AMPA and NMDA responses respectively). Amplitude of NMDA responses was measured 60ms after the peak response to ensure the absence of AMPAR component. For calculating AMPAR rectification index 30-60 stable sweeps were recorded at -60mV and +40mV (and 10-40 sweeps at 0mV). NMDA receptors responses were blocked by 50μM APV (Ascent, UK) and 100μM spermine (Roth) was present in the internal solution. For minimal stimulation protocol, the electric stimulus was adjusted to obtain both responses and failures. Every 20-30 sweeps the holding potential was changed between -60mV and +40mV to ensure stability of failures/responses number for both AMPA and NMDA currents. Percentage of silent synapses was calculated from the following equation: % silent synapses $= 1 - \frac{\ln(F_{-60mV})}{\ln(F_{+40mV})}$, where F_{-60mV} and F_{+40mV} are failure rates at -60 and +40mV respectively. For all experiments the ACSF solution contained additionally 50μM picrotoxin.

2.6.5. Data analysis

All results are shown as a mean ± standard error of the mean, calculated as:

$$\mathrm{SEM} = \frac{\sigma}{\sqrt{n}},$$

where σ is the standard deviation of the sample and n is the size of the sample. Student t-test and one-way ANOVA with Tukey post-tests was used for statistical analysis.

2.6.5.1. Variance-mean analysis

30-100 sweeps of stable AMPAR responses were analyzed. Peak amplitude of each sweep was subtracted for baseline (max 2ms section right before each peak) and averaged. Variance of each peak was calculated and plotted on a graph against mean amplitude of the response. Amplitudes of postsynaptic responses (I) and their variance (σ^2), show a parabolic relationship, if recorded at different release probability conditions (Clements and Silver, 2000). It can be described by two equations:

$$I = NPQ \quad (1)$$

$$\sigma^2 = NQ^2P(1-P) \quad (2).$$

Combination of equations 1 and 2 shows the parabolic relationship between mean amplitude and variance:

$$\sigma^2 = IQ(1/N)^2 \quad (3).$$

From this relationship, three quantal parameters can be determined: the amplitude of a response to a single quantum of neurotransmitter (Q), the number of functional release sites (N) and the probability of neurotransmitter release (P). A parabolic fit was added to 5 data points and from its equation (3) N and Q calculated. Release probability for each of 5 peaks can be calculated from equation 1. Cells were discarded when parabola didn't fit well to the data ($R^2<0.9$), was distorted or bent in opposite direction (e.g. when variance for $P \approx 0.5$ was lower than for $P \approx 0.1$). In few cases, when fifth peak showed too many failures and therefore had an unusually big variance compared to other peaks, parabolic fit was added to 4 remaining data points.

3. Cocaine-induced changes in quantal parameters of nucleus accumbens afferents

The excitatory synapses in the nucleus accumbens shell have been recently extensively studied, because of their importance in development of addiction-related behaviours (Kalivas and O'Brien, 2008). The nucleus accumbens receives massive glutamatergic input from different cortical and limbic structures, hijacked by drugs of abuse to transmit differential aspects of addiction-associated information. While most studies focused on postsynaptic adaptations, the presynaptic effect of repeated cocaine exposure remains unknown. In order to study cocaine-induced alterations of presynaptic properties of glutamatergic synapses it is essential to address the afferents separately, as various pathways might be modified by cocaine in different ways. The following sections describe a pathway-specific analysis of the presynaptic component of PFC- and amygdala-to-NAc synapses using variance-mean analysis. Dissection of separate pathways was enabled by an optogenetic approach.

3.1. Variance-mean analysis in a model system

In order to characterize synaptic adaptations in cocaine-induced plasticity, I used the variance-mean analysis, a powerful tool to measure both pre- and postsynaptic properties of synaptic transmission. The binomial model of this quantal analysis predicts a parabolic relationship between the mean amplitude of synaptic responses and its variance, if recorded at different release probability conditions (Clements and Silver, 2000). Changes in one or more quantal parameters estimated from this model reflect modifications of synaptic transmission. Typically, different release probabilities can be achieved by altering the extracellular calcium concentrations and steady-state recordings are carried out for each of those conditions separately. Scheuss and Neher (Scheuss and Neher, 2001) however, described a more straightforward

method, where the probability of release is transiently altered by short-term plasticity happening at a synapse during short trains of stimulations. The release probability during the train of action potentials is changed by two opposing mechanisms. Repetitive stimulations deplete synaptic vesicles on one hand but also lead to build up of calcium inside axon terminals to increase the calcium secretion coupling. This approach is more reliable, because different probability states are analysed simultaneously.

In this study, quantal analysis of synaptic properties was combined with optical stimulation, enabled by expression of channelrhodopsin-2 – a cation channel with light-gated conductance. Upon illumination with blue light, the channel opens (as a result of isomerisation of a chromophore all-*trans* retinal), which causes cation influx that, when expressed in neurons, leads to the generation of action potentials (Boyden et al., 2005; Nagel et al., 2005). The channelrhodopsin used in this study is fused with a yellow fluorescent protein – Venus (Figure 1), which allows identifying transduced neurons.

Figure 1: The map of AAV vector encoding channelrhodopsin 2-Venus fusion protein
A fragment of a plasmid map, showing elements of the AAV vector with ChR2-Venus fusion cDNA under the control of a CAG promoter. ITRs – inverted terminal repeats, CAG – CAG promoter, ChR2 – channelrhodopsin 2, WPRE - woodchuck hepatitis post-transcriptional regulatory element.

In our experimental setup, expressing the ChR2-Venus in neurons allows the triggering of stable trains of action potentials in response to illumination with blue light. Recordings in whole-cell current clamp mode showed that light pulses of 1ms duration were able to evoke reliably the desired number of action potentials at 20 and 50Hz frequencies (Figure 2).

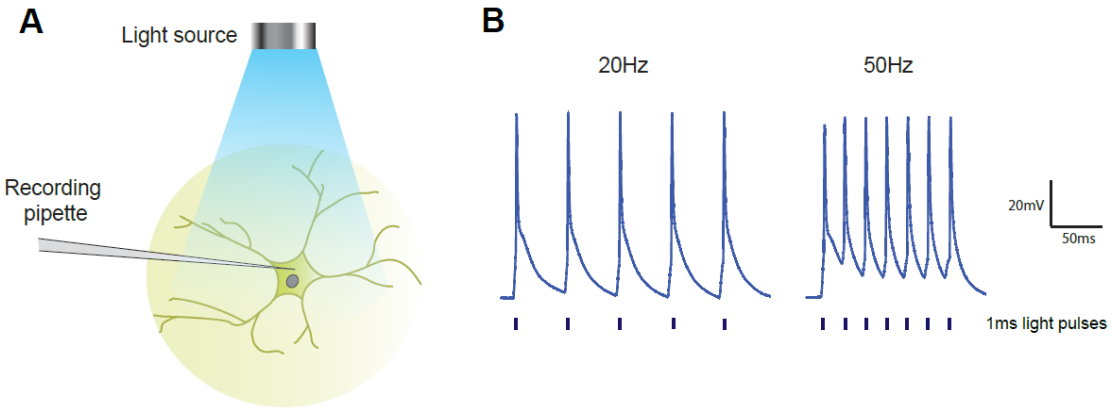

Figure 2: Blue-light illumination generates action potentials in ChR2-Venus expressing neurons
A A pyramidal neuron in somatosensory cortex, transduced with ChR2-Venus was stimulated with 1ms light pulses. B Example traces of action potentials generated by light stimulation at different frequencies. The stereotaxic viral injections into somatosensory cortex in mice were carried out by Dr Oliver Schlüter and Franziska Greifzu at Systems Neuroscience Group, Johann-Friedrich-Blumenbach-Institute of Zoology and Anthropology, Bernstein Focus for Neurotechnology, University of Göttingen.

Since variance-mean analysis has never been utilized in combination with optogenetics, it was therefore crucial to validate it in a defined model system. Results in Figure 2 confirm the applicability of 20Hz light stimulation for variance-mean analysis, showing that it would not introduce additional variance due to failures in AP generation. The accuracy of variance-mean analysis combined with light stimulation in estimating changes in synaptic quantal parameters still remained to be validated. For this purpose, I used rat hippocampal slice cultures and characterized their well-preserved CA3-CA1 glutamatergic connections, as well as PFC-to-NAc synapses in mouse acute slice preparations.

3.1.1. Characterization of quantal parameters of CA3-CA1 glutamatergic synapses in rat hippocampal slice cultures

The following experiments were performed in hippocampal organotypic slice preparations derived from P8 – P9 Wistar rats. The slices were transduced with ChR2-Venus-encoding AAV in the CA3 region in order to render the CA3-CA1 pathway light sensitive. The AMPA receptor-mediated post-synaptic currents were therefore evoked by light and recorded from CA1 pyramidal neurons in whole-cell voltage clamp (at -60 mV) mode. To ensure sufficient channelrhodopsin expression, recordings were made at least 8 days after viral transduction. In order to estimate

quantal parameters with variance-mean analysis, recordings were carried out at different release probability conditions, achieved by applying a train of 5 stimuli, 50 ms apart (Figure 3).

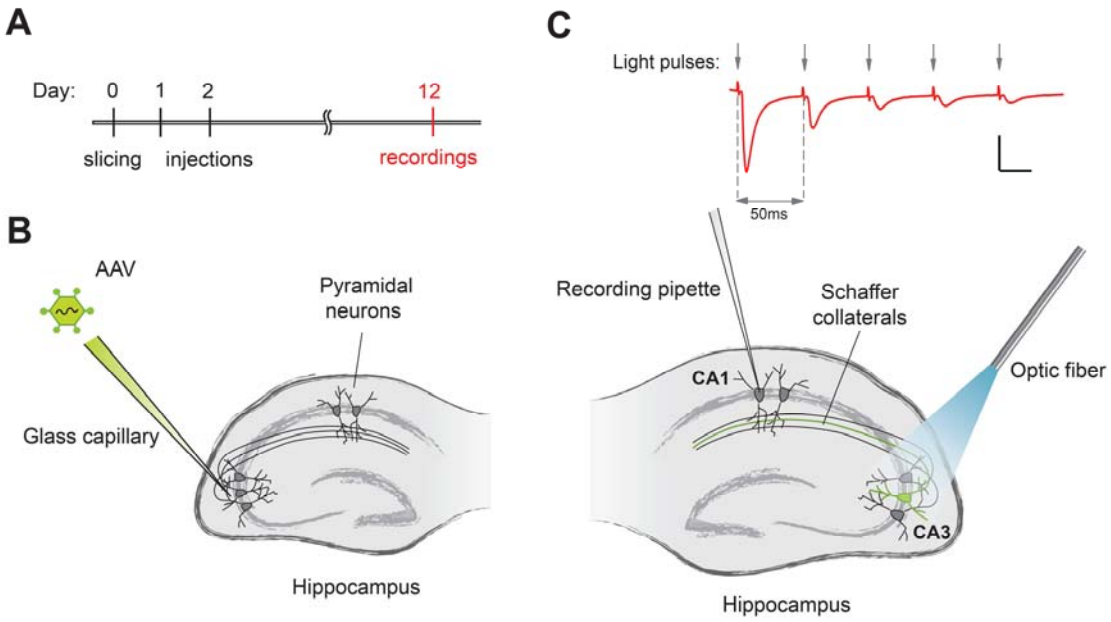

Figure 3: A strategy for optical stimulation in hippocampal organotypic slice cultures

A Time course of the experiment. **B** Injection of ChR2-Venus-encoding AAV into the CA3 region of the slice. **C** Electrophysiological analysis of CA1 pyramidal neurons. A train of 5 light flashes onto the CA3 region evoked postsynaptic responses in CA1 neuron. Scale bar for AMPAR EPSCs: 50pA and 25ms.

3.1.1.1. Variance-mean analysis of CA3-CA1 synapses in organotypic slice cultures.

In order to make sure that the combination of light stimulation and variance-mean analysis allows estimation of quantal parameters and detects their changes, I performed the quantal analysis under pharmacology induced variations of the release probability. A series of recordings was conducted in three different pharmacological conditions:

- control, where no drugs were added,
- low release probability, with addition of picrotoxin (PTX) and chloroadenosine (CA),
- high release probability, with picrotoxin, chloroadenosine and 4-aminopyridine (4-AP).

Picrotoxin is a non-competitive $GABA_A$ receptor antagonist, used to block inhibitory transmission and to study excitatory synaptic transmission in isolation. Chloroadenosine is an A1 adenosine receptor agonist, routinely used in electrophysiology to prevent epileptic activity (Ehrlich and Malinow, 2004; Hayashi, 2000). 4-AP, on the other hand, blocks preferentially the Kv1 family of voltage-dependent potassium channels and therefore prolongs the action potential duration. As a result, more calcium ions enter the synaptic terminal and cause more synaptic vesicles to fuse (Hjelmstad et al., 1997).

The recorded trains of 5 AMPAR EPSCs were used for variance-mean analysis and the quantal parameters were estimated from a parabolic fit (Figure 4). The experiment showed that the release probability of glutamatergic CA3-CA1 synapses was 58 ± 3% (n = 8) in the control conditions, which corresponds well with previous studies (Bolshakov and Siegelbaum, 1995). A combination of picrotoxin and chloroadenosine decreased it to 48 ± 1% ($p<0.01$, n = 22), whereas, adding 4-AP resulted in an increase to 68 ± 1% ($p<0.05$ vs. control and $p<0.001$ vs. PTX + CA, n = 21). The estimated number of release sites was quite variable, because each cell was stimulated by recruiting different number of ChR2-expressing axons. It decreased from 10 ± 3 (n = 8) to 7 ± 1 after adding PTX and CA ($p=0.16$, n = 22) and decreased further, to 5 ± 1 by adding 4-AP ($p<0.05$, n = 21). The apparent significant reduction of N after adding 4-AP was caused solely by lowering the strength of stimulation, which led to the recruitment of fewer synapses. Lowering the stimulation strength was necessary, because in hippocampal slice cultures, many CA3-CA3, as well as unphysiological CA1-CA1 connections, decreased the threshold for epileptic activity and rendered the slices susceptible to epileptic bursts after 4-AP addition. Surprisingly the quantum size also changed, following pharmacological manipulation. It decreased after adding PTX and CA from -32.06 ± 7.26 pA (n = 8) to -17.12 ± 1.33 pA ($p<0.01$, n = 22) and remained unchanged (compared to control) in the presence of 4-AP -28.49 ± 2.88 pA ($p=0.50$ vs. control and $p<0.01$ vs. PTX + CA, n = 21). This might suggest that CA reduces AMPAR transmission by a postsynaptic mechanism or that in control conditions and in the presence of 4-AP, the glutamate release is multivesicular (see section 3.1.1.3), which caused Q estimated by variance-mean analysis to increase.

Not all of the analysed cells, however, could be used for the above analysis. Out of 73 cells analysed, 22 did not fit the criteria (see methods for details). Some of the

difficulties were caused by a low signal to noise ratio or polysynaptic responses, which led to an unnaturally big variance especially in a high release probability condition.

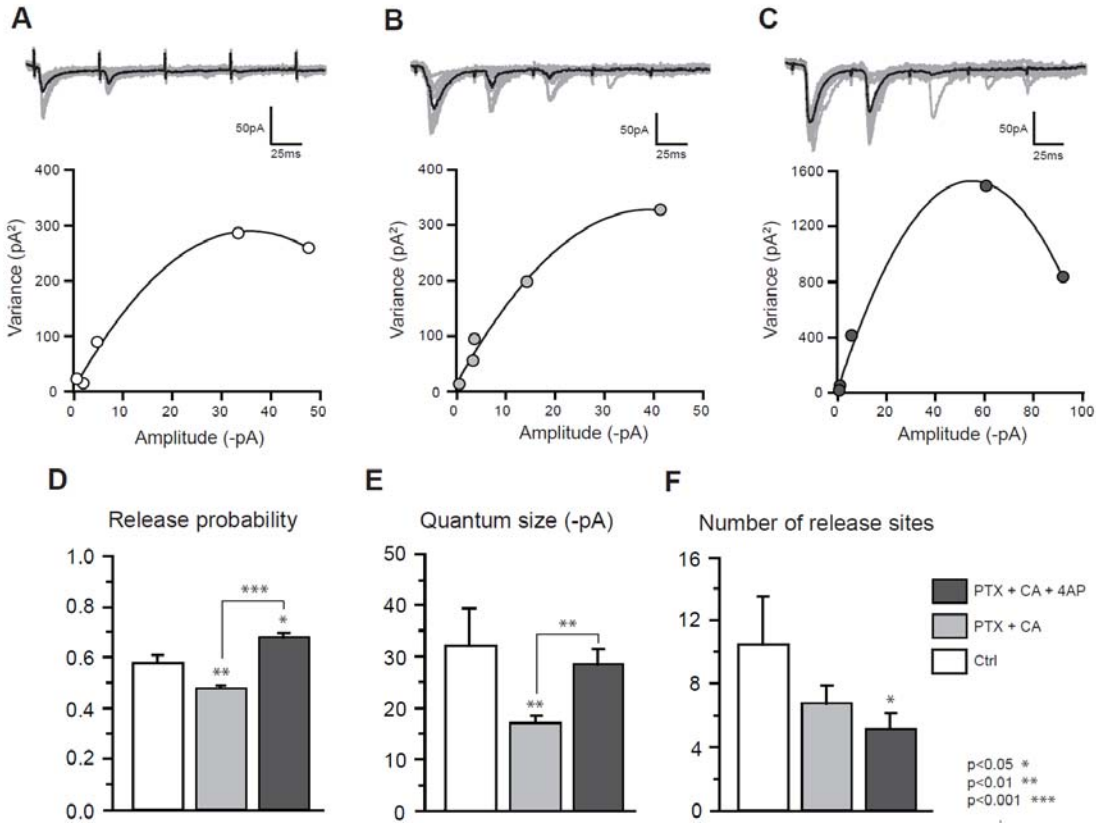

Figure 4: Variance-mean analysis of hippocampal CA3-CA1 synapses detects pharmacological modifications of release probability.

A, B, C Variance-mean curve and 15 consecutive example traces of AMPAR EPSCs recorded in the absence of drugs (A), 50µM picrotoxin and 1µM chloroadenosine (B), 50µM picrotoxin, 1µM chloroadenosine and 5µM 4-aminopyridine (C). Sample traces in grey, average trace in black. **D** Bar graph showing significant changes in release probability, after pharmacological manipulation with 50µM picrotoxin, 1µM chloroadenosine and 5µM 4-aminopyridine. **E** Bar graph showing significant changes in quantum size, after pharmacological manipulation with 50µM picrotoxin, 1µM chloroadenosine and 5µM 4-aminopyridine. **F** Bar graph showing estimated number of release sites.

This experiment proves that variance-mean analysis, combined with optical stimulation is able to detect changes in release probability. Estimation of other quantal parameters remained to be further validated, as unexpected changes in quantal size occurred at low release probability.

3.1.1.2. Estimation of quantum size of CA3-CA1 synapses

Quantum size can also be estimated from the amplitudes of AMPAR EPSCs (R. A. Silver et al., 1996). By plotting the histograms of amplitudes of AMPAR EPSCs, one can read out the size of response to a single vesicle from evenly distributed quantal peaks (Figure 5). I used the same AMPAR EPSCs amplitudes as in variance-mean analysis and plotted their histograms with a bin width of 2 pA. The first peak, with the average amplitude around 0pA represents failures. Quantum size is represented by the mean amplitude of the second peak. This reanalysis showed a similar range of quantum sizes compared to Q calculated from the variance-mean plots, in the presence of chloroadenosine. Here however, the Q values were similar in all conditions tested, suggesting that quantum size was not affected by pharmacological manipulation.

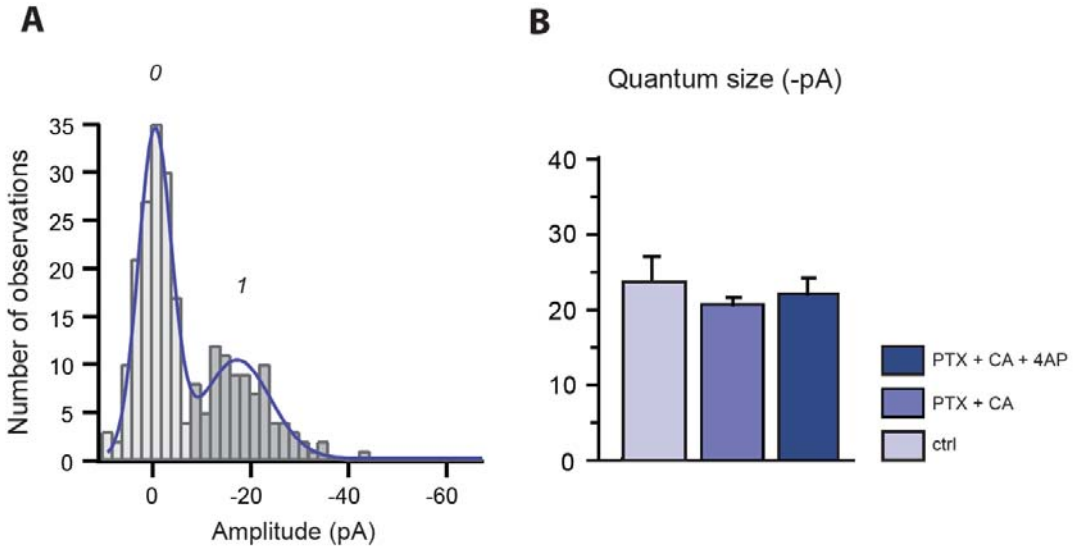

Figure 5: Quantum size of CA3-CA1 synapses, estimated from distributions of AMPA EPSCs amplitudes.

A Example AMPAR EPSC amplitude histogram showing quantal peaks, where peak 0 represents failures and peak 1 – responses to a single vesicle of neurotransmitter. EPSCs were obtained from a cell recorded in the presence of 50μM picrotoxin, 1μM chloroadenosine and 5μM 4-aminopyridine. The distributions were fitted with double Gaussian function (blue). **B** Bar graph showing the average quantum size and illustrating that pharmacological manipulation did not alter the Q value (estimated from Gaussian fits).

In the absence of drugs, a single quantum of neurotransmitter evoked a response of -23.9 ± 3.0 pA. It was similar for the combination of PTX and CA -20.4 ± 0.7 pA and PTX, CA and 4-AP -21.4 ± 2.9 pA. If indeed a single vesicle evokes ≈20pA

AMPAR responses, it would support the notion that under normal conditions and in the presence of 4-AP some multivesicular release may occur. The discrepancy between the quantum size of -20pA and, based on variance-mean method -30pA, suggests that the multiple vesicles are not released independently of each other or that multivesicular release saturates postsynaptic receptors.

3.1.1.3. Uniquantal vs. multiquantal release

The variance-mean analysis described above allows to estimate the quantal parameters if the quantal responses sum linearly, which means that each active zone releases only one vesicle or when more than one vesicle is released, but independently from each other (one released vesicle has no influence on the probability of releasing the others). This model however does not apply to synapses where multivesicular release leads to receptor saturation. In such cases the quantal responses do not sum linearly and the quantum size will change together with the release probability (Silver, 2003). It will also reduce the variance of the responses at the highest P causing the parabolic curve to bend, falsely over-estimating the release probability. It is therefore crucial to investigate whether a binomial model of variance-mean analysis applies. One way to do that, is to perform recordings at high and low release probability with the presence of a fast equilibrating AMPA receptor competitive antagonist - kynurenic acid (Diamond and Jahr, 1997). If multivesicular release (at high release probability) is indeed causing receptor saturation, the reduction of postsynaptic responses by kynurenate will be weak. On the contrary, when uniquantal release dominates, the blockage is independent of release probability. I compared the fractional block (the ratio of amplitude of a response in the presence and absence of the blocker) of AMPAR EPSCs caused by kynurenate, at control and elevated (4-AP) release probability and discovered no change between the two conditions: 0.28 ± 0.05 ($n = 19$) and 0.26 ± 0.06 ($n = 23$, $p = 0.79$, Figure 6). It therefore shows that in this model system, increased release probability causes no saturation. Together with the difference in quantum size estimations described earlier (Figure 4, 5) suggests that at some synapses, the release of one vesicle increased the likelihood of releasing another one, from the same release site. Nonetheless, the amount of glutamate released simultaneously from multiple vesicles was not enough to saturate the receptors.

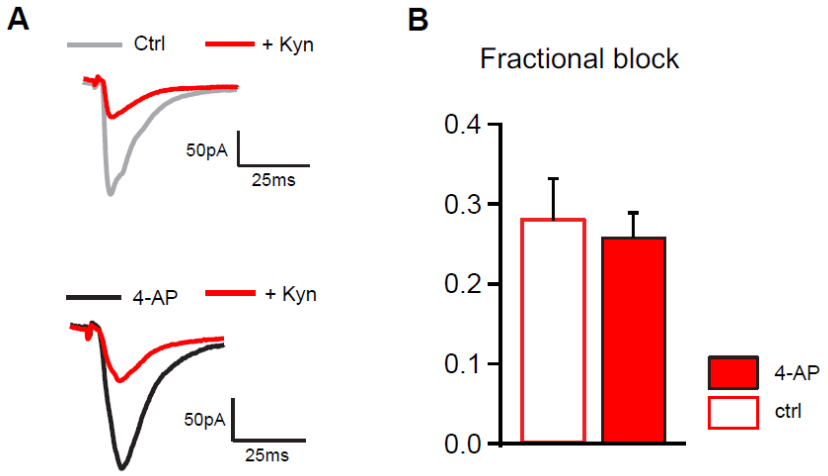

Figure 6: Increased glutamate release does not saturate AMPA receptors in rat hippocampal CA3-CA1 synapses.

A Average traces of AMPAR EPSCs showing a decrease of amplitude caused by 0.5mM kynurenic acid (red) compared to control condition (grey). This reduction remains similar in a high release probability condition in the presence of 5µM 4-aminopyridine (black). **B** Bar graph illustrating that the fractional block (amplitude of a response in the presence of Kyn divided by the amplitude of a response without the blocker) is independent of release probability.

The above experiments show that AAV-mediated expression of channelrhodopsin in CA3 region of hippocampal slices provides a reliable light-controlled stimulation method. Variance-mean analysis performed in this system, allows a straightforward estimate of quantal parameters and to monitor their changes during pharmacological manipulations. Interestingly, significant changes in quantum size calculated from variance-mean relationship and no change in Q observed from distributions of AMPAR EPSCs amplitudes, hint a possible multivesicular release, one where a binomial model of this assay does not apply. Nevertheless, this multiquantal release doesn't saturate AMPA receptors and therefore has no influence on estimation of the release probability and synapse number.

3.1.2. Estimating the quantal parameters of glutamatergic synapses in PFC to NAc pathway

In the previous set of experiments, the variance-mean analysis was tested in ChR2-transduced hippocampal slice cultures, where two out of three quantal parameters (P and N) were accurately determined. Moreover, these results gave important insights on the limitations of this approach, which was the case of an estimate of a quantum size. It therefore became important to check the accuracy of the variance-mean method in synapses in the nucleus accumbens shell. The analysis of synapses in the NAc requires preparation of acute slices, where connections from afferent structures are cut during slicing. The light stimulation can be therefore focused exclusively on axon terminals. Unlike in hippocampus, where owing to the preservation of the entire connection, the light stimulation could be focused on CA3 neuron cell bodies as well as axons.

A similar pharmacological approach was used to validate the use of binomial model of variance-mean analysis in PFC-to-NAc synapses.

The following experiments were performed in acute slices prepared from P20-P30 mice. The animals were injected with ChR2-Venus-encoding AAV into their prefrontal cortices of both hemispheres, around postnatal day 1. Three to four weeks later, the level of ChR2-Venus expression in axons projecting from the PFC to the NAc was sufficient for a successful light stimulation. This approach allows isolating PFC-to-NAc pathway among other afferents, which might differ in quantal parameters. Recordings were performed in medium spiny neurons of the nucleus accumbens shell. Similar to the experiments in hippocampal slice cultures, AMPAR EPSCs were recorded in whole-cell voltage clamp mode at -60mV. Additionally NMDA receptor-mediated EPSCs were measured at +40mV, in the presence of the AMPA receptors blocker, NBQX.

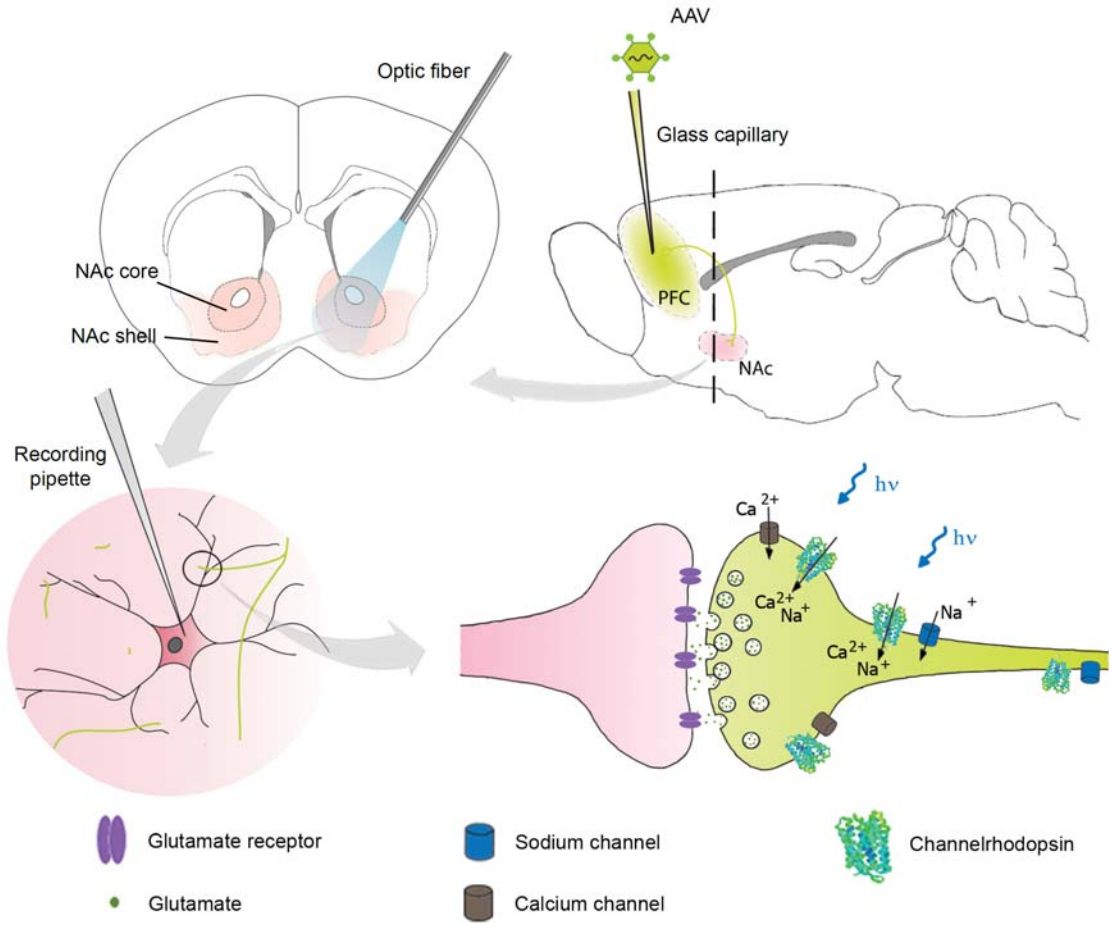

Figure 7: Optogenetic targeting of PFC-to-NAc pathway

Glutamatergic pyramidal neurons of PFC (green-yellow) that project to the nucleus accumbens (pink) are transduced by ChR2-Venus-encoding AAV, injected into PFC of P0 mouse pups. After several days allowing sufficient ChR2 expression, coronal slices of the NAc are prepared (dashed line). Illumination with blue light activates ChR2-expressing axon terminals and leads to glutamate release. Postsynaptic responses of medium spiny neurons located in the NAc shell can be recorded with a patch pipette.

3.1.2.1. Variance-mean analysis of PFC-to-NAc synapses

Pharmacological modification of release probability with 4-aminopyridine was used once more, to evaluate the accuracy of variance-mean analysis in PFC – nucleus accumbens pathway. Isolation of this pathway from among others projecting to NAc was ensured by using optogenetics, as mentioned before. The AMPAR EPSCs evoked by light were analysed as previously. This experiment had one major advantage over previous characterization of variance-mean analysis in hippocampal organotypic slice cultures, because it enabled subsequent recordings of cells in control condition

followed by a wash-in of 4-AP. It therefore allowed a direct comparison of control and increased release probability in one cell. Moreover, medium spiny neurons are inhibitory, GABAergic neurons, therefore epileptic activity was not observed.

The wash-in of 4-AP slightly increased the mean amplitude of AMPAR EPSCs simultaneously decreasing the variance (Figure 8A, B). An increase in asynchronous release was observed as well, as more events were detected shortly after each stimulus. The release probability of PFC-to-NAc glutamatergic synapses in the presence of picrotoxin (the control condition) was 50 ± 5% (n = 6) and increased significantly by adding 4-AP to the extracellular solution - 75 ± 4% (paired t-test, $p<0.01$, n = 6, Figure 8). Other quantal parameters remained unchanged after pharmacological manipulation. The unchanged number of release sites represented a stable stimulation over the same number of synapses in both conditions tested. In the control condition N was estimated to 22 ± 4 (n = 6) and in the presence of 4-AP – 21 ± 6 (n = 6). In parallel to that, the quantum size was estimated to -9.6 ± 2.3 pA (n = 6) and -9.4 ± 2.3 pA (n = 6). Stable quantum size in both conditions, estimated to ≈10pA suggests uniquantal release and no increase of multiquantal events following an increase of P. In this experiment 3 animals were used and 8 stable recordings analysed. Two cells were discarded according to the criteria mentioned before.

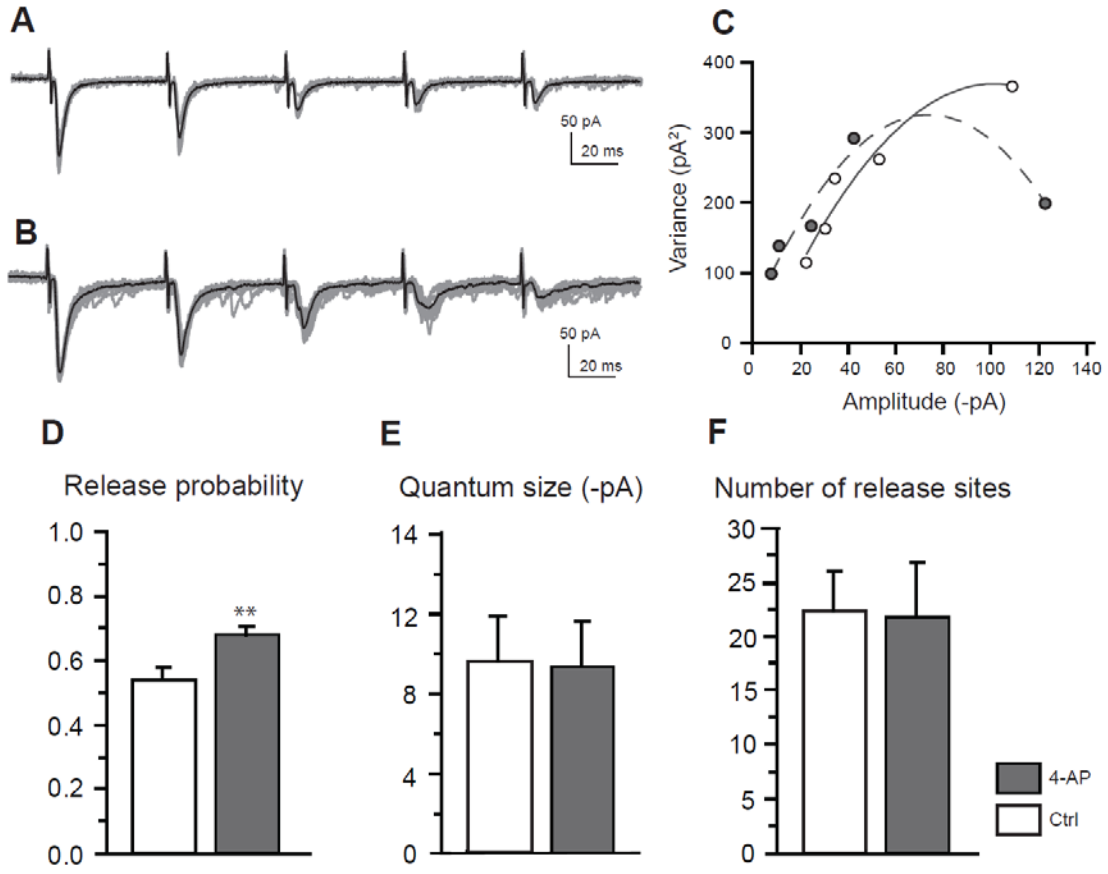

Figure 8: Estimation of quantal parameters by variance-mean analysis in mouse PFC-to-NAc synapses.

A Example traces of a train of AMPAR EPSCs recorded from a control cell; average trace in black. **B** Example traces of a train of AMPAR EPSCs recorded from the same cell in the presence of 10µM 4-aminopyridine; average trace in black. **C** Variance-mean plots for control cell (white) and in the presence of 4-AP (grey). **D** Bar graph showing a significant increase in release probability after bath application of 10µM 4-AP. **E**, **F** Bar graphs showing that other quantal parameters (quantum size and number of release sites accordingly) remained unchanged in the presence of 10µM 4-AP.

3.1.2.2. Estimating the release probability with a paired-pulse ratio analysis

To further confirm the change of release probability in PFC-to-NAc synapses after application of 4-AP, I used the paired-pulse ratio (PPR) analysis - the amplitude of the second post-synaptic response divided by the amplitude of the first, when two stimuli are elicited shortly after each other. The PPR is inversely related to the probability of neurotransmitter release (Dobrunz and Stevens, 1997; Manabe et al., 1993). The first stimulus will cause some vesicles to fuse, leaving many vesicles that failed to be released, docked to pre-synaptic membrane. At the same time, the residual calcium,

which has not been cleared after the previous action potential, will greatly increase the chance of fusion of the remaining vesicles, as the second stimulus follows shortly after the first one. Depending on the relative contribution of the size of the readily-releasable pool (number of vesicles primed at release sites) and intrinsic release probability, the synapse will be facilitating or depressing. For instance, if the release probability is high, the first stimulus will cause many vesicles to be released from the stimulated population of synapses, depleting their readily-releasable pools. In such situation, even though the calcium concentration is still elevated at the time of the second action potential, there are fewer vesicles left to be released. The amplitude of the first postsynaptic response will therefore be higher than the second (low PPR).

In my recordings, using a train of stimulating light pulses every 50ms, allowed me to calculate the paired-pulse ratio between the amplitude of the second and first post-synaptic response in the same set of cells analysed for quantal parameters. I observed a significant decrease in PPR after treatment with 4-AP, from 0.44 ± 0.06 to 0.32 ± 0.05 (paired t-test p=0.03, n=8), suggesting an increase of the release probability (Figure 9), consistent with the results of the variance-mean analysis above.

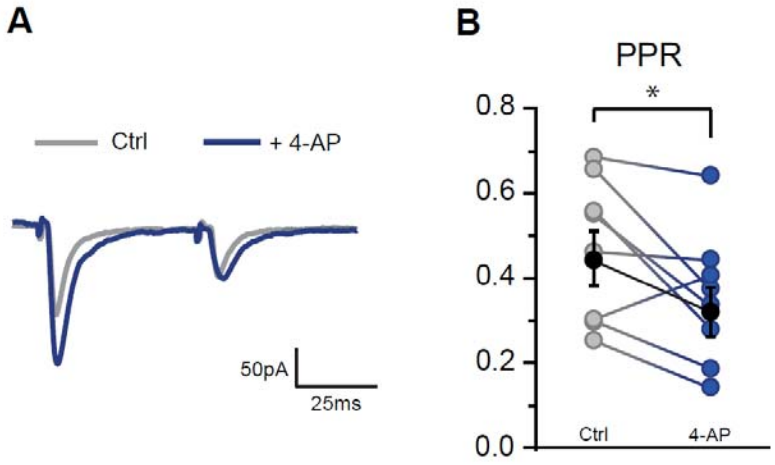

Figure 9: Paired-pulse ratio analysis shows an increase of release probability in PFC-to-NAc synapses caused by 4-AP.

A Average traces showing paired AMPAR EPSCs (50ms apart) in control condition (grey) and in the presence of 10µM 4-aminopyridine (blue). **B** A decrease in paired pulse ratio in the presence of 10µM 4-AP. Average paired-pulse ratios shown in black.

3.1.2.3. Analysis of the change in release probability using MK801

The previous results allow estimation of the release probability based on AMPAR-mediated postsynaptic responses. It was shown however, that PPR can be affected by AMPAR desensitization (Heine et al., 2008). To confirm the effect of 4-AP on the release probability I used the MK801 – an irreversible NMDA receptor open-channel blocker, for AMPAR-independent assessment of release probability (Hessler et al., 1993; Rosenmund et al., 1993). When recording post-synaptic responses mediated by NMDA receptors (whole-cell recordings from cells voltage clamped at +40mV, in the presence of NBQX to block the AMPA receptor-mediated transmission), MK801 binds to NMDA receptors in their open-channel state and renders them irresponsive to further stimuli. As a result, decay in the amplitude of postsynaptic response is observed. If the release probability of stimulated synapses is high, more release causes a higher number of NMDA receptors to open, hence the blocker inactivates them faster.

As illustrated in Figure 10, the decay of the post-synaptic amplitude response caused by MK801 was faster in the presence of 4-AP, which confirms the ability of 4-AP to increase the probability of glutamate release. A trend towards a decreased decay constant calculated from double exponential fit (fast component) was observed: from $\tau = 2.3 \pm 0.4$ (n=8) to $\tau = 1.5 \pm 0.2$ (n = 11, p = 0.06).

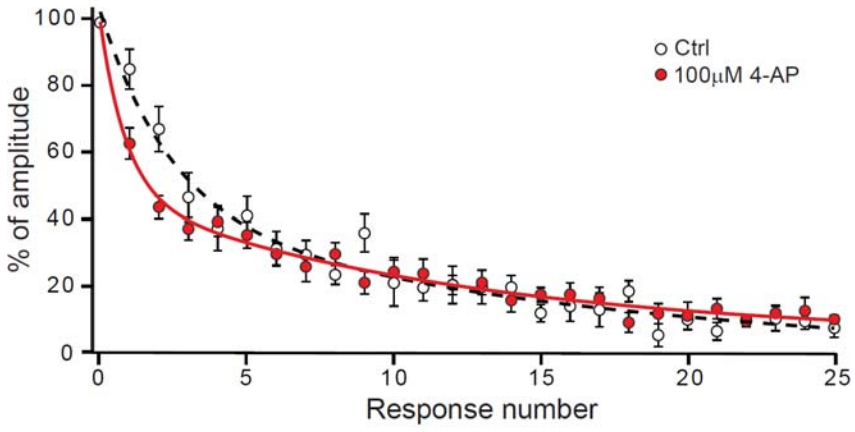

Figure 10: 4-AP-mediated increase of the release probability shown by the faster decay of NMDAR responses in the presence of MK801.

A decay of the amplitude of NMDAR EPSCs in the presence of 20μM MK801 is faster with bath applied 100μM 4-aminopyridine (red) compared to control (white). The amplitudes were normalized to the size of the first NMDA response in the presence of MK801. Data points were fitted with double exponential function.

Taken together, the above results confirm that a combination of optogenetics with variance-mean analysis enables precise estimates of all three quantal parameters in PFC-to-NAc pathway.

3.2. Pathway-specific analysis of cocaine-induced plasticity in the rat NAc shell

In this study, I investigated the properties of synapses in the NAc shell after exposure to cocaine in a pathway-specific manner. Acute slice preparations of the NAc do not preserve its entire long-range connections from afferent structures, because axons projecting from PFC, amygdala and other structures are cut during slicing. With traditional, electrical stimulation one is unable to specifically target a single pathway, because they are not sufficiently separated from each other. In such cases, an optogenetic approach is useful, because through gene delivery a single structure can be targeted and its connections with NAc, although cut, will be light-responsive. Owing to the activation of fibers of a single identity, simultaneous activation of other systems (e.g. modulatory) is excluded. In the following experiments, neurons in PFC and amygdala were separately transduced with channelrhodopsin-2, which enabled light stimulation of only one pathway at a time (Figure 11).

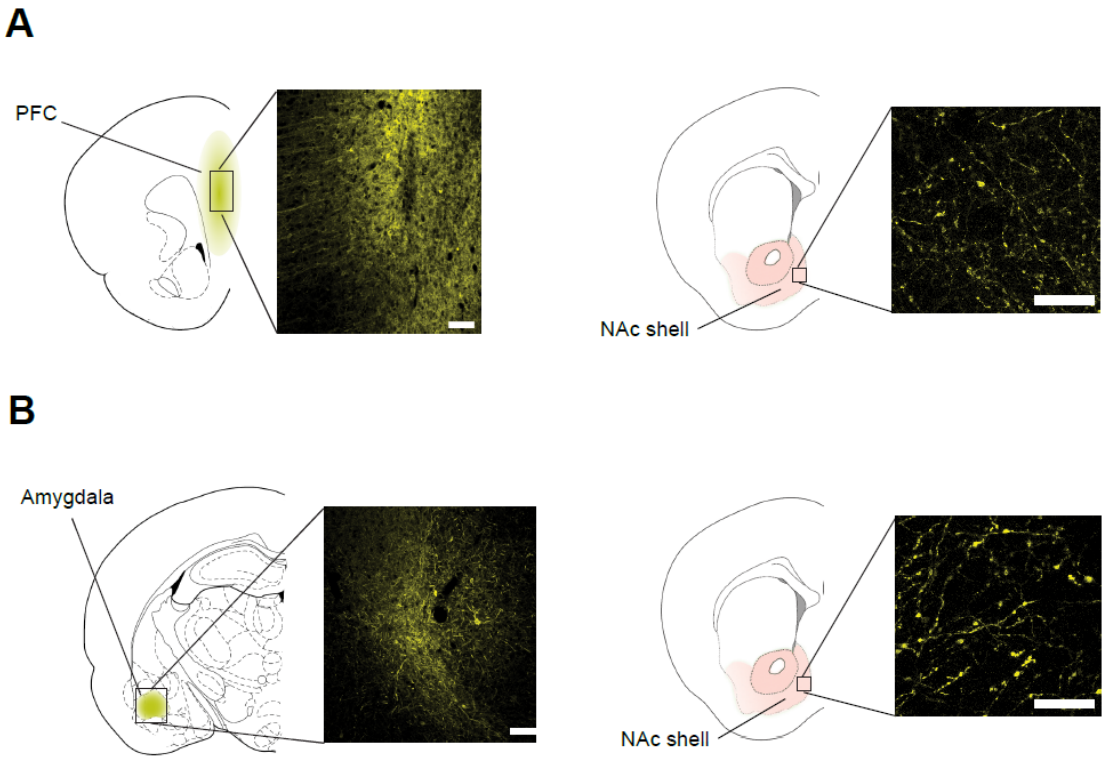

Figure 11: Optogenetic isolation of single afferents in rat NAc shell.

A Example confocal images showing ChR2-Venus expression in the injection spot (PFC) and in projection area, NAc shell. **B** Example confocal images showing ChR2-Venus expression in the injection spot (amygdala) and in the NAc shell. Sample preparation and imaging was carried out by Brian Lee (Department of VCAPP, Washington State University, Pullman, WA, USA), scale bar 100μm.

I performed variance-mean analysis to estimate quantal parameters of NAc shell, MSN synapses and monitor their changes after repeated cocaine exposure. Two different cocaine administration paradigms were used – passive intra-peritoneal injections and self-administration. During passive injections, animals received 15mg/kg of cocaine (or saline in control group) for 5 consecutive days, while during 2h of self-administration sessions, each animal received as many infusions of cocaine as desired. The dose of cocaine self-administered during the 2h session was similar to the amount of drug delivered in a single i.p. injection (15mg/kg) as illustrated on Figure 12.

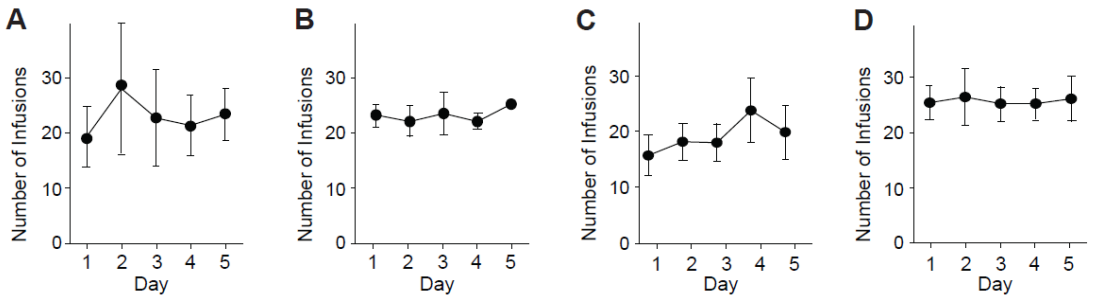

Figure 12: Performance of cocaine self-administration in rats.

Graphs showing the number of cocaine infusions received by rats during 2h self-administration sessions, on 5 consecutive days. Each infusion delivered 0.75 mg/kg of cocaine in 0.10 ml solution volume. **A**, **B** Rats with ChR2-Venus expressed in PFC analyzed for short-term (n=3) and long-term (n=4) cocaine withdrawal respectively. **C**, **D** Animals with ChR2-Venus expressed in amygdala analyzed for short-term (n=7) and long-term (n=5) cocaine withdrawal respectively.

The animal's response to both cocaine procedures was identical (increased locomotor activity). However, the self-administration paradigm is nowadays routinely used for studies of addiction mechanisms, because compared to passive i.p. injections cocaine administered intravenously has a stronger effect on brain structures implicated in drug dependence, like PFC and nucleus accumbens (Porrino, 1993). Furthermore, it is also very important that in this procedure, laboratory animal self-administers the drug voluntarily.

3.2.1. Prefrontal cortex pathway – cocaine-induced changes in quantal parameters

Previous experiments showed that our approach of combining variance-mean analysis with optogenetics is able to detect changes in quantal parameters of glutamatergic synapses both in hippocampus and nucleus accumbens shell. In the following experiments, I used this method to investigate changes in the quantal parameters subsequent to cocaine exposure. The AMPAR EPSCs of MSN voltage-clamped at -70mV were evoked and analysed as previously.

The variance-mean analysis revealed that the glutamatergic synapses in rat PFC-to-NAc shell pathway have 48 ± 3% chance of neurotransmitter release in control conditions (number of animals – n = 4, number of cells – m = 12, Figure 13). Exposure to cocaine, both passively injected and self-administered increased this probability to 65 ± 3% (p = 0.007, n/m = 3/14) and 62 ± 3% accordingly (p = 0.02, n/m = 3/14). Those changes became even more prominent when cocaine paradigms (especially self-administration) were followed by a long-term withdrawal time (45-50 days). The probability of neurotransmitter release for the saline-treated animals remained unchanged during long-term withdrawal – 53 ± 3% (n/m = 3/15), which validates the stability of the assay. The release probability increased to 64 ± 2% for animals which received cocaine passively (p = 0.01, n/m = 4/19) and 73 ± 1% for animals that self-administered cocaine (p = 0.001 vs. saline and p = 0.006 vs. cocaine i.p., n/m = 4/19).

Other quantal parameters were not affected by cocaine. Quantal size of the studied synapses in saline-treated rats was estimated to -17.1 ± 4.2 pA (n/m = 4/12). After cocaine treatments i.p. and SA it was slightly (but not significantly) elevated to -24.4 ± 9.6 pA (p = 0.4, n/m = 3/14) and -31.2 ± 9.7 pA accordingly (p = 0.2, n/m = 3/14). In long term withdrawal studies the quantal size remained stable in all examined conditions. In control, saline-treated group it was -15.8 ± 2.3 pA (n/m = 3/15), in i.p. cocaine-treated group -13.6 ± 3.0 pA (p = 0.3, n/m = 4/19) and in cocaine self-administration group -13.2 ± 2.8 pA (p = 0.6, n/m = 4/19).

Influence of cocaine treatment on the number of release sites cannot be determined in this approach, due to sampling over different set of synapses for each cell. The number of release sites was nonetheless calculated: for saline-treated rats: 20 ± 6 (n/m = 4/12), cocaine i.p: 11 ± 4 (p = 0.3, n/m = 3/14), cocaine SA: 15 ± 5 (p = 0.6, n/m = 3/14). In long term withdrawal, saline: 23 ± 4 (n/m = 3/15), in i.p. cocaine: 26 ± 8 (n/m = 4/19) and cocaine self-administration: 23 ± 10 (n/m = 4/19). 17 out of 110 recorded neurons did not fulfil the criteria for variance-mean analysis.

It appears that repeated cocaine experience increases the activity of prefrontal cortex – nucleus accumbens synapses, by increasing the probability of glutamate release. This enhanced activity is long-lasting and becomes more prominent in case of drug self-administration, which might correspond to addiction-related plasticity changes.

3. 2BCocaine-induced changes in quantal parameters of nucleus accumbens afferents

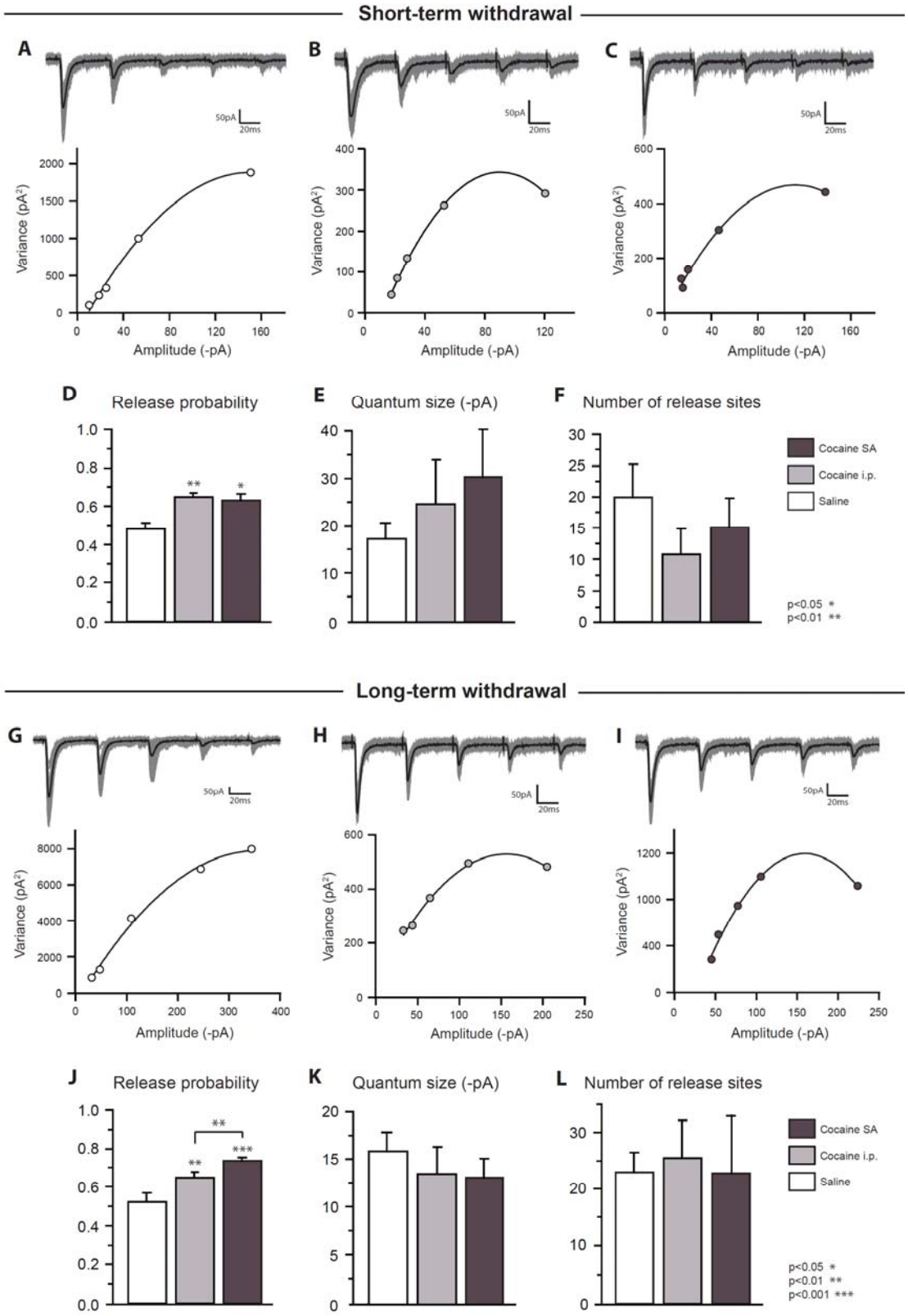

3.2.2. Amygdala pathway – cocaine-induced changes in quantal parameters

I next examined the glutamatergic synapses between amygdala pyramidal neurons and medium spiny neurons in the nucleus accumbens shell and discovered that the amygdala pathway has a higher chance of neurotransmitter release than the PFC pathway (Figure 14). Based on variance-mean analysis, saline treated rats showed in amygdala-to-NAc pathway the release probability of 65 ± 1% which is significantly higher than those of the PFC pathway ($p = 0.002$, n/m = 4/10). Cocaine treatment (both i.p. and SA) had no effect on this parameter, even when the treatment was followed by a long-term withdrawal. Cocaine i.p: 65 ± 4% (n/m = 4/12) and 66 ± 3% in long-term withdrawal (n/m = 4/14), cocaine SA: 68 ± 2% (n/m = 7/18) and 70 ± 4 in long-term withdrawal (n/m = 5/14).

Figure 13 (*facing page*): Cocaine experience increases the probability of glutamate release in PFC-to-NAc synapses.

A – F Results obtained 1 day after cocaine treatment from rat NAc medium spiny neurons. **A – C** Example traces of trains of AMPAR EPSCs (grey) and an average response (black). Below – a variance-mean plot from a cell of: **A** control – saline treated rat, **B** cocaine treated rat – i.p. injections, **C** cocaine treated rat – self administration. **D – F** Quantal parameters determined by variance-mean analysis. **D** Bar graph showing an increase in the probability of glutamate release after cocaine treatment – both passive i.p. injections and self-administration. **E** Bar graph showing cocaine effect on quantum size. **F** Bar graph showing the estimated number of release sites. **G – L** Results obtained 45 days after cocaine treatment from rat NAc medium spiny neurons. **G – I** Example traces of trains of AMPAR EPSCs (grey) and an average response (black). Below – a variance-mean plot from a cell of: **G** control – saline treated rat, **H** cocaine treated rat – i.p. injections, **I** cocaine treated rat – self administration. **J – L** Quantal parameters determined by variance-mean analysis. **J** Bar graph showing an increase in the probability of glutamate release after 45 days withdrawal from cocaine passive i.p. injections and self-administration. **K, L** Bar graphs showing that 45 days of withdrawal after cocaine treatment had no effect neither on quantum size nor on the number of release sites accordingly.

3. 2BCocaine-induced changes in quantal parameters of nucleus accumbens afferents

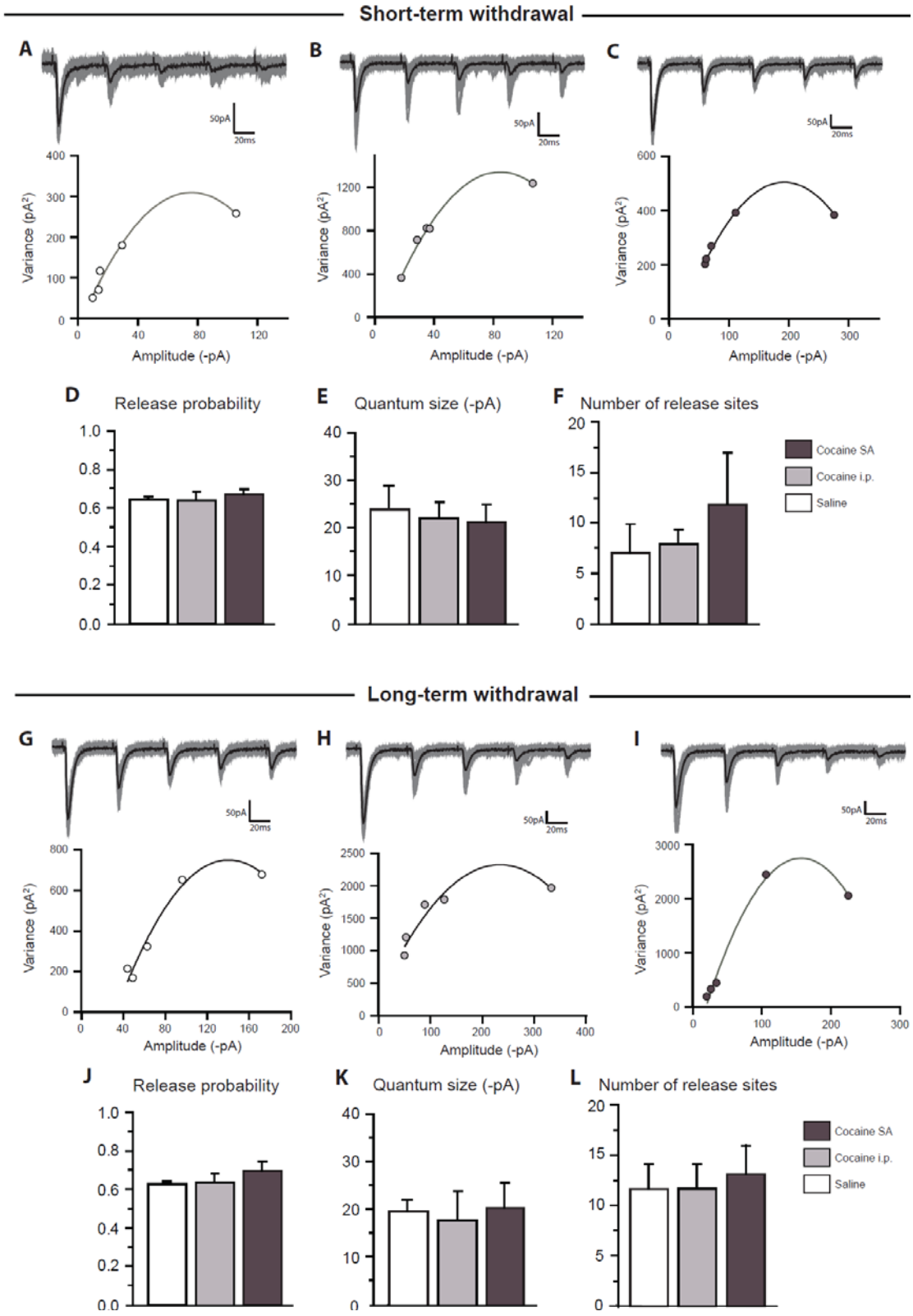

Like in PFC-to-NAc pathway, cocaine had no effect on other quantal parameters in amygdala-to-NAc synapses. Quantal size remained stable in all examined conditions, both in short and long-term withdrawal: saline: -24.7 ± 5.1 pA (n/m = 4/10) and -19.7 ± 2.4 pA (n/m = 2/13) respectively, cocaine i.p: -21.9 ± 3.7 pA (n/m = 4/12) and -17.7 ± 6.0 pA (n/m = 4/14) respectively, finally cocaine SA: -21.1 ± 3.8 pA (n/m = 7/18) and -20.0 ± 5.8 pA (n/m = 5/14) respectively. The changes in the number of release sites could not be detected by this analysis: saline 7 ± 3 (n/m = 4/10) and 12 ± 2 for short and long-term withdrawal respectively (n/m = 2/13), cocaine i.p: 8 ± 1 (n/m = 4/12) and 12 ± 2 for short and long-term withdrawal respectively (n/m = 4/14), cocaine SA: 12 ± 5 (n/m = 7/18) and 13 ± 3 for short and long-term withdrawal respectively (n/m = 5/14). Fifteen out of 93 analysed cells did not fit the criteria for variance-mean analysis.

Taken together, a pathway-specific analysis of quantal parameters of glutamatergic synapses on NAc shell medium spiny neurons revealed a cocaine-induced selective up-regulation of the PFC pathway but not the amygdala-to-NAc synapses, which compared to the PFC pathway, had a higher initial release probability. This specific up-regulation was long-lasting and further enhanced by withdrawal from cocaine self-administration. No changes in other quantal parameters were observed.

Figure 14 (*facing page*): Cocaine treatment had no effect on quantal parameters of synapses from amygdala-to-NAc pathway.

A – F Results obtained 1 day after cocaine treatment from rat NAc medium spiny neurons. **A – C** Example traces of trains of AMPAR EPSCs (grey) and an average response (black). Below – a variance-mean plot from a cell of: **A** control – saline treated rat, **B** cocaine treated rat – i.p. injections, **C** cocaine treated rat –self administration. **D – F** Quantal parameters determined by variance-mean analysis. **D** Bar graph showing that the probability of glutamate release remained unchanged all conditions tested. **E** Bar graph showing that cocaine had no effect on quantum size. **F** Bar graph showing estimated number of release sites.**G – L** Results obtained 45 days after cocaine treatment from rat NAc medium spiny neurons. **G – I** Example traces of trains of AMPAR EPSCs (grey) and an average response (black). Below – a variance-mean plot from a cell of: **G** control – saline treated rat, **H** cocaine treated rat – i.p. injections, **I** cocaine treated rat – self administration. **J – L** Quantal parameters determined by variance-mean analysis. **J** Bar graph showing no change in the probability of glutamate release **K, L** Bar graphs showing no change neither in quantum size nor in the number of release sites accordingly.

3.2.3. Cocaine-induced increases in release probability do not cause AMPA receptors saturation

As stated in section 3.1.1.3, due to a high release probability, an increased neurotransmitter release may cause receptor saturation. In such case, a binomial model of variance-mean analysis is invalid, because the quantal responses do not sum linearly. In order to make sure that no saturation (due to possible multivesicular release) occurs, I performed recordings of trains of AMPAR EPSCs in the presence of kynurenate, from cells of cocaine-treated rats. I calculated the fractional block caused by kynurenic acid for three highest release probability conditions (represented by first 3 peaks in recorded trains of postsynaptic AMPAR responses). In contrast to the variance-mean analysis, in this approach, the last two peaks carried very little information. Their mean amplitudes, due to many failures were very small. Further decrease of amplitude by the kynurenate was therefore not representative, because it resulted in a poor signal to noise ratio.

If the inhibition caused by the antagonist was weaker for the first peak (highest release probability) than on the remaining ones, it would be the indication of receptor saturation. As shown on Figure 15 no changes in fractional block were observed in any of examined conditions, which demonstrates that even in the case of a cocaine-induced higher glutamate release in PFC-to-NAc pathway, no saturation is indicated.

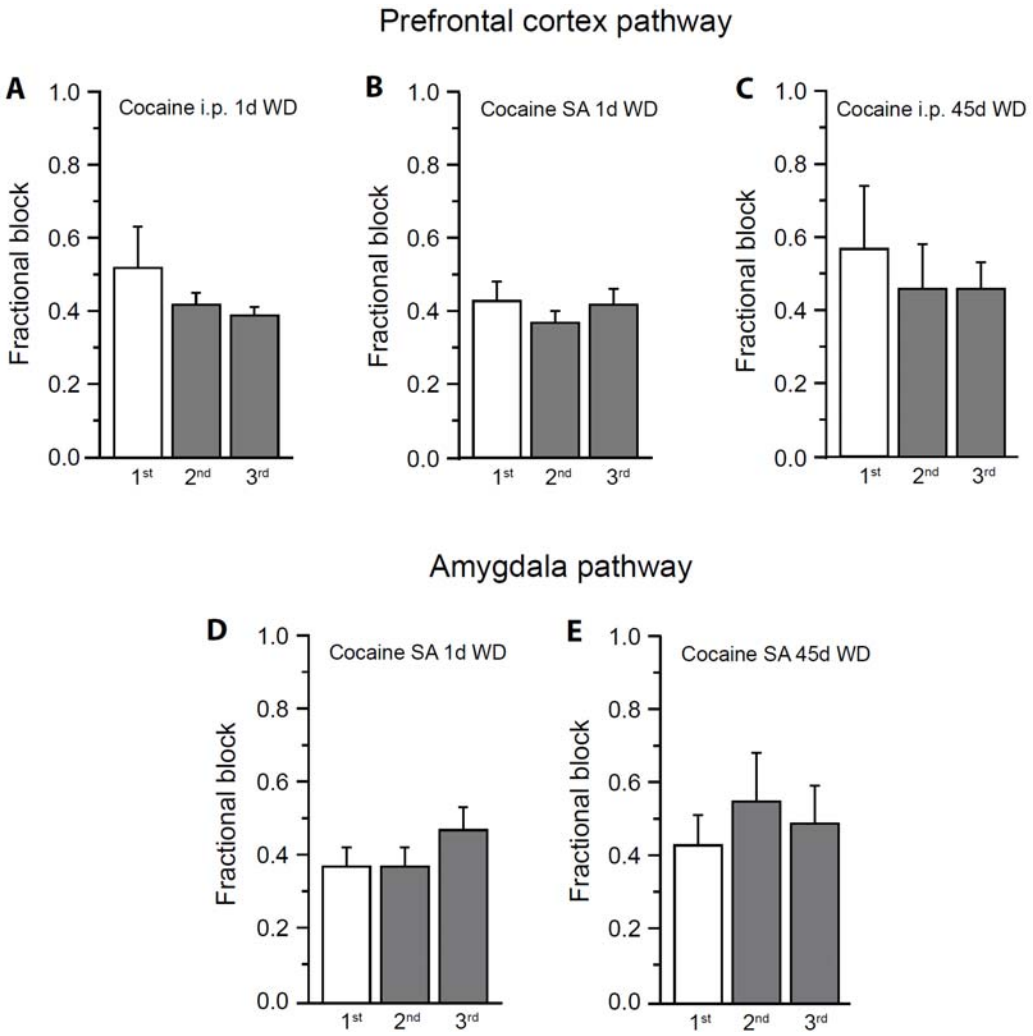

Figure 15: Increased release after cocaine treatment does not saturate AMPA receptors in MSN of rat NAc.

A-C Bar graphs showing no change in fractional block between 3 highest release probability conditions, represented by first 3 peaks from the train of AMPAR EPSCs in cells from rats treated with i.p. cocaine injections, cocaine self-administration and i.p. cocaine injections followed by long-term withdrawal respectively. **D-E** Bar graphs showing no change in fractional block between 3 different release probability conditions in cells from rats self-administrating the cocaine in short and long term withdrawal respectively.

3.2.4. Estimation of quantal size from mEPSCs

Variance-mean analysis revealed that cocaine had no effect on quantal size in both analysed pathways; however the results for PFC pathway were quite variable, ranging from -13 to -30pA. As shown in section 3.1.1.2, the quantal size can be estimated from the amplitudes of EPSCs. I performed the reanalysis of recorded cells by plotting the histograms of AMPAR EPSCs amplitude. Unfortunately, unlike in the

hippocampus the distribution did not show single peaks from which the Q value could be estimated, likely because of the bigger EPSC sizes.

Miniature EPSCs are thought to be responses to single vesicles, spontaneously released at the synapse. From measuring their amplitude it is also possible to estimate quantal size.

In the recordings performed from cocaine-treated rats, alongside with the train of 5 AMPAR EPSCs peaks, evoked by light stimulation, many miniature events could be found as well. Analysis of those mEPSCs however, loses the pathway specificity, as it was impossible to know, from which axons the vesicles were released. I averaged the amplitudes of the first 50 mEPSCs derived from the recorded sweeps and discovered no change in the quantum size in neither of cocaine paradigms. The Q was estimated as follows: for short term withdrawal, saline: -21.23 ± 2.65pA (n/m = 6/10), cocaine i.p: -20.85 ± 0.77pA (n/m = 6/10), cocaine SA: -20.83 ± 1.78pA (n/m = 6/10), for long term withdrawal, saline: -21.76 ± 1.35pA (n/m = 5/10), cocaine i.p: -21.81 ± 1.35pA (n/m = 6/10) and cocaine SA: -21.80 ± 1.37pA (n/m = 6/10).

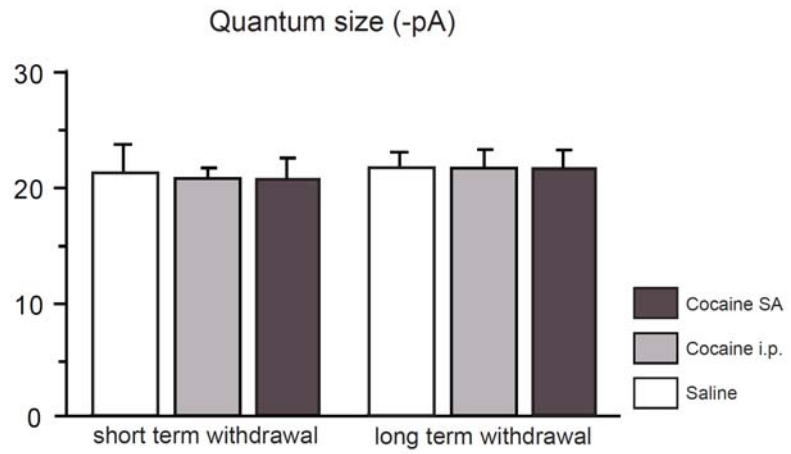

Figure 16: Quantum size estimated from AMPAR mEPSCs in rat NAc shell MSNs.
Bar graph showing no change in quantum size based on the amplitudes of mEPSCs both in short-term (left) and long-term withdrawal from cocaine.

These results are consistent with Q estimated from variance-mean analysis, where similar quantum size and no change between different cocaine procedures and withdrawal times were observed.

Taken together the above results obtained with variance-mean analysis show a specific, long-lasting up-regulation of prefrontal cortex to nucleus accumbens pathway after repeated cocaine exposure, although in basal conditions it is amygdala-to-NAc pathway that exhibit higher probability of glutamate release.

4. Cocaine-induced adaptations in AMPA receptors function

Recent studies of mechanisms underlying addiction allowed formulating a hypothesis that drugs of abuse feed in to natural reward learning processes (Hyman et al., 2006). Cocaine easily induces synaptic plasticity that leads to formation of pathological forms of memory, because it hijacks the mesolimbic dopamine system, creating rapid adaptations. Strengthening of AMPA receptor-mediated transmission in glutamatergic drive to NAc during withdrawal is believed to be responsible for drug-seeking behaviour, incubation of cocaine craving and sensitization (Conrad et al., 2008; Kalivas, 2004; Thomas et al., 2001). Cocaine experience induces silent synapses in the NAc (Huang et al., 2009) and PSD-95, a protein involved in trafficking and retention of AMPARs in the synapse is involved in silent synapse formation and cocaine-induced adaptations (Béïque at al., 2006; Yao et al., 2004; Zhang et al. 2011). The following sections describe the role of silent synapses in the formation of cocaine-associated memories, as well as the involvement of the PSD-95 protein in cocaine-induced adaptations of AMPAR-mediated synaptic transmission. The persistence of cocaine-induced memories, correlated with the formation of silent synapses, as well as short- and long-term effects of cocaine on AMPAR-mediated synaptic transmission were analysed in PSD-95 KO animals.

4.1. Conditioned place preference in cocaine-treated mice

One of the common ways of testing the long-term effects of cocaine experience in animals is a measurement of behavioural sensitization, defined as a progressive enhancement of locomotor activity occurring after repeated cocaine treatment

(Kalivas and Stewart, 1991; Robinson and Berridge, 1993). Repeated cocaine exposure however, had no effect of behavioural sensitization in PSD-95 KO mice, as the response to an initial cocaine injection was already saturating (Yao et al., 2004). Therefore, in order to test the persistence of cocaine-induced memories, I used the conditioned place preference (CPP) behavioural model. The CPP behavioural experiments measure rewarding or aversive properties of substances. Animals are placed in a two-compartment chamber and are allowed to explore one part of it under the influence of a drug and the other part after saline administration. The drug has positive reinforcing effects, when after the conditioning an animal prefers to spend more time in the drug-associated compartment. I tested the long-term effects of cocaine treatment, comparing the preference towards the cocaine-associated compartment after short and long-term drug withdrawal in PSD-95 KO animals.

During the conditioning phase PSD-95 KO as well as wild-type animals were given once daily (for 10 days) alternate i.p. injections of either 20mg/kg of cocaine or saline in the assigned compartments. One day after the last injection, a place preference test was performed, in which the time spent in both compartments was measured and calculated as a place preference score (PPS, see methods for details). Both wild-type animals and PSD-95 knockouts displayed a strong preference to the cocaine-associated compartment. Before the conditioning, wild-type animals did not show preference towards any of the compartments: PPS was 561 ± 32 and increased to 719 ± 18 ($n = 10$ paired t-test $p<0.001$) after cocaine administration. Similarly in PSD-95 KO animals initial PPS increased from 538 ± 39 (no preference) to 797 ± 37 ($n = 5$, paired t-test $p<0.001$) as illustrated on Figure 17. Simultaneously, control animals, which received saline injections in both compartments, did not show preference either before, or after the conditioning procedure: WT PPS before saline treatment 487 ± 59 and 495 ± 62 after the treatment ($n = 7$), PSD-95 KO PPS before 508 ± 33 and 546 ± 80 after saline treatment ($n = 8$). When cocaine treatment was followed by 21-25 days of drug withdrawal (during which, animals remained undisturbed in their home cages) the preference for the cocaine associated chamber did not extinguish in wild-type animals and a strong preference towards it remained, while PSD-95 KO animals failed to recognize the previously preferred compartment. PPS of wild-type animals didn't change after the withdrawal: PPS = 711 ± 26 ($n =$

10), while in PSD-95 KO animals decreased significantly to 580 ± 21 (n=4, paired t-test $p<0.01$, Figure 17)

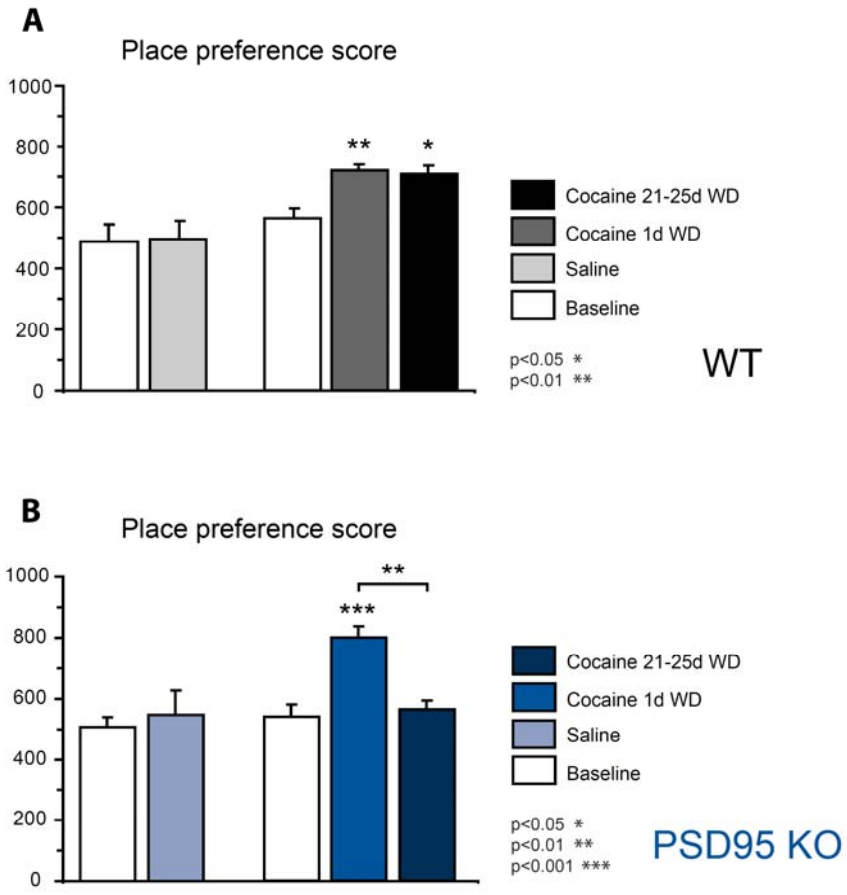

Figure 17: PSD-95 is required for long-term memories in cocaine conditioned place preference test in mice.

Bar graphs showing the place preference score (PPS) of wild-type and PSD-95 KO animals before and after cocaine conditioning. PPS around 500 represents no preference towards any compartment, while PPS over 700 shows strong preference towards conditioned compartment, indicating rewarding properties of cocaine. **A** Place preference score of wild-type animals before (baseline, shown in white) and after the conditioning. Animals showed no preference after saline injections (bright gray) and a strong, long-lasting preference following cocaine treatment (grey and black). **B** PPS of PSD-95 KO animals before (baseline, in white) and after the conditioning. Animals showed no preference after saline injections (bright blue) and a strong preference 1 day after the last cocaine injection (blue). After 21-25 days of withdrawal this preference was gone (dark blue).

The above experiment showed that in PSD-95 KOs cocaine-associated memories extinguished during withdrawal; lack of PSD-95, however, does not seem to prevent initial learning. Moreover, a higher PPS of PSD-95 KO animals compared to wild-types suggested a reduced threshold for learning. This observation was confirmed while trying an alternative protocol for conditioned place preference. In a protocol

typically used with rats, two daily, alternate cocaine and saline injections (administered at least 6 hours apart) are performed during 5 days of conditioning (Roux et al., 2003). Wild-type mice after 5 days treatment did not show a preference towards the cocaine-associated compartment. Such "shorter" protocol was however enough for PSD-95 KO's to develop a very strong preference towards the room where cocaine was administered; correctly displaying the drug's positive reinforcing properties. As illustrated in figure 18, PPS of wild-type mice didn't change after cocaine conditioning: 581 ± 14 before the treatment and 535 ± 55 after (n = 4), but increased significantly for PSD-95 KO animals: 492 ± 32 before the treatment and 856 ± 62 after (n = 4, $p<0.01$ paired t-test).

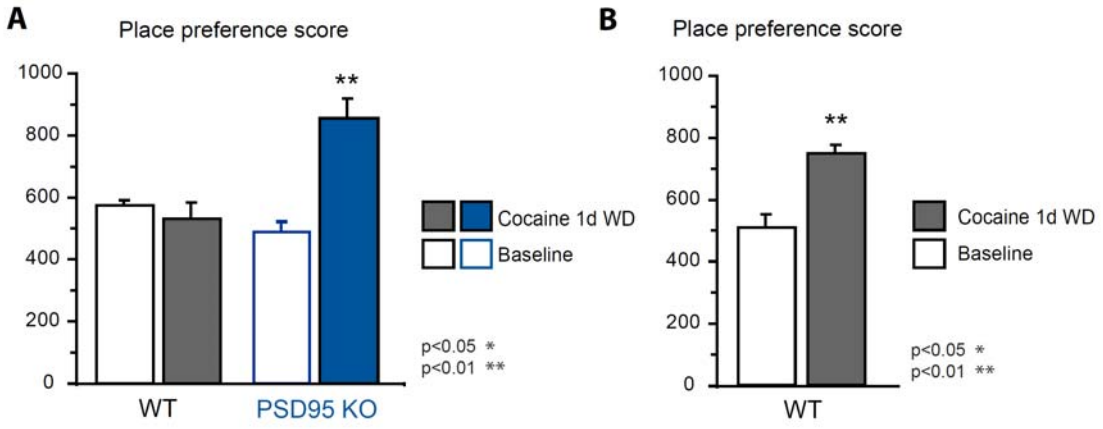

Figure 18: Absence of PSD-95 reduces the threshold for development of cocaine conditioned place preference in mice.

Bar graphs showing the place preference score (PPS) of wild-type and PSD-95 KO animals before and after conditioning with cocaine, using an alternative protocol of twice daily drug and vehicle injections. **A** PPS of wild-type animals didn't change after 5 days of cocaine injections (grey) compared to baseline, measured before the treatment (white). PSD-95 KO animals, however, displayed a strong increase of place preference score in response to this protocol (blue). **B** An increase of PPS of wild-type mice following cocaine treatment with a standard, 10 day conditioning protocol (see also Figure 17).

4.2. Cocaine experience generates silent synapses

In order to identify the cellular correlates of cocaine-induced memories acquired during the conditioning, I performed electrophysiological analysis of AMPAR-mediated transmission.

In the following experiments, the animals tested for CPP were sacrificed either 1 day after (short-term withdrawal) or 21-25 days after cocaine/saline treatment. The recordings were performed in medium spiny neurons of the nucleus accumbens shell, similar to previous experiments with pathway specific variance-mean analysis. This time however, I was focusing on the comparison of cocaine-induced changes between wild-type and PSD-95 KO animals. At this stage, the pathway specificity was not required and an electrical stimulation was used.

It was known that cocaine treatment decreases AMPA/NMDA ratio in the NAc shell, probably due to an increase in the number of silent synapses (Thomas et al. 2001; Kourrich et al. 2007; Huang et al. 2009). It was however unknown whether cocaine experience will have the same effect on PSD-95 KO animals, because in contrast to wild-types they express higher locomotor activity to acute cocaine administration but do not develop behavioural sensitization after repeated treatment (Yao et al., 2004). In the hippocampus of PSD-95 KO animals, AMPA/NMDA ratio is lower compared to their wild-type littermates, due to a high number of silent synapses (Béïque et al., 2006). If a similar phenomenon is present in the NAc, perhaps cocaine treatment does not increase this already elevated number of nascent synapses, hence no sensitization in PSD-95-deficient mice. To test this hypothesis I performed AMPA/NMDA ratio analysis and estimated the number of silent synapses using the minimal stimulation protocol.

For AMPA/NMDA ratio measurements, AMPAR EPSCs were recorded in whole-cell voltage clamp at -60mV and NMDA receptor-mediated EPSCs at +40mV, measured 60ms after the peak. This assay informs about a change in cell's sensitivity to glutamate, as it can be easily modified by insertion/removal of AMPA receptors from the synapse.

The experiment showed that in wild-type animals, cocaine experience significantly decreased the ratio of AMPA/NMDA EPSCs amplitudes in MSN of NAc, from 4.0 ± 0.6 to 2.8 ± 0.2 (n/m = 4/18, $p<0.05$). This ratio increased during drug withdrawal to 4.7 ± 0.3 (n/m = 6/28, $p<0.001$ vs. cocaine 1 day WD). Consistent with previous findings in the hippocampus (Béïque et al., 2006), AMPA/NMDA ratio of saline treated KO mice was significantly lower compared to wild-type controls: 2.8 ± 0.2 (n/m = 5/27, $p<0.05$ t-test). Cocaine treatment decreased it even further to 1.9 ± 0.1 (n/m = 4/22, $p<0.01$) after short-term withdrawal, but in contrast to wild-type

controls, it did not recover after long-term withdrawal and remained at 1.7 ± 0.2 (n/m = 4/16, p<0.01), (Figure 19).

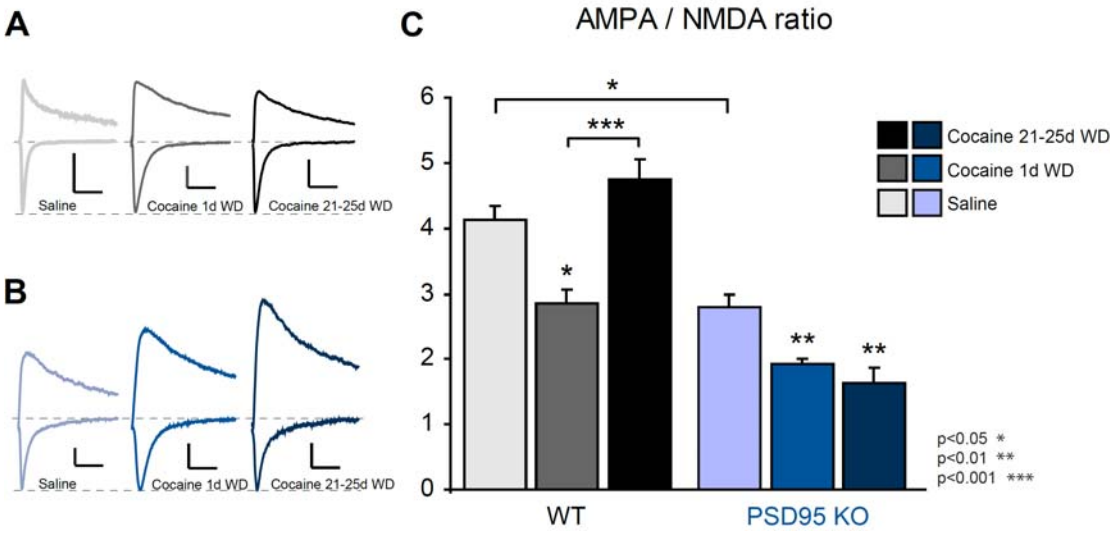

Figure 19: Cocaine experience reduces the ratio of AMPA- versus NMDA-mediated EPSCs in mouse NAc shell.

A Example average traces of AMPA EPSCs recorded at -60mV and composite AMPA and NMDA EPSCs recorded at +40mV, peak-scaled to the size of AMPA response in saline treated, wild-type mice (light grey). Traces from cocaine treated animals recorded after 1 day of withdrawal shown in grey and 21-25days of withdrawal shown in black. **B** Example average traces of AMPA EPSCs recorded at -60mV and composite AMPA and NMDA EPSCs recorded at +40mV, peak-scaled to the size of AMPA response in saline treated, PSD-95 KO mice (light blue). Traces from cocaine treated animals recorded after 1 day of withdrawal shown in blue and 21-25days of withdrawal shown in dark blue. **C** Bar graphs showing a decrease of ratio of AMPA compared to NMDA EPSCs amplitudes shortly after cocaine treatment in wild-type mice (light grey and grey). During long-term withdrawal the ratio increases (black). The absence of PSD-95 leads to a decrease of AMPA/NMDA ratio (light blue) and exposure to cocaine further decreases this parameter (cocaine 1 day withdrawal in blue and 21-25 days withdrawal in dark blue). Scale bars 50pA, 20ms.

The relative decrease of AMPAR-, compared to NMDAR-mediated transmission suggests that following cocaine exposure, the number of silent synapses increases. Indeed, the minimal stimulation assay, which provides the number of silent synapses based on the fraction of failures of AMPAR- compared to NMDAR-mediated EPSCs, showed a significant increase in the percentage of silent synapses in MSN of NAc shell, following cocaine administration. The number of silent synapses in saline treated wild-type animals was estimated to 23 ± 6% (n/m = 4/16) and doubled after cocaine procedure to 46 ± 5% (n/m = 6/18, p<0.05, Figure 20). Following long-term

cocaine withdrawal, the percentage of silent synapses was no longer elevated and returned to the control level (20 ± 5%, n/m = 6/22, p<0.01 vs. cocaine 1d WD). In saline treated PSD-95 KO animals, 57 ± 5% of MSN synapses in the NAc shell were silent (m/n = 5/18). Cocaine experience elevated this number even higher, to 74 ± 2% (n/m = 4/13, p<0.05) after short-term withdrawal and 72 ± 6% after long-term withdrawal (n/m = 4/15, p = 0.1).

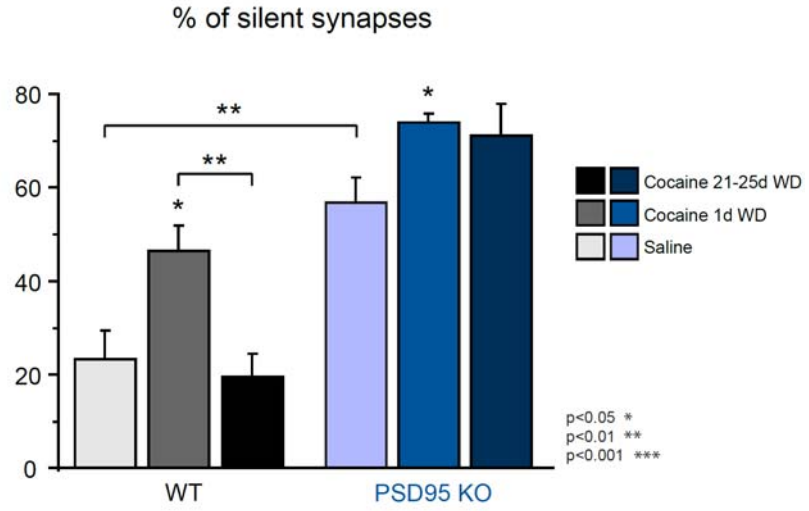

Figure 20: Cocaine experience induces silent synapses in mouse NAc medium spiny neurons.
Bar graphs showing an increase in number of silent synapses following cocaine experience in wild-type mice (grey). During long-term withdrawal the number of silent synapses goes back to baseline level (black). The Absence of PSD-95 leads to a strong increase in the number of silent synapses (light blue), which becomes even higher after cocaine treatment (blue) and stays elevated during long-term withdrawal (dark blue).

The above results are directly correlated with changes in AMPA/NMDA ratio (Figure 19), where the initial decrease recovers during withdrawal in wild-type animals, but not in PSD-95 KO mice. Despite the elevated number of silent synapses in the NAc shell of PSD-95-deficient mice, cocaine treatment increased this number even higher, discarding my initial hypothesis that KO animals have reached the maximum capacity for silent synapses. Therefore, combined with the results from behavioural tests (Figure 17 and Yao et al., 2004), this data suggest that silent synapses might be important in formation of cocaine-associated memories, but it is their unsilencing that could influence the behaviour after withdrawal.

4.3. Cocaine-induced changes in AMPA receptors subunit composition

The decrease in number of silent synapses, after 3 weeks of cocaine withdrawal, combined with an increase of AMPA/NMDA ratio in cocaine treated wild-type mice, suggests that new AMPA receptors were recruited to previously silent synapses. AMPA receptors in adult rodents are tetramers containing two GluR2 subunits (Wolf, 2010) and are calcium impermeable. GluR2-lacking receptors, on the other hand, are calcium permeable (CP) and therefore have a higher channel conductance. Previous studies showed that cocaine experience increases the number of CP-AMPARs in the synapse during extended withdrawal (Conrad et al 2008, Mameli et al. 2009). Their accumulation in the synapse however, is detected at least after 35 days of withdrawal (Mameli et al. 2009), while silent synapses are no longer detected within 1 week after cocaine treatment (Huang et al. 2009). Such difference in the timeline suggests that nascent synapses are unsilenced by recruitment of GluR2-containing AMPARs, which are later substituted by GluR2-lacking ones.

One way to test the accumulation of CP-AMPARs is to perform recordings of AMPAR-mediated EPSCs at different holding potentials (-60 mV and +40mV) in the presence of polyamines. GluR2-lacking receptors are inwardly rectifying (reduced outward current at positive membrane potentials), because of voltage-dependent inhibition by intracellular polyamines. The amplitudes of CP-AMPAR EPSCs at positive holding potential will therefore be lower, compared to GluR2-containing AMPA receptors and a rectification index (amplitude of AMPA EPSCs at -60mV divided by EPSC amplitude at +40mV) will increase.

The experiment showed, as expected, that shortly after cocaine exposure there was no change in composition of AMPA receptors, neither in wild-type nor in KO mice (Figure 21). The rectification index of wild-type animals estimated to 1.85 ± 0.16 (n/m = 4/14) remained unchanged 1 day after cocaine treatment: 1.85 ± 0.14 (n/m = 6/16). Similarly, in PSD-95KO animals there was no change in rectification index: saline: 1.74 ± 0.09 (n/m = 4/24), cocaine 1d WD: 1.88 ± 0.35 (n/m = 4/15). This data suggest that CP-AMPARs are not required for development of CPP. Among the new AMPA receptors inserted to the synapse during long-term withdrawal, a significant number of GluR2-lacking receptors was present in wild-type animals, but not in the absence of PSD-95. Rectification index increased after 3 weeks of withdrawal in

wild-type animals: 2.43 ± 0.12 (n/m = 6/23, p=0.03 vs. saline, p=0.02 vs. cocaine 1d WD) and remained unchanged in knockouts: 1.90 ± 0.20 (n/m = 4/14).

Taken together, these results show that in conditioned place preference model in mice, PSD-95 is important for recalling cocaine-associated memories during extended withdrawal. Its absence however facilitates formation of silent synapses in response to repeated cocaine exposure.

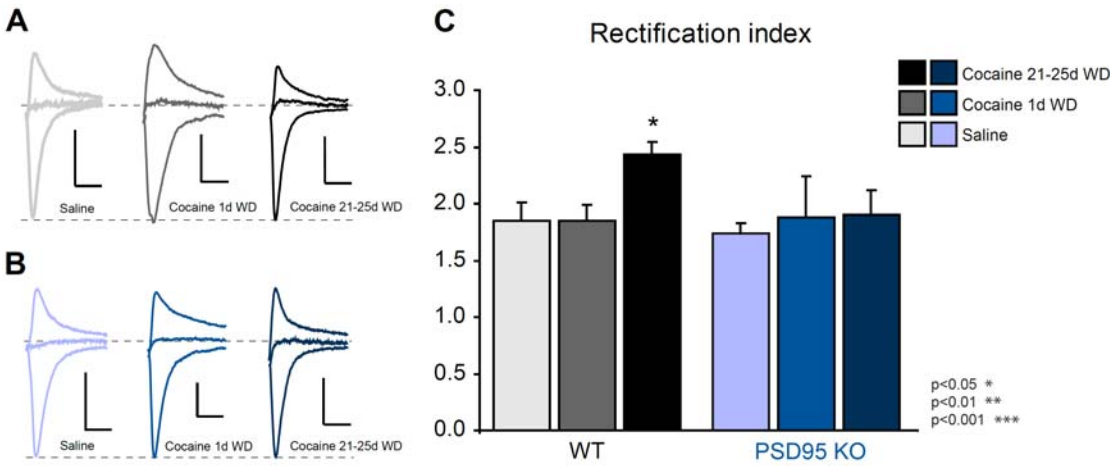

Figure 21: GluR2-lacking AMPA receptors are inserted into the synapse during long-term withdrawal in cocaine-treated mice.

A Example average traces of AMPA EPSCs recorded at -60mV, 0mV and +40mV, peak-scaled to the size of AMPA response at -60mV in saline treated, wild-type mice (light grey). Traces from cocaine treated animals recorded after 1 day of withdrawal shown in grey and 21-25days of withdrawal shown in black. **B** Example average traces of AMPA EPSCs recorded at -60mV, 0mV and +40mV, peak-scaled to the size of AMPA response at -60mV in saline treated, PSD-95 KO mice (light blue). Traces from cocaine treated animals recorded after 1 day of withdrawal shown in blue and 21-25days of withdrawal shown in dark blue. **C** Bar graphs showing that in wild-type mice, shortly after cocaine treatment the rectification index (amplitude of AMPA EPSCs at -60mV divided by amplitude at +40mV) doesn't change (light grey and grey). During long-term withdrawal the rectification index increases (black). This increase is abolished in PSD-95 KO mice (dark blue), but the absence of that protein has no influence on AMPA receptors composition, neither in saline treated mice (light blue) nor 1 day after cocaine treatment (blue). Recordings were made in the presence of 50µM picrotoxin in the extracellular solution and 100µM spermine in the internal solution. Scale bars 50pA, 20ms.

5. Discussion

Recent studies shed much light on our understanding of how drugs of abuse influence neural communication, leading to two major discoveries. Firstly, the midbrain dopamine system is a common target of all addictive substances and drug use triggers adaptations in brain regions responsible for emotions, decision making and motivated behaviours (Goldstein and Volkow, 2011; Hyman et al., 2006). Secondly, drug-induced plasticity is mediated through the same mechanisms as the natural reinforcement learning; only the addiction-related memories are extremely persistent and lead to pathological behaviour (Hyman et al., 2006). One of the structures strongly influenced in addiction is the nucleus accumbens, which mediates execution of motivated behaviours and is implicated in development of drug craving and relapse (Hyman and Malenka, 2001).

In this study, I focused on elucidating the influence of repeated cocaine exposure and extended drug withdrawal on pre- and postsynaptic properties of glutamatergic synapses in the NAc shell. I discovered that repeated cocaine treatment led to a specific, long-lasting up-regulation of glutamatergic projections from the PFC to the NAc. Moreover, cocaine treatment generated silent synapses in the NAc of wild-type and PSD-95 KO mice, but only in wild-type animals did the silent synapse number decrease during drug withdrawal. Similarly, CP-AMPARs accumulated in the synapse during extended withdrawal in wild-type animals but not in PSD-95 KO mice.

5.1. Variance-mean analysis as a tool to study cocaine-induced changes in synaptic quantal parameters.

Variance-mean analysis is a powerful method for estimating the quantal parameters of a synapse (Clements and Silver, 2000). One of the goals of this study was to elucidate whether repeated cocaine exposure has an effect on quantal parameters in different glutamatergic afferents in rat NAc shell. To this end, variance-

mean analysis was combined with an optogenetic approach, to study the projections from PFC and amygdala specifically.

Measurements of quantal parameters of CA3-CA1 synapses in rat hippocampal organotypic slice cultures, in pharmacologically altered release probability conditions, provided important information regarding the applicability and accuracy of variance-mean analysis (Figure 3, 4). Firstly, the analysis confirmed the pharmacologically-induced changes in the release probability, as 2-chloroadenosine is known to decrease (Wu and Saggau, 1994) and 4-aminopyridine to increase (Thomsen and Wilson, 1983) the probability of neurotransmitter release. Indeed, the recordings made in the presence of CA showed a 10% decrease, while in the presence of 4-AP a 10% increase of the release probability, compared to the control condition.

A significant decrease observed in the estimated number of release sites in rat organotypic slice cultures are due to a reduced stimulation strength in recordings from cells at high release probability (in the presence of 4-AP). In general, the number of stimulated synapses strongly depends on the number of axons that express ChR2-Venus as well as on the channel's expression level. In hippocampal slice cultures, owing to the ease of AAV-mediated transduction of CA3 pyramidal neurons with ChR2-Venus, a high number of neurons expressed the protein very efficiently. Yet in this culture system, the obstacle was the high degree of connectivity, both between CA3-CA3 and CA1-CA1 neurons that further increased with prolonged culture time. During recordings, wash-in of 4-AP inevitably led to induction of epileptic activity. Therefore, the solution to this problem was to record cells in each pharmacological condition separately, rather than wash-in different drug combinations one by one while recording from the same cell. This way, the stimulation strength was individually adjusted to obtain postsynaptic responses between -200 and -50pA. This meant that for cells recorded in the presence of 4-AP, in order to avoid epileptic activity, the stimulation strength had to be greatly reduced, which in turn activated fever connections. Importantly, such a reduction didn't come unnoticed by the variance-mean analysis approach, which detected ≈50% decrease in the number of release sites in the presence of 4-AP.

Estimations of the quantum size by different methods of analysis – variance-mean approach and amplitudes distribution, led to different results. In hippocampal organotypic slice cultures, based on the amplitudes of mEPSCs, Q was previously estimated to ≈ -20pA (rat cultures: (Baxter and Wyllie, 2006; Ehrlich and Malinow,

2004; Tyler and Pozzo-Miller, 2001), mouse cultures: (Elias et al., 2006). It is similar to the quantum size, in the presence of 2-chloroadenosine, which was estimated by variance-mean relationship to -17pA. However, the Q was almost 50% higher in the control condition when the release probability was increased by 4-AP. It was reported that in CA3-CA1 synapses of rat hippocampal pyramidal neurons, with an increasing release probability, more glutamate is released per a single AP, as a result of an increasing contribution of multivesicular release (Oertner et al., 2002). It is likely that in the present study, the reduction in release probability by 1μM CA leads to a decrease in the number of multiquantal events, making uniquantal release predominant. It is further supported by the analysis of quantal peaks from AMPAR-mediated EPSCs amplitude histograms, where the size of the response to a single quantum was estimated to ≈ -20pA, similar to the Q in the presence of CA based on the variance-mean approach. Moreover, the quantum size estimated from amplitude distribution was stable, regardless of the release probability, suggesting that Q is not altered by any of the drugs (Figure 5). The discrepancy of the Q estimated by the two methods – amplitude histograms and the variance-mean analysis, suggest that the latter is affected by multivesicular release, where the release of one vesicle increases the likelihood of releasing another one. Only this way the Q would be overestimated by binomial model of the variance-mean analysis.

Nonetheless, multiquantal release, occurring at high release probability, did not saturate AMPA receptors, as shown by fractional block in the presence of rapidly equilibrating competitive antagonist – kynurenic acid (Figure 6).

The reason for the discrepancy of the quantum size estimates lies in different properties of the used methods. Variance-mean analysis is very advantageous when dealing with synapses of substantial inter- and intrasite variabilities, especially under non-saturating conditions (reviewed by Silver, 2003). Nonuniform release, dendritic filtering or low signal to noise ratio may obscure quantal peaks in amplitude histograms. However, when multivesicular release occurs, such that the release of one vesicle affects the probability of releasing the others, the quantal responses do not summate linearly and Q calculated from the variance-mean relationship might vary from the actual quantum size. Therefore, in cases of relatively low inter- and intrasite variability and a high signal to noise ratio, estimation of Q based on Gaussian fitting to amplitude histograms might be more advisable (Redman, 1990; Silver, 2003). The

most accurate quantum size analysis based on fluctuations of EPSCs amplitudes can be performed if the variance of EPSCs is small. The work of Wall and Usowicz (1998), in cerebellar mossy fiber-granule cell synapses is an example, because due to an extremely low variance, up to 5 quantal peaks could be easily distinguished. In general, however, other types of synapses express relatively higher variance of EPSCs and the quantal peaks are not so properly resolved, therefore Q can not be estimated. In my study, in rat hippocampal slice cultures, the histograms of EPSCs amplitudes provided additional information regarding the quantum size and combining this approach with the variance-mean analysis, led to a successful estimation of quantal parameters and their changes, following pharmacological manipulation in CA3-CA1 synapses.

The pharmacological approach of increasing the release probability by 10μM 4-AP (Figure 8), used to evaluate the variance-mean analysis of PFC-to-NAc afferents is an excellent way to validate the method. NAc shell is composed of 90% inhibitory (GABAergic) medium spiny neurons (Meredith et al., 1999) therefore epileptic activity was not observed, in spite of a strong stimulation and high release probability, which was a great advantage, in contrast to recordings from hippocampal slices. It was thus possible to directly compare high and low release probabilities in the same cell, because recordings in control conditions were directly followed by a wash in of 4-AP and no readjustments of stimulation strength were necessary. Similarly to results from hippocampal slice cultures, a 15% increase in the probability of release was detected in the presence of 4-AP (Figure 8) and was further confirmed by a decrease in PPR and a faster decay kinetics in the presence of MK801 (Figure 9 and 10 respectively). The initial release probability estimated to 50% goes in accordance with a previous study, where electrical stimulation of axons at the border between PFC and NAc was combined with variance-mean analysis in 3 different extracellular calcium concentrations (Casassus et al., 2005). Similar values of P estimated by optical and electrical stimulations also suggest that channelrhodopsin-2, despite its calcium permeability, does not increase the release probability. Perhaps, owing to application of very short light pulses (1ms).

The number of release sites remained unchanged, as expected (Figure 8), because in NAc slices, the same number of synapses was recruited during the entire recording. Unlike in CA3-CA1 synapses in hippocampus, increased release probability did not affect the quantum size, which estimated to -10pA, is similar to the previous estimates

based on mEPSCs amplitudes of NAc afferents in mice: ≈ -10pA (Kourrich et al. 2007). Measurements in the presence of kynurenate revealed that at high release probability no saturation occurs (Figure 10), which further supports the validity of variance-mean analysis in studying quantal properties of NAc afferents.

A direct comparison between the control and elevated release probability done sequentially within each cell, showed a change only on one quantal parameter (P) leaving the other parameters (Q and N) unchanged, proving that 4-AP has an impact solely on the release probability, which, based on recordings from the hippocampus, was at the first glance not so clear and required additional analysis. It is also possible that in PFC-to-NAc synapses, unlike in the hippocampus, the quantal responses summate linearly, hence estimated Q did not change with the release probability.

Finally, the variance-mean analysis, which was utilized to estimate the cocaine-induced changes in the quantal parameters, provided new information about the properties of NAc shell MSN. It proved to be necessary to analyze presynaptic properties of different afferents separately, because the analysis of quantal parameters led to a discovery that various glutamatergic afferents of NAc display different probabilities of neurotransmitter release. In rats, amygdala-to-NAc pathway has a basal release probability higher than PFC-to-NAc: around 65% and 50% respectively (Figure 13, 14), consistent with previous estimation in mice (Figure 8).

5.2. Cocaine-induced selective increase in the release probability of PFC-NAc synapses

The variance-mean analysis of the release probability showed that only the PFC-to-NAc pathway was selectively up-regulated upon cocaine administration – both contingent and non-contingent, by about 30%. This enhancement was long-lasting and further increased during long-term withdrawal from cocaine self-administration. Previous studies, based on mEPSCs frequency analysis showed contradictory results regarding a possible presynaptic effect of cocaine on NAc MSN. Thomas and co-workers (2001) reported no change in mEPSCs frequency, suggesting no change in presynaptic mechanisms, which was further supported by unaltered paired-pulse ratio. On the other hand, other studies showed an increase in mEPSCs frequency, which could be an indication of a presynaptic enhancement (Kourrich et al., 2007; Moussawi

et al., 2011). It was however attributed to a postsynaptic change, as PPR measurements were not altered, suggesting no global change in the release probability upon cocaine experience. This however might have been an effect of a simultaneous recruitment of different pathways with electrical stimulation, as different afferents of NAc display different release probabilities, e.g. corticostriatal synapses being facilitating and thalamostriatal – depressing (Ding et al., 2008). In such an approach, a specific up-regulation of a single pathway would be masked, because the result will strongly depend on where the electrode was placed – an obstacle easily avoided by optical stimulation.

The estimated number of release sites remained unchanged, regardless of the stimulated afferents (PFC or amygdala axons), the cocaine paradigm or withdrawal time (Figure 13, 14). It was however quite variable (between 7 and 25), but solely due to a different number of ChR2-Venus-expressing axons stimulated during each recording. At a first glance, this result appeared at odds, as cocaine induced an increase in the number of dendritic spines (Huang et al., 2009). However, these are partially silent synapses, which can not be detected by variance-mean analysis. The method samples over AMPAR-mediated EPSCs, which are absent in nascent synapses, rendering them "invisible" in the analysis.

The quantum size also remained unaltered in each examined group and similar to the number of release sites, varied between different conditions. Although variable, the Q ranging between -13pA and -30pA is not far different from quantum size hitherto estimated from mEPSCs amplitudes: -15pA – -20pA in rats (Moussawi et al., 2011; Nicola et al., 1996). The variability in EPSCs size was too high, so that the amplitude distribution analysis did not reveal separable peaks to estimate Q. Lastly, the mEPSCs amplitudes, at the level of -20pA remained stable in all conditions tested, further indicating a stable quantum size. This result however was not obtained in a pathway-specific analysis.

5.3. Possible implications of cocaine-induced specific enhancement of PFC-NAc projections

In their study on cocaine self-administration in rats Sun and Rebec (Sun and Rebec, 2006) discovered that during the 3 weeks of contingent cocaine intake, the basal activity of PFC decreases. However re-exposure to the drug caused an increased PFC firing rate, suggesting that PFC becomes potentiated to specifically process cocaine-related information. Glutamatergic efferents from PFC to nucleus accumbens are believed to be the final common pathway for initiation of drug-seeking behaviour and it was observed that exposure to stress or re-exposure to drugs causes an increase in the glutamate release in the NAc (Kalivas and Volkow, 2005).

A possible mechanism that could explain the potentiation of glutamate release in the NAc is the disturbance of cystine-glutamate exchange system occurring during withdrawal from repeated cocaine exposure (Pierce et al., 1996). The cystine-glutamate exchange system is responsible for maintaining basal levels of extracellular glutamate. Baker and co-workers (Baker et al., 2002) discovered that the source of glutamate in the extracellular space is the cystine-glutamate antiporter, not the synaptic glutamate release. It has nonetheless a major impact on synaptic glutamate release, because the level of extracellular glutamate influences the tone of mGluR2/3 presynaptic autoreceptors that control synaptic release (Manzoni et al., 1997) and prevent excitatory neurotoxicity (Murphy et al., 1989). It was reported that in rats, during withdrawal from repeated cocaine treatment, the extracellular levels of glutamate are reduced specifically in the nucleus accumbens (Baker et al., 2003; Madayag et al., 2007; Pierce et al., 1996) which caused a higher susceptibility for cocaine-induced reinstatement of drug-seeking (Baker et al. 2003). The reinstatement of drug seeking is a commonly used animal model of drug craving and relapse in humans (Shalev et al., 2002). Decreased extracellular glutamate, in turn increased glutamate release in the NAc by affecting the inhibitory function of mGluR2/3 receptors (Moran et al., 2005), which might explain the increased release probability of cortical afferents. Importantly, restoration of normal levels of glutamate by infusing cystine into NAc or systemic administration of N-acetylcysteine prevents reinstatement of drug-seeking behaviour (Baker et al. 2003, Moran et al. 2005, Moussawi 2010).

Brain-derived neurotrophic factor (BDNF) might potentially be involved in mechanisms specifically up-regulating PFC-to-NAc afferents. BDNF is a potent modulator of synaptic plasticity and plays an important role in the development of long-term changes underlying learning and memory formation (Minichiello, 2009; Poo, 2001). It was discovered in hippocampal slices that application of BDNF resulted in an increase of mEPSCs frequency but not amplitude, suggesting an increase in release probability, which was due to an increase in the number of vesicles docked in the synaptic active zones (Tyler and Pozzo-Miller, 2001). Moreover, this increase was not associated with changes in other quantal parameters, leaving the quantum size and the number of release sites unaltered (Tyler et al., 2006). In regard to addiction, BDNF levels in NAc and amygdala increase during withdrawal from cocaine, but not in withdrawal from natural rewards (sucrose), which was correlated with incubation of drug craving (Grimm et al., 2003). Cocaine treatment transiently increases BDNF levels in the NAc, by local mRNA translation (Graham et al., 2007). However, the gradual accumulation of BDNF during withdrawal might be a result of anterograde transport from the medial PFC (Altar et al., 1997; Lu et al., 2010). This might indicate the biological relevance of specific PFC afferents enhancement in regard to cocaine-induced drug-seeking behaviour.

5.4. The role of PSD-95 in formation and retrieval of cocaine-induced memories

The conditioned place preference paradigm is a widely used, simple model to evaluate the reinforcing effects of drugs in animals (Tzschentke, 1998). This way, positive reinforcing effects of cocaine and other drugs of abuse were discovered (Durazzo et al., 1994; Lepore et al., 1995; Sora et al., 2001). Therefore, in this study, I took advantage of positive reinforcing effects of cocaine in a CPP paradigm in mice, to measure the persistence of cocaine-induced memories, which indirectly correspond to the cue-induced drug seeking behaviour (Roux et al. 2003). The experiment revealed that PSD-95 KO mice as well as the wild-type controls displayed a preference towards the cocaine-associated compartment (Figure 17). In contrast to wild-type mice however, after 3 weeks of withdrawal, in PSD-95 KO mice CPP was extinguished. Importantly, the loss of PSD-95 did not impair memory formation. On

the contrary, PSD-95 KO animals had a lower threshold to acquire the place preference towards the cocaine-associated chamber (Figure 18). The above results suggest a crucial role of PSD-95 in consolidation of long-term, cocaine-induced memory during withdrawal. On the other hand, learning impairments could also interfere with the outcome of CPP test in long-term withdrawal.

Indeed, when comparing results of CPP tests in WT vs. genetically modified animals, it is important to know whether the genetic modification does not severely impair the spatial memory, learning or locomotion as it might give false positive/negative results. PSD-95 KO animals were shown to have slightly impaired spatial learning in water maze tasks, requiring more training trials to learn the position of the platform and more time to find the platform in test trials, compared to their wild-type littermates (Migaud et al. 1998). This phenomenon was attributed to modified NMDAR-dependent long-term plasticity in the hippocampus. Another strain of PSD-95 KO animals exhibited a slightly lower locomotor activity in the open-field test, but a much stronger locomotor response to drugs of abuse (Yao et al. 2004, Zhang et al. 2007). Moreover, in the context of place preference-related learning, I showed a better performance in CPP tests in these KOs compared to wild-type animals (Figure 18). It should be noted, that the mentioned strains of PSD-95 knockout mice were generated with different strategies. In the work of Yao et al. (2004), a genetic deletion of a GK domain led to a complete removal of the entire PSD-95 protein, while in the work of Migaud et al. (1998), a truncated version of PSD-95 carrying the first two PDZ domains is still present, but not translocated to the synapse and physiologically inactive. It is unknown, whether this difference could account for opposing spatial learning abilities in various behavioural tests. What is important however is the fact that spatial learning in water maze tasks depends mostly on hippocampal learning, while memory formation in the place preference paradigm combined with cocaine administration involves midbrain, striatum and cortical structures as well (Brown et al., 2010). Moreover, this study showed that despite the possible spatial learning impairments, PSD-95 KO mice successfully associated cocaine administration with the correct compartment and compared to wild-type animals, showed a major difference in the observed effects after long-term cocaine withdrawal, suggesting the importance of PSD-95 in consolidating memories, rather than interfering with memory formation.

5.5. Cocaine induces formation of silent synapses

Recordings using minimal stimulation protocol on mice subjected to CPP paradigm allowed investigating the influence of repeated cocaine treatment and subsequent prolonged withdrawal on formation of silent synapses in the NAc shell. The recordings revealed a 2-fold increase in the nascent synapse number, 1 day after completed cocaine treatment in wild-type animals. The number of silent synapses decreased to baseline during the 3-week withdrawal (Figure 20A). It is in agreement with the discovery of the increase in silent synapse number in rat NAc shell, following 5 days of cocaine i.p. injections (Huang et al. 2009). This is the first study however, which shows that in NAc shell of PSD-95 KO animals 60% of glutamatergic synapses are AMPAR-silent. Moreover, subsequent to cocaine treatment, this number increased by further 15% and remained elevated for at least 3 weeks of withdrawal (Figure 20B). The above results show, that the lack of PSD-95 did not prevent cocaine-induced silent synapse formation, but did prevent the unsilencing of nascent synapses during extended withdrawal. In control animals, the decrease in silent synapse number during withdrawal was probably due to insertion of new AMPARs to the synapse. The silent synapse formation with subsequent conversion to a functional synapse could be the underlying mechanism of cocaine-induced long-term changes like drug-related associations. PSD-95, a protein involved in trafficking of AMPARs to the synapse, has an impact on silent synapses as well, since a higher number of nascent synapses was observed in the hippocampus of PSD-95 knockout mice (Béïque et al. 2006). The observed decrease in silent synapse number after 3-week withdrawal correlates with the ability of wild-type animals to recognize the cocaine-associated chamber in conditioned place preference. Simultaneously, the increased nascent synapse number in PSD-95 KO mice, remaining throughout the withdrawal was correlated with the inability to recall which compartment was paired with cocaine. On the other hand, the elevated number of synapses 1 day after the conditioning procedure does not prevent correct, short-term CPP associations. It seems, therefore that unsilencing of nascent synapses in the NAc underlie formation of cocaine-induced long-term, but not short-term associations, a process where PSD-95 protein is involved. It might be that PSD-95-deficient synapses are easier to undergo plasticity changes, as shown in previous reports on enhanced LTP in PSD-95 KO mice (Migaud et al. 1998, Beique et al. 2006, Yao et al. 2004).

Although it might complicate hippocampal spatial learning (Migaud et al. 1998) in cocaine-induced plasticity, enhanced LTP may be displayed by the reduced threshold for CPP induction. However, it also appears that PSD-95 is necessary to make cocaine-associated memories long-lasting. It is unclear why silent synapses are not facilitating spatial learning in water maze tasks, but it might be partially due to their abundance in different brain structures, where learning and memory consolidation might occur in different time course. For instance, drug naïve PSD-95 KO animals have 60% of silent synapses in NAc but 40% in visual cortex (personal communication from X. Huang). The exact number of nascent synapses in hippocampus of PSD-95 knockouts remains to be elucidated.

Changes in the number of silent synapses in wild-type and PSD-95-deficient mice following repeated cocaine treatment and extended withdrawal, directly correlate with alterations of AMPA/NMDA EPSCs ratio (Figure 19). Previous studies described a decrease in AMPA/NMDA ratio in NAc synapses, shortly after cocaine treatment (Kourrich et al. 2007, Thomas et al. 2001). At that time, however, it was attributed to a LTD mechanism that removes AMPAR from the synapse. The pathway-specific analysis of quantal parameters of NAc shell synapses revealed that repeated cocaine experience did not have an influence on the quantum size of neither of the NAc afferents tested (Figure 13, 14). A change in this parameter informs about alterations in both pre and postsynaptic properties, like the change in number of synaptic vesicles released, amount of neurotransmitter inside the vesicle and the number of postsynaptic receptors (Clements and Sliver 2000). Lack of change in Q estimated from variance-mean relationship, combined with unchanged mEPSCs amplitudes (Figure 16) indicate that the postsynaptic input into quantum size is unaltered by cocaine treatment, meaning that the number of postsynaptic AMPA receptors remained stable. Another explanation would be a presynaptic LTD, which would reduce AMPAR EPSCs without affecting the Q. Such mechanism however was ruled out, because of the observed increase in release probability (Figure 13). If a postsynaptic LTD mechanism occurred and the number of AMPARs in the synapse was reduced, it should have been detected as a decrease in Q. Because no such decrease was observed, the reduction of AMPA/NMDA ratio after short-term withdrawal is not due to the loss of AMPARs, but rather as a result of an increase in NMDARs number (Figure 19). In fact, those new NMDA receptors are recruited to newly formed spines (Brown et al., 2011; Robinson et al., 2001). As mentioned before

(section 5.1), the cocaine-induced increase in the number of silent synapses is undetectable by the variance-mean analysis due to sampling over fully functional synapses only. Lack of change in Q, however, indirectly points to conclusions in favour of silent synapses-based mechanism of cocaine-induced long-term changes in synaptic plasticity, rather than the LTD-like mechanism proposed in previous studies. It therefore appears that cocaine experience triggers the formation of silent synapses in NAc, priming these connections for enhanced learning. The fate of newly formed nascent synapses might be determined by subsequent experiences, which turn them into fully functional connections. The electrophysiological data obtained after 3 weeks of cocaine withdrawal show a normalization of both: the silent synapse number and the AMPA/NMDA ratio (Figure 19, 18), suggesting that AMPARs are indeed being recruited to form a functional synapse.

5.6. The fate of silent synapses in cocaine-induced circuitry reorganization

During the course of withdrawal, the number of silent synapses induced by cocaine treatment in the NAc shell gradually decreases (Huang et al., 2009). It is possible that new AMPARs – homomers of GluR1 and hetero-oligomers of GluR1/GluR2 are recruited to those synapses in an activity dependent manner in the process of LTP and later replaced by GluR2/GluR3 containing AMPARs, as it was shown in hippocampal slices (Shi et al., 2001; Shi et al., 1999). Recent evidence in the context of cocaine-induced plasticity, however, points to another mechanism that in NAc, GluR2-containing receptors are gradually replaced by GluR2-lacking, calcium permeable AMPARs during extended cocaine withdrawal – a phenomenon associated with the incubation of cocaine craving (Conrad et al., 2008, Mameli et al., 2009, McCutcheon et al., 2011). In this concept, the gradual recruitment of CP-AMPARs is not a result of LTP, but rather an ongoing process of circuitry remodelling. The rectification indices analysis showed that in wild-type animals, on withdrawal day 1 no CP-AMPARs were detectable, but after 3 weeks of withdrawal a substantial fraction of AMPARs was calcium permeable (Figure 21). PSD-95 has to be involved in this process, because in the absence of this protein no accumulation of CP-AMPARs occured. Due to calcium permeability (causing higher channel

conductance), GluR2-lacking AMPAR are important players in regulating synaptic strength (Liu and Cull-Candy, 2000) and subsequent plasticity by influencing calcium-dependent signalling pathways (Isaac et al., 2007) and could act as molecular correlates of drug dependence.

A possible mechanism, by which PSD-95 might be important in the accumulation of calcium-permeable AMPA receptors during cocaine withdrawal, is its involvement in BDNF signalling cascades mediated by TrkB – a member of the neurotrophin receptor tyrosine kinase family. As mentioned before, the levels of BDNF in NAc and amygdala gradually increase during prolonged withdrawal after cocaine treatment and similarly to increase in the number of CP-AMPARs, no changes are detected on withdrawal day 1 (Grimm et al., 2003). These increased levels of BDNF in NAc, following cocaine treatment, increase synaptic delivery of CP-AMPAR via TrkB signalling pathway (Caldeira et al., 2007; Li and Wolf, 2011). Activation of BDNF-TrkB signalling increases trafficking of PSD-95 to the synapse (Yoshii and Constantine-Paton, 2007), which might be an immediate link with an increase in synaptic AMPA receptors. One of the three major signalling pathways activated by TrkB is the recruitment and activation of phospholipase Cγ, which in turn leads to activation of protein kinase C (PKC, reviewed by Minichiello, 2009). It was shown that in NAc of cocaine self-administrating rats the activity of PKC is involved in trafficking of CP-AMPARs to the synapse (McCutcheon et al., 2011).

5.7. A possible role of calcium-permeable AMPA receptors in memory formation

Silent synapses in NAc shell, induced by cocaine treatment, disappear after a week (Huang et al., 2009), but CP-AMPARs are undetectable within the first 2 weeks of withdrawal (Kourrich et al., 2007). In the VTA however, CP-AMPARs are incorporated immediately, after even a single injection of cocaine and within 24 hours an increase in rectification index is observed (Bellone and Lüscher, 2006). Similarly in the amygdala of animals subjected to fear conditioning, CP-AMPARs accumulate gradually, reaching the peak at 24h after conditioning and disappearing within 7 days (Clem and Huganir, 2010). According to the studies mentioned above, despite the differences in the timeline of CP-AMPARs appearance, their involvement in the

process of making memories durable is consistent. Also in this study, PSD-95 KO animals, due to the lack of CP-AMPARs, were unable to consolidate cocaine-associated memories. CP-AMPARs might be the hallmarks of a labile period, when synapses undergo intensive plasticity changes that will shape the memories. Interfering with that window, by blocking the accumulation of CP-AMPARs or removing them by mGluR1-dependent mechanism, leads to erasure of the fear memory and prevents from reinstatement of drug-seeking behaviour (Clem and Huganir, 2010, Bellone and Lüscher, 2006, Mameli et al., 2009, McCutcheon et al., 2011).

PSD-95 KO animals are unable to accumulate CP-AMPARs during withdrawal from repeated cocaine exposure (Figure 21), which doesn't interfere with induction of CPP, but renders them unable to consolidate cocaine-associated memory traces, or retrieve the memories later (Figure 17). It suggests that insertion of GluR2-lacking AMPARs is not responsible for formation of memories, but rather establishing pathways to consolidate them. Similarly, removing CP-AMPARs might not erase memories, but instead provide a way to reshape them.

5.8. Conclusions and outlook

This study, focused on properties of glutamatergic synapses in the nucleus accumbens shell, provided important new insights into mechanisms underlying the formation of cocaine-induced memories.

The optogenetic targeting of two brain structures responsible for the main glutamatergic drive to NAc shell, PFC and amygdala, combined with electrophysiology, showed a specific, long-lasting up-regulation of cortical afferents only. This up-regulation was long-lasting and may represent a shift of the NAc glutamatergic drive towards the PFC in development of addiction. Future experiments combining ChR2 expression with shRNA-mediated knockdown of various proteins, like BDNF, will help to elucidate, in a pathway-specific manner, their role in the presynaptic enhancement of PFC-to-NAc synapses.

The study confirmed, in agreement with previous reports, that repeated cocaine experience generates silent synapses in the NAc shell. For the first time however, it was shown in this study that in PDS-95-deficient animals, more than half of

glutamatergic synapses in the NAc shell are silent and cocaine exposure elevated this number even higher. It would be interesting to investigate the involvement of other DLG-MAGUKs in cocaine-induced formation of silent synapses and also, whether inhibition of this process will prevent the formation of drug-associated memories.

In the nucleus accumbens, the appearance of silent synapses correlates with the formation of addiction-related memory traces. In the long-term however, the unsilencing of nascent synapses is what mediates memory consolidation. Similarly, accumulation of calcium-permeable AMPA receptors seemed to be involved in establishing long-term memories. This study therefore, supports the hypothesis that silent synapses provide new connections, primed for enhanced plasticity, while unsilencing, followed by the insertion of CP-AMPARs during withdrawal, represents ongoing reorganization, potentially leading to memory consolidation.

References

Altar, C. A., Cai, N., Bliven, T., Juhasz, M., Conner, J. M., Acheson, A. L., Lindsay, R. M., & Wiegand, S. J. (1997). Anterograde transport of brain-derived neurotrophic factor and its role in the brain. *Nature, 389*(6653), 856-860.

Baker, D. A., McFarland, K., Lake, R. W., Shen, H., Tang, X. C., Toda, S., & Kalivas, P. W. (2003). Neuroadaptations in cystine-glutamate exchange underlie cocaine relapse. *Nat Neurosci, 6*(7), 743-749.

Baker, D. A., Xi, Z. X., Shen, H., Swanson, C. J., & Kalivas, P. W. (2002). The origin and neuronal function of in vivo nonsynaptic glutamate. *J Neurosci, 22*(20), 9134-9141.

Baxter, A. W., & Wyllie, D. J. (2006). Phosphatidylinositol 3 kinase activation and AMPA receptor subunit trafficking underlie the potentiation of miniature EPSC amplitudes triggered by the activation of L-type calcium channels. *J Neurosci, 26*(20), 5456-5469.

Bear, M. F. (1996). A synaptic basis for memory storage in the cerebral cortex. *Proc Natl Acad Sci U S A, 93*(24), 13453-13459.

Bear, M. F., & Malenka, R. C. (1994). Synaptic plasticity: LTP and LTD. *Curr Opin Neurobiol, 4*(3), 389-399.

Beique, J. C., Lin, D. T., Kang, M. G., Aizawa, H., Takamiya, K., & Huganir, R. L. (2006). Synapse-specific regulation of AMPA receptor function by PSD-95. *Proc Natl Acad Sci U S A, 103*(51), 19535-19540.

Bellone, C., & Luscher, C. (2006). Cocaine triggered AMPA receptor redistribution is reversed in vivo by mGluR-dependent long-term depression. *Nat Neurosci, 9*(5), 636-641.

Berridge, M. J. (1998). Neuronal calcium signaling. *Neuron, 21*(1), 13-26.

Bolshakov, V. Y., & Siegelbaum, S. A. (1995). Regulation of hippocampal transmitter release during development and long-term potentiation. *Science, 269*(5231), 1730-1734.

Boyden, E. S., Zhang, F., Bamberg, E., Nagel, G., & Deisseroth, K. (2005). Millisecond-timescale, genetically targeted optical control of neural activity. *Nat Neurosci, 8*(9), 1263-1268.

Brown, R. M., Short, J. L., & Lawrence, A. J. (2010). Identification of brain nuclei implicated in cocaine-primed reinstatement of conditioned place preference: a behaviour dissociable from sensitization. *PLoS One, 5*(12), e15889.

Brown, T. E., Lee, B. R., Mu, P., Ferguson, D., Dietz, D., Ohnishi, Y. N., Lin, Y., Suska, A., Ishikawa, M., Huang, Y. H., Shen, H., Kalivas, P. W., Sorg, B. A., Zukin, R. S., Nestler, E. J., Dong, Y., & Schluter, O. M. (2011). A silent synapse-based mechanism for cocaine-induced locomotor sensitization. *J Neurosci, 31*(22), 8163-8174.

Caldeira, M. V., Melo, C. V., Pereira, D. B., Carvalho, R., Correia, S. S., Backos, D. S., Carvalho, A. L., Esteban, J. A., & Duarte, C. B. (2007). Brain-derived neurotrophic factor regulates the expression and synaptic delivery of alpha-amino-3-hydroxy-5-methyl-4-isoxazole propionic acid receptor subunits in hippocampal neurons. *J Biol Chem, 282*(17), 12619-12628.

Carlisle, H. J., Fink, A. E., Grant, S. G., & O'Dell, T. J. (2008). Opposing effects of PSD-93 and PSD-95 on long-term potentiation and spike timing-dependent plasticity. *J Physiol, 586*(Pt 24), 5885-5900.

Casassus, G., Blanchet, C., & Mulle, C. (2005). Short-term regulation of information processing at the corticoaccumbens synapse. *J Neurosci, 25*(50), 11504-11512.

Clem, R. L., & Huganir, R. L. (2010). Calcium-permeable AMPA receptor dynamics mediate fear memory erasure. *Science, 330*(6007), 1108-1112.

Clements, J. D., & Silver, R. A. (2000). Unveiling synaptic plasticity: a new graphical and analytical approach. *Trends Neurosci, 23*(3), 105-113.

Conrad, K. L., Tseng, K. Y., Uejima, J. L., Reimers, J. M., Heng, L. J., Shaham, Y., Marinelli, M., & Wolf, M. E. (2008). Formation of accumbens GluR2-lacking AMPA receptors mediates incubation of cocaine craving. *Nature, 454*(7200), 118-121.

Cuthbert, P. C., Stanford, L. E., Coba, M. P., Ainge, J. A., Fink, A. E., Opazo, P., Delgado, J. Y., Komiyama, N. H., O'Dell, T. J., & Grant, S. G. (2007). Synapse-associated protein 102/dlgh3 couples the NMDA receptor to specific plasticity pathways and learning strategies. *J Neurosci, 27*(10), 2673-2682.

Di Chiara, G. (1998). A motivational learning hypothesis of the role of mesolimbic dopamine in compulsive drug use. *J Psychopharmacol, 12*(1), 54-67.

Di Chiara, G. (2002). Nucleus accumbens shell and core dopamine: differential role in behavior and addiction. *Behav Brain Res, 137*(1-2), 75-114.

Diamond, J. S., & Jahr, C. E. (1997). Transporters buffer synaptically released glutamate on a submillisecond time scale. *J Neurosci, 17*(12), 4672-4687.

Ding, J., Peterson, J. D., & Surmeier, D. J. (2008). Corticostriatal and thalamostriatal synapses have distinctive properties. *J Neurosci, 28*(25), 6483-6492.

Dobrunz, L. E., & Stevens, C. F. (1997). Heterogeneity of release probability, facilitation, and depletion at central synapses. *Neuron, 18*(6), 995-1008.

Durazzo, T. C., Gauvin, D. V., Goulden, K. L., Briscoe, R. J., & Holloway, F. A. (1994). Cocaine-induced conditioned place approach in rats: the role of dose and route of administration. *Pharmacol Biochem Behav, 49*(4), 1001-1005.

Ehrlich, I., & Malinow, R. (2004). Postsynaptic density 95 controls AMPA receptor incorporation during long-term potentiation and experience-driven synaptic plasticity. *J Neurosci, 24*(4), 916-927.

El-Husseini, A. E., Schnell, E., Chetkovich, D. M., Nicoll, R. A., & Bredt, D. S. (2000). PSD-95 involvement in maturation of excitatory synapses. *Science, 290*(5495), 1364-1368.

Elias, G. M., Funke, L., Stein, V., Grant, S. G., Bredt, D. S., & Nicoll, R. A. (2006). Synapse-specific and developmentally regulated targeting of AMPA receptors by a family of MAGUK scaffolding proteins. *Neuron, 52*(2), 307-320.

Goebel, D. J., & Poosch, M. S. (1999). NMDA receptor subunit gene expression in the rat brain: a quantitative analysis of endogenous mRNA levels of NR1Com, NR2A, NR2B, NR2C, NR2D and NR3A. *Brain Res Mol Brain Res, 69*(2), 164-170.

Golding, N. L., Staff, N. P., & Spruston, N. (2002). Dendritic spikes as a mechanism for cooperative long-term potentiation. *Nature, 418*(6895), 326-331.

Goldstein, R. Z., & Volkow, N. D. (2011). Dysfunction of the prefrontal cortex in addiction: neuroimaging findings and clinical implications. *Nat Rev Neurosci, 12*(11), 652-669.

Graham, D. L., Edwards, S., Bachtell, R. K., DiLeone, R. J., Rios, M., & Self, D. W. (2007). Dynamic BDNF activity in nucleus accumbens with cocaine use increases self-administration and relapse. *Nat Neurosci, 10*(8), 1029-1037.

Gray, J. A., Shi, Y., Usui, H., During, M. J., Sakimura, K., & Nicoll, R. A. (2011). Distinct modes of AMPA receptor suppression at developing synapses by GluN2A and GluN2B: single-cell NMDA receptor subunit deletion in vivo. *Neuron, 71*(6), 1085-1101.

Grimm, J. W., Lu, L., Hayashi, T., Hope, B. T., Su, T. P., & Shaham, Y. (2003). Time-dependent increases in brain-derived neurotrophic factor protein levels within the mesolimbic dopamine system after withdrawal from cocaine: implications for incubation of cocaine craving. *J Neurosci, 23*(3), 742-747.

Groc, L., Gustafsson, B., & Hanse, E. (2006). AMPA signalling in nascent glutamatergic synapses: there and not there! *Trends Neurosci, 29*(3), 132-139.

Hayashi, Y. (2000). Driving AMPA Receptors into Synapses by LTP and CaMKII: Requirement for GluR1 and PDZ Domain Interaction. *Science, 287*(5461), 2262-2267.

Heine, M., Groc, L., Frischknecht, R., Beique, J. C., Lounis, B., Rumbaugh, G., Huganir, R. L., Cognet, L., & Choquet, D. (2008). Surface mobility of postsynaptic AMPARs tunes synaptic transmission. *Science, 320*(5873), 201-205.

Hessler, N. A., Shirke, A. M., & Malinow, R. (1993). The probability of transmitter release at a mammalian central synapse. *Nature, 366*(6455), 569-572.

Hjelmstad, G. O., Nicoll, R. A., & Malenka, R. C. (1997). Synaptic refractory period provides a measure of probability of release in the hippocampus. *Neuron, 19*(6), 1309-1318.

Howe, J. R., Cull-Candy, S. G., & Colquhoun, D. (1991). Currents through single glutamate receptor channels in outside-out patches from rat cerebellar granule cells. *J Physiol, 432*, 143-202.

Huang, Y. H., Lin, Y., Mu, P., Lee, B. R., Brown, T. E., Wayman, G., Marie, H., Liu, W., Yan, Z., Sorg, B. A., Schluter, O. M., Zukin, R. S., & Dong, Y. (2009). In vivo cocaine experience generates silent synapses. *Neuron, 63*(1), 40-47.

Hyman, S. E., & Malenka, R. C. (2001). Addiction and the brain: the neurobiology of compulsion and its persistence. *Nat Rev Neurosci, 2*(10), 695-703.

Hyman, S. E., Malenka, R. C., & Nestler, E. J. (2006). Neural mechanisms of addiction: the role of reward-related learning and memory. *Annu Rev Neurosci, 29*, 565-598.

Isaac, J. T., Ashby, M. C., & McBain, C. J. (2007). The role of the GluR2 subunit in AMPA receptor function and synaptic plasticity. *Neuron, 54*(6), 859-871.

Isaac, J. T., Nicoll, R. A., & Malenka, R. C. (1995). Evidence for silent synapses: implications for the expression of LTP. *Neuron, 15*(2), 427-434.

Kalivas, P. W. (2004). Glutamate systems in cocaine addiction. *Curr Opin Pharmacol, 4*(1), 23-29.

Kalivas, P. W., & O'Brien, C. (2008). Drug addiction as a pathology of staged neuroplasticity. *Neuropsychopharmacology, 33*(1), 166-180.

Kalivas, P. W., & Stewart, J. (1991). Dopamine transmission in the initiation and expression of drug- and stress-induced sensitization of motor activity. *Brain Res Brain Res Rev, 16*(3), 223-244.

Kalivas, P. W., & Volkow, N. D. (2005). The neural basis of addiction: a pathology of motivation and choice. *Am J Psychiatry, 162*(8), 1403-1413.

Kelley, A. E., & Berridge, K. C. (2002). The neuroscience of natural rewards: relevance to addictive drugs. *J Neurosci, 22*(9), 3306-3311.

Kerchner, G. A., & Nicoll, R. A. (2008). Silent synapses and the emergence of a postsynaptic mechanism for LTP. *Nat Rev Neurosci, 9*(11), 813-825.

Kornau, H. C., Schenker, L. T., Kennedy, M. B., & Seeburg, P. H. (1995). Domain interaction between NMDA receptor subunits and the postsynaptic density protein PSD-95. *Science, 269*(5231), 1737-1740.

Kourrich, S., Rothwell, P. E., Klug, J. R., & Thomas, M. J. (2007). Cocaine experience controls bidirectional synaptic plasticity in the nucleus accumbens. *J Neurosci, 27*(30), 7921-7928.

Kullmann, D. M. (1994). Amplitude fluctuations of dual-component EPSCs in hippocampal pyramidal cells: implications for long-term potentiation. *Neuron, 12*(5), 1111-1120.

Kuroda, H., Kutner, R. H., Bazan, N. G., & Reiser, J. (2009). Simplified lentivirus vector production in protein-free media using polyethylenimine-mediated transfection. *J Virol Methods, 157*(2), 113-121.

Lepore, M., Vorel, S. R., Lowinson, J., & Gardner, E. L. (1995). Conditioned place preference induced by delta 9-tetrahydrocannabinol: comparison with cocaine, morphine, and food reward. *Life Sci, 56*(23-24), 2073-2080.

Li, X., & Wolf, M. E. (2011). Brain-derived neurotrophic factor rapidly increases AMPA receptor surface expression in rat nucleus accumbens. *Eur J Neurosci, 34*(2), 190-198.

Liao, D., Hessler, N. A., & Malinow, R. (1995). Activation of postsynaptically silent synapses during pairing-induced LTP in CA1 region of hippocampal slice. *Nature, 375*(6530), 400-404.

Lieberman, D. N., & Mody, I. (1999). Properties of single NMDA receptor channels in human dentate gyrus granule cells. *J Physiol, 518 (Pt 1)*, 55-70.

Liu, S. Q., & Cull-Candy, S. G. (2000). Synaptic activity at calcium-permeable AMPA receptors induces a switch in receptor subtype. *Nature, 405*(6785), 454-458.

Liu, X. B., Murray, K. D., & Jones, E. G. (2004). Switching of NMDA receptor 2A and 2B subunits at thalamic and cortical synapses during early postnatal development. *J Neurosci, 24*(40), 8885-8895.

Lu, H., Cheng, P. L., Lim, B. K., Khoshnevisrad, N., & Poo, M. M. (2010). Elevated BDNF after cocaine withdrawal facilitates LTP in medial prefrontal cortex by suppressing GABA inhibition. *Neuron, 67*(5), 821-833.

Madayag, A., Lobner, D., Kau, K. S., Mantsch, J. R., Abdulhameed, O., Hearing, M., Grier, M. D., & Baker, D. A. (2007). Repeated N-acetylcysteine administration alters plasticity-dependent effects of cocaine. *J Neurosci, 27*(51), 13968-13976.

Magee, J. C., & Johnston, D. (1997). A synaptically controlled, associative signal for Hebbian plasticity in hippocampal neurons. *Science, 275*(5297), 209-213.

Malinow, R., & Malenka, R. C. (2002). AMPA receptor trafficking and synaptic plasticity. *Annu Rev Neurosci, 25*, 103-126.

Mameli, M., Balland, B., Lujan, R., & Luscher, C. (2007). Rapid synthesis and synaptic insertion of GluR2 for mGluR-LTD in the ventral tegmental area. *Science, 317*(5837), 530-533.

Mameli, M., Halbout, B., Creton, C., Engblom, D., Parkitna, J. R., Spanagel, R., & Luscher, C. (2009). Cocaine-evoked synaptic plasticity: persistence in the VTA triggers adaptations in the NAc. *Nat Neurosci, 12*(8), 1036-1041.

Mameli, M., & Luscher, C. (2011). Synaptic plasticity and addiction: learning mechanisms gone awry. *Neuropharmacology, 61*(7), 1052-1059.

Manabe, T., Wyllie, D. J., Perkel, D. J., & Nicoll, R. A. (1993). Modulation of synaptic transmission and long-term potentiation: effects on paired pulse facilitation and EPSC variance in the CA1 region of the hippocampus. *J Neurophysiol, 70*(4), 1451-1459.

Mansour, M., Nagarajan, N., Nehring, R. B., Clements, J. D., & Rosenmund, C. (2001). Heteromeric AMPA receptors assemble with a preferred subunit stoichiometry and spatial arrangement. *Neuron, 32*(5), 841-853.

Manzoni, O., Michel, J. M., & Bockaert, J. (1997). Metabotropic glutamate receptors in the rat nucleus accumbens. *Eur J Neurosci, 9*(7), 1514-1523.

McCutcheon, J. E., Loweth, J. A., Ford, K. A., Marinelli, M., Wolf, M. E., & Tseng, K. Y. (2011). Group I mGluR activation reverses cocaine-induced accumulation of calcium-permeable AMPA receptors in nucleus accumbens synapses via a protein kinase C-dependent mechanism. *J Neurosci, 31*(41), 14536-14541.

McGee, A. W., Topinka, J. R., Hashimoto, K., Petralia, R. S., Kakizawa, S., Kauer, F. W., Aguilera-Moreno, A., Wenthold, R. J., Kano, M., & Bredt, D. S. (2001). PSD-93 knock-out mice reveal that neuronal MAGUKs are not required for development or function of parallel fiber synapses in cerebellum. *J Neurosci, 21*(9), 3085-3091.

Meredith, G. E., Farrell, T., Kellaghan, P., Tan, Y., Zahm, D. S., & Totterdell, S. (1999). Immunocytochemical characterization of catecholaminergic neurons in the rat striatum following dopamine-depleting lesions. *Eur J Neurosci, 11*(10), 3585-3596.

Migaud, M., Charlesworth, P., Dempster, M., Webster, L. C., Watabe, A. M., Makhinson, M., He, Y., Ramsay, M. F., Morris, R. G., Morrison, J. H., O'Dell, T. J., & Grant, S. G. (1998). Enhanced long-term potentiation and impaired learning in mice with mutant postsynaptic density-95 protein. *Nature, 396*(6710), 433-439.

Miller, E. K., & Cohen, J. D. (2001). An integrative theory of prefrontal cortex function. *Annu Rev Neurosci, 24*, 167-202.

Minichiello, L. (2009). TrkB signalling pathways in LTP and learning. *Nat Rev Neurosci, 10*(12), 850-860.

Moran, M. M., McFarland, K., Melendez, R. I., Kalivas, P. W., & Seamans, J. K. (2005). Cystine/glutamate exchange regulates metabotropic glutamate receptor presynaptic inhibition of excitatory transmission and vulnerability to cocaine seeking. *J Neurosci, 25*(27), 6389-6393.

Moussawi, K., Zhou, W., Shen, H., Reichel, C. M., See, R. E., Carr, D. B., & Kalivas, P. W. (2011). Reversing cocaine-induced synaptic potentiation provides enduring protection from relapse. *Proc Natl Acad Sci U S A, 108*(1), 385-390.

Murphy, T. H., Miyamoto, M., Sastre, A., Schnaar, R. L., & Coyle, J. T. (1989). Glutamate toxicity in a neuronal cell line involves inhibition of cystine transport leading to oxidative stress. *Neuron, 2*(6), 1547-1558.

Nagel, G., Szellas, T., Kateriya, S., Adeishvili, N., Hegemann, P., & Bamberg, E. (2005). Channelrhodopsins: directly light-gated cation channels. *Biochem Soc Trans, 33*(Pt 4), 863-866.

Nicola, S. M., Kombian, S. B., & Malenka, R. C. (1996). Psychostimulants depress excitatory synaptic transmission in the nucleus accumbens via presynaptic D1-like dopamine receptors. *J Neurosci, 16*(5), 1591-1604.

Oertner, T. G., Sabatini, B. L., Nimchinsky, E. A., & Svoboda, K. (2002). Facilitation at single synapses probed with optical quantal analysis. *Nat Neurosci, 5*(7), 657-664.

Petreanu, L., Mao, T., Sternson, S. M., & Svoboda, K. (2009). The subcellular organization of neocortical excitatory connections. *Nature, 457*(7233), 1142-1145.

Pierce, R. C., Bell, K., Duffy, P., & Kalivas, P. W. (1996). Repeated cocaine augments excitatory amino acid transmission in the nucleus accumbens only in rats having developed behavioral sensitization. *J Neurosci, 16*(4), 1550-1560.

Poo, M. M. (2001). Neurotrophins as synaptic modulators. *Nat Rev Neurosci, 2*(1), 24-32.

Porrino, L. J. (1993). Functional consequences of acute cocaine treatment depend on route of administration. *Psychopharmacology (Berl), 112*(2-3), 343-351.

Redman, S. (1990). Quantal analysis of synaptic potentials in neurons of the central nervous system. *Physiol Rev, 70*(1), 165-198.

Rekling, J. C., Shao, X. M., & Feldman, J. L. (2000). Electrical coupling and excitatory synaptic transmission between rhythmogenic respiratory neurons in the preBotzinger complex. *J Neurosci, 20*(23), RC113.

Robinson, T. E., & Berridge, K. C. (1993). The neural basis of drug craving: an incentive-sensitization theory of addiction. *Brain Res Brain Res Rev, 18*(3), 247-291.

Robinson, T. E., Gorny, G., Mitton, E., & Kolb, B. (2001). Cocaine self-administration alters the morphology of dendrites and dendritic spines in the nucleus accumbens and neocortex. *Synapse, 39*(3), 257-266.

Roche, K. W., Standley, S., McCallum, J., Dune Ly, C., Ehlers, M. D., & Wenthold, R. J. (2001). Molecular determinants of NMDA receptor internalization. *Nat Neurosci, 4*(8), 794-802.

Rodrigues, S. M., Schafe, G. E., & LeDoux, J. E. (2004). Molecular mechanisms underlying emotional learning and memory in the lateral amygdala. *Neuron, 44*(1), 75-91.

Rosenmund, C., Clements, J. D., & Westbrook, G. L. (1993). Nonuniform probability of glutamate release at a hippocampal synapse. *Science, 262*(5134), 754-757.

Roux, S., Froger, C., Porsolt, R. D., Valverde, O., & Maldonado, R. (2003). Place preference test in rodents. *Curr Protoc Neurosci, Chapter 9*, Unit 9 15.

Saiki, R. K., Scharf, S., Faloona, F., Mullis, K. B., Horn, G. T., Erlich, H. A., & Arnheim, N. (1985). Enzymatic amplification of beta-globin genomic sequences and restriction site analysis for diagnosis of sickle cell anemia. *Science, 230*(4732), 1350-1354.

Scheuss, V., & Neher, E. (2001). Estimating synaptic parameters from mean, variance, and covariance in trains of synaptic responses. *Biophys J, 81*(4), 1970-1989.

Schluter, O. M., Xu, W., & Malenka, R. C. (2006). Alternative N-terminal domains of PSD-95 and SAP97 govern activity-dependent regulation of synaptic AMPA receptor function. *Neuron, 51*(1), 99-111.

Schoepfer, R., Monyer, H., Sommer, B., Wisden, W., Sprengel, R., Kuner, T., Lomeli, H., Herb, A., Kohler, M., Burnashev, N., & et al. (1994). Molecular biology of glutamate receptors. *Prog Neurobiol, 42*(2), 353-357.

Schultz, W., Apicella, P., & Ljungberg, T. (1993). Responses of monkey dopamine neurons to reward and conditioned stimuli during successive steps of learning a delayed response task. *J Neurosci, 13*(3), 900-913.

Schultz, W., Dayan, P., & Montague, P. R. (1997). A neural substrate of prediction and reward. *Science, 275*(5306), 1593-1599.

Seeburg, P. H., Higuchi, M., & Sprengel, R. (1998). RNA editing of brain glutamate receptor channels: mechanism and physiology. *Brain Res Brain Res Rev, 26*(2-3), 217-229.

Shalev, U., Grimm, J. W., & Shaham, Y. (2002). Neurobiology of relapse to heroin and cocaine seeking: a review. *Pharmacol Rev, 54*(1), 1-42.

Shepherd, J. D., & Huganir, R. L. (2007). The cell biology of synaptic plasticity: AMPA receptor trafficking. *Annu Rev Cell Dev Biol, 23*, 613-643.

Shi, S., Hayashi, Y., Esteban, J. A., & Malinow, R. (2001). Subunit-specific rules governing AMPA receptor trafficking to synapses in hippocampal pyramidal neurons. *Cell, 105*(3), 331-343.

Shi, S. H., Hayashi, Y., Petralia, R. S., Zaman, S. H., Wenthold, R. J., Svoboda, K., & Malinow, R. (1999). Rapid spine delivery and redistribution of AMPA receptors after synaptic NMDA receptor activation. *Science, 284*(5421), 1811-1816.

Silver, R. A. (2003). Estimation of nonuniform quantal parameters with multiple-probability fluctuation analysis: theory, application and limitations. *J Neurosci Methods, 130*(2), 127-141.

Silver, R. A., Cull-Candy, S. G., & Takahashi, T. (1996). Non-NMDA glutamate receptor occupancy and open probability at a rat cerebellar synapse with single and multiple release sites. *J Physiol, 494 (Pt 1)*, 231-250.

Sora, I., Hall, F. S., Andrews, A. M., Itokawa, M., Li, X. F., Wei, H. B., Wichems, C., Lesch, K. P., Murphy, D. L., & Uhl, G. R. (2001). Molecular mechanisms of cocaine reward: combined dopamine and serotonin transporter knockouts eliminate cocaine place preference. *Proc Natl Acad Sci U S A, 98*(9), 5300-5305.

Sun, W., & Rebec, G. V. (2006). Repeated cocaine self-administration alters processing of cocaine-related information in rat prefrontal cortex. *J Neurosci, 26*(30), 8004-8008.

Swanson, L. W. (1982). The projections of the ventral tegmental area and adjacent regions: a combined fluorescent retrograde tracer and immunofluorescence study in the rat. *Brain Res Bull, 9*(1-6), 321-353.

Thomas, M. J., Beurrier, C., Bonci, A., & Malenka, R. C. (2001). Long-term depression in the nucleus accumbens: a neural correlate of behavioral sensitization to cocaine. *Nat Neurosci, 4*(12), 1217-1223.

Thomsen, R. H., & Wilson, D. F. (1983). Effects of 4-aminopyridine and 3,4-diaminopyridine on transmitter release at the neuromuscular junction. *J Pharmacol Exp Ther, 227*(1), 260-265.

Tyler, W. J., & Pozzo-Miller, L. D. (2001). BDNF enhances quantal neurotransmitter release and increases the number of docked vesicles at the active zones of hippocampal excitatory synapses. *J Neurosci, 21*(12), 4249-4258.

Tyler, W. J., Zhang, X. L., Hartman, K., Winterer, J., Muller, W., Stanton, P. K., & Pozzo-Miller, L. (2006). BDNF increases release probability and the size of a rapidly recycling vesicle pool within rat hippocampal excitatory synapses. *J Physiol, 574*(Pt 3), 787-803.

Tzschentke, T. M. (1998). Measuring reward with the conditioned place preference paradigm: a comprehensive review of drug effects, recent progress and new issues. *Prog Neurobiol, 56*(6), 613-672.

Ungless, M. A., Whistler, J. L., Malenka, R. C., & Bonci, A. (2001). Single cocaine exposure in vivo induces long-term potentiation in dopamine neurons. *Nature, 411*(6837), 583-587.

Wall, M. J., & Usowicz, M. M. (1998). Development of the quantal properties of evoked and spontaneous synaptic currents at a brain synapse. *Nat Neurosci, 1*(8), 675-682.

Wolf, M. E. (2010). Regulation of AMPA receptor trafficking in the nucleus accumbens by dopamine and cocaine. *Neurotox Res, 18*(3-4), 393-409.

Wu, G.-Y., Malinow, R., & Cline, H. T. (1996). Maturation of a Central Glutamatergic Synapse. *Science, 274*(5289), 972-976.

Wu, L. G., & Saggau, P. (1994). Adenosine inhibits evoked synaptic transmission primarily by reducing presynaptic calcium influx in area CA1 of hippocampus. *Neuron, 12*(5), 1139-1148.

Xiao, M. Y., Wasling, P., Hanse, E., & Gustafsson, B. (2004). Creation of AMPA-silent synapses in the neonatal hippocampus. *Nat Neurosci, 7*(3), 236-243.

Xu, W., Schluter, O. M., Steiner, P., Czervionke, B. L., Sabatini, B., & Malenka, R. C. (2008). Molecular dissociation of the role of PSD-95 in regulating synaptic strength and LTD. *Neuron, 57*(2), 248-262.

Yao, W. D., Gainetdinov, R. R., Arbuckle, M. I., Sotnikova, T. D., Cyr, M., Beaulieu, J. M., Torres, G. E., Grant, S. G., & Caron, M. G. (2004). Identification of PSD-95 as a regulator of dopamine-mediated synaptic and behavioral plasticity. *Neuron, 41*(4), 625-638.

Yoshii, A., & Constantine-Paton, M. (2007). BDNF induces transport of PSD-95 to dendrites through PI3K-AKT signaling after NMDA receptor activation. *Nat Neurosci, 10*(6), 702-711.

Zhang, X., Liu, X., Wang, D., Liu, H., & Hao, W. (2011). Conditioned place preference associated with level of palmitoylation of PSD-95 in rat hippocampus and nucleus accumbens. *Neuropsychobiology, 64*(4), 211-218.

Acknowledgements

First and foremost I would like to express my sincere gratitude to Dr. Oliver Schlüter, for giving me the opportunity to join his wonderful team. I'm very thankful for his, invaluable guidance, encouragement, tremendous knowledge and creativity. Thank you for your constant support and belief in my abilities.

I would like to thank the members of my thesis committee, Prof. André Fischer and Prof. Tobias Moser for their supervision and constructive input to this PhD project.

It was a pleasure to work in such a wonderful team made by the past and present Members of the Molecular Neurobiology Group at the European Neuroscience Institute. Juliane, Stephanie, Derya, Sandra, Huang, Yanling, Martina, Peter, Plino, Tanmoy, Albrecht, you guys created an amazing atmosphere. Thank you for all your support and countless lunch sessions.

My special thanks to Juliane, Stephanie, Derya and Sandra for your joy and laughter during the good times and the words of comfort when things got rocky. Juliane, thank you for becoming my role model. Stephanie, you have been a constant Sunshine in this rainy Göttingen. Derya, thank you for sharing the frustrations during our tea breaks and Sandra, thank you for caring so much. But most of all, thank you for becoming my friends!

I am thankful to our collaborator Prof. Yan Dong for allowing me to carry out a part of my project at his laboratory, for his substantial scientific input and stimulating discussions. Special thanks to Dr. Brian Lee for his tremendous help with animal surgeries and sharing his setup, taking the early morning shift. Many thanks to other lab members Dr. Yanhua Huang, Dr. Masago Ishikawa and Mami Otaka for helpful discussions and support; Peter Neumann and Brandon Roberts for their wonderful company during my three months in Pullman.

I am very grateful to the GGNB School for the privilege of becoming their student. I felt deeply honored for awarding me the Excellence Stipend. Many thanks to the CMPB program coordinator, Prof. Michael Hörner and the members of the GGNB coordination office for an exceptional organization and an incredible support during the course of my PhD.
Many thanks to EMBO for the award of a travel fellowship enabling me to work in the group of Prof. Yan Dong at Washington State University.

My stay in Göttingen wouldn't be so incredible hadn't I met Tolga Soykan. I am extremely grateful you for your emotional support, care and affection that kept me going throughout those years.
I thank Jonas Barth for his friendship and all the wonderful and extraordinary people I was fortunate to live among, for bringing joy to my stay in Germany and making me feel like home. Many thanks to my amazing girls: Marysia Mrozek, Kasia Hanzelka and Asia Łoboda for their friendship and support despite hundreds of kilometers between us.

Lastly, I would like to express my utmost gratitude to my family, to whom I dedicate this work. To my incredible mom Elżbieta for her sacrifice, unconditional love and affection. To my wonderful brothers Maciej and Piotr for their care of their little sister. Without you none of this would have been possible.

Curriculum Vitae

Personal data

Name, surname: **Anna Elżbieta Suska**

Date of birth: **31.07.1984, Kraków**

Address: **Friedrichstr 1, 37073 Göttingen**

E-mail: **asuska@gwdg.de**

Education

2008 – 2012	**Molecular Physiology of the Brain program at GGNB, Georg-August University, Göttingen, Germany –** PhD student
2003 – 2008	**Faculty of Biotechnology, Jagiellonian University, Kraków, Poland** MSc course in biotechnology, specialized in biochemistry, final grade: A
1999 – 2003	**Bartłomiej Nowodworski's Secondary School no.1, Kraków, Poland,** profile: biology and chemistry, final grade: A

Awards

2003 –	Jagiellonian University Contest of Chemical Knowledge for secondary school students: first place

Laboratory experience

2008 – 2012	Dr. Oliver Schlüter's research group – Molecular Neurobiology at European Neuroscience Institute, Göttingen, Germany – PhD student
2011	Professor Yan Dong's research group – Department of Veterinary and Comparative Anatomy, Pharmacology and Physiology, Washington State University, Pullman, WA, USA
2007 – 2008	Dr. Oliver Schlüter's research group – Molecular Neurobiology at European Neuroscience Institute, Göttingen, Germany – ERASMUS program
2005 – 2008	Professor Władysław Lasoń's research group – Experimental Neuroendocrinology, Institute of Pharmacology, Polish Academy of Sciences

Scholarships

2009 – 2012	GGNB Excellence Stipend
2011	EMBO Short-term Fellowship
2010	GGNB Travel Grant

Publication list

Suska, A., Lee, B.R., Huang, Y.H., Dong, Y., & Schlüter, O.M., (2012). Selective Presynaptic Enhancement of the prefrontal cortex to nucleus accumbens pathway by cocaine exposure. *PNAS in press*

Szymanska, M., **Suska, A**., Budziszewska, B., Jaworska-Feil, L., Basta-Kaim, A., Leskiewicz, M., Kubera, M., Gergont, A., Kroczka, S., Kacinski, M., & Lason, W. (2009). Prenatal stress decreases glycogen synthase kinase-3 phosphorylation in the rat frontal cortex. *Pharmacol Rep, 61*(4), 612-620.

Fiala, A., **Suska, A**., & Schlüter, O. M. (2010). Optogenetic approaches in neuroscience. *Curr Biol, 20*(20), R897-903.

Brown, T. E., Lee, B. R., Mu, P., Ferguson, D., Dietz, D., Ohnishi, Y. N., Lin, Y., **Suska, A**., Ishikawa, M., Huang, Y. H., Shen, H., Kalivas, P. W., Sorg, B. A., Zukin, R. S., Nestler, E. J., Dong, Y., & Schluter, O. M. (2011). A silent synapse-based mechanism for cocaine-induced locomotor sensitization. *J Neurosci, 31*(22), 8163-8174.